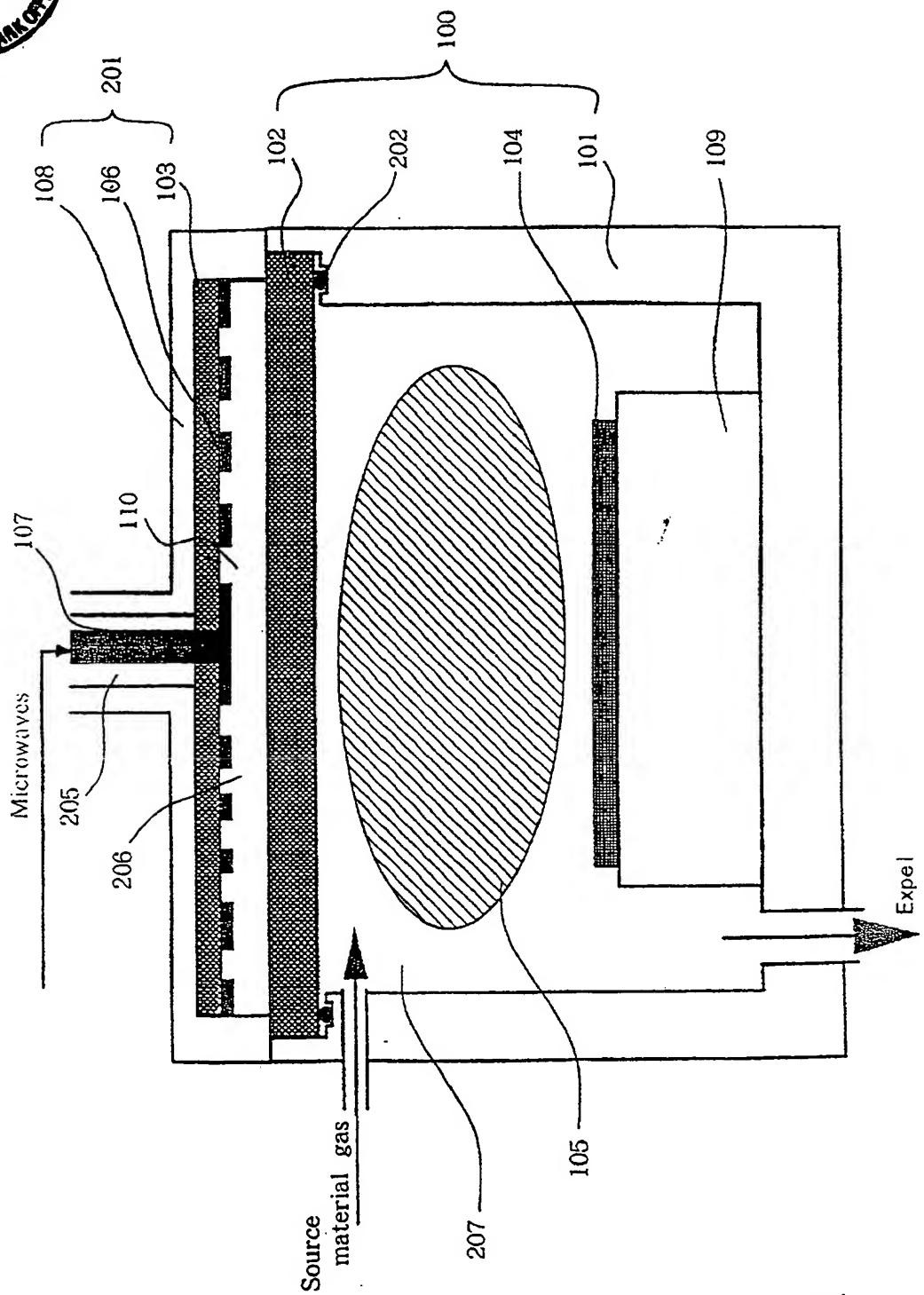

Fig. 1

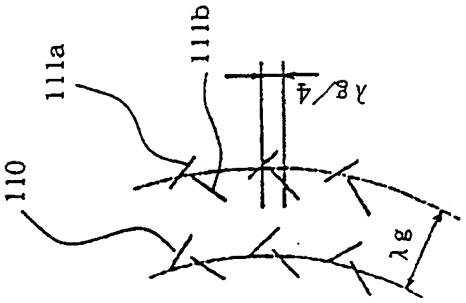

Fig. 2B

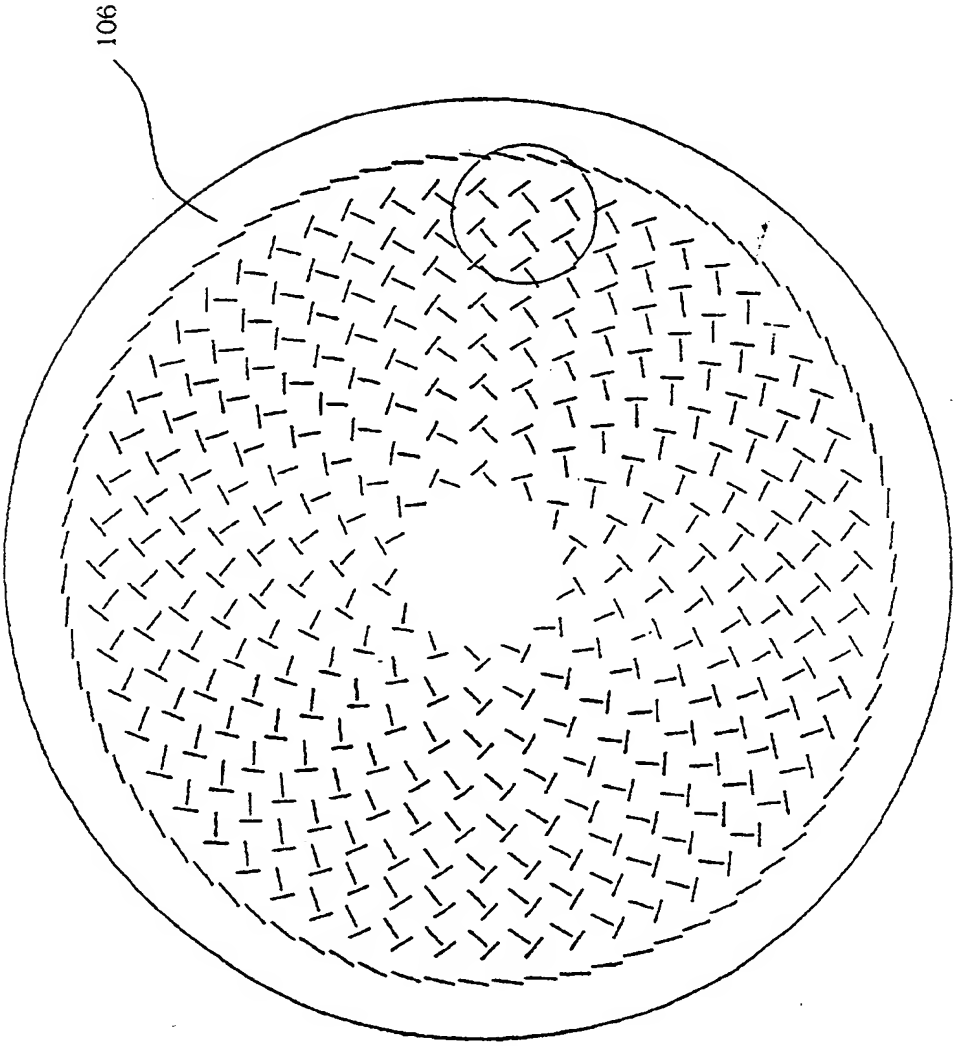

Fig. 2A

Microwave power (W) / Chamber material and inner surface processing conductivity($\Omega^{-1}\cdot m^{-1}$)	400	800	1200	1600
SUS (no inner surface processing) 1.4×10^{6}	×	×	×	×
Pb (inner surface processing onto SUS) 4.8×10^{6}	×	×	×	△
Ta (inner surface processing onto SUS) 8.0×10^{6}	×	×	○	○
W (inner surface processing onto SUS) 1.7×10^{7}	×	○	○	○
Al (inner surface processing onto SUS) 3.7×10^{7}	○	○	○	○
Au (inner surface processing onto SUS) 4.3×10^{7}	○	○	○	○
Cu (inner surface processing onto SUS) 6.0×10^{7}	○	○	○	○
Ag (inner surface processing onto SUS) 6.3×10^{7}	○	○	○	○

Inner surface processing thickness: 10 μm

○ plasma stable △ plasma unstable × no activation of plasma caused

Fig. 3

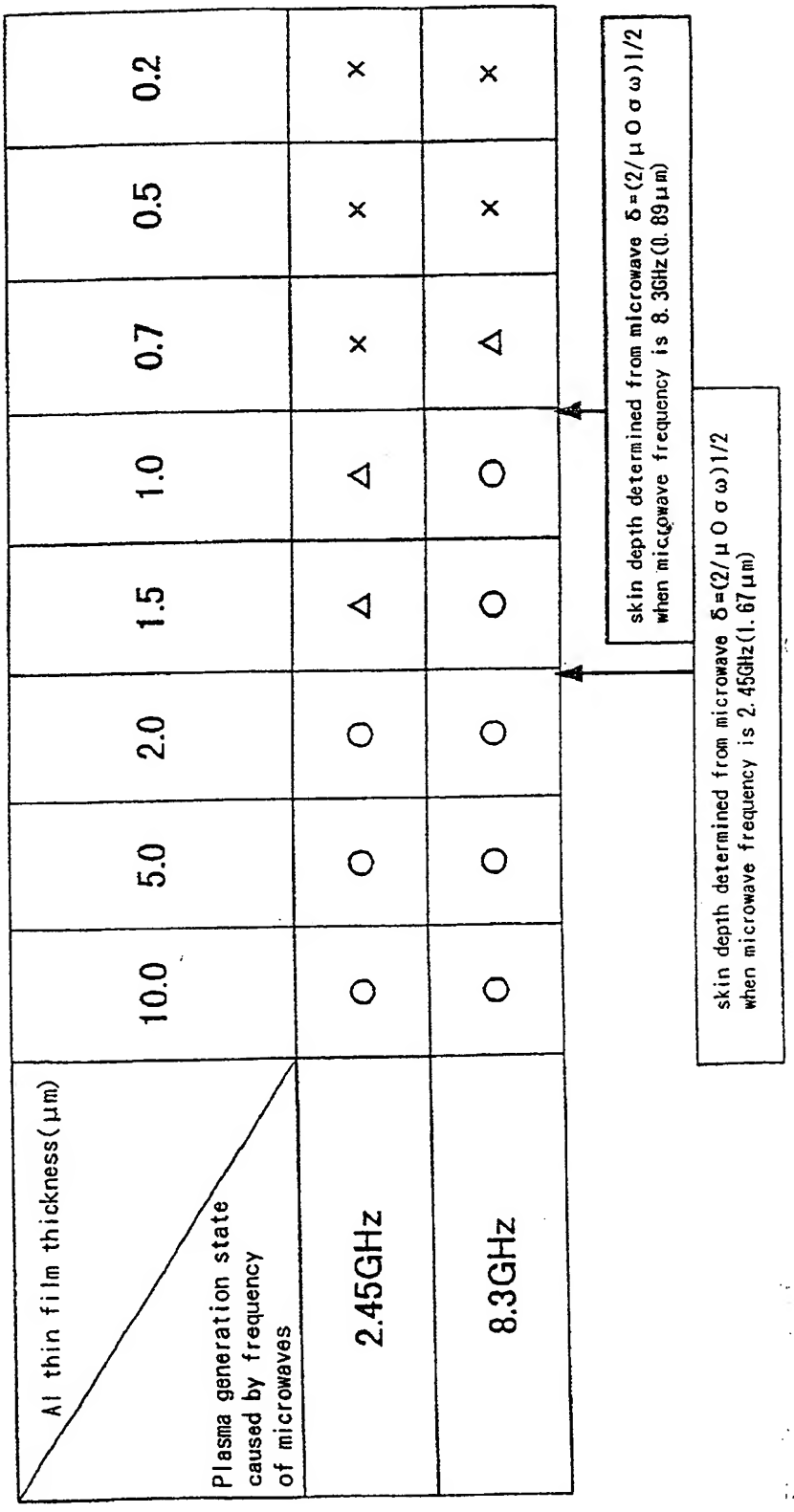

Plasma generation state caused by frequency of microwaves / Al thin film thickness(μm)	10.0	5.0	2.0	1.5	1.0	0.7	0.5	0.2
2.45GHz	○	○	○	△	△	×	×	×
8.3GHz	○	○	○	○	○	△	×	×

skin depth determined from microwave $\delta=(2/\mu O \sigma \omega)1/2$ when microwave frequency is 8.3GHz(0.89μm)

skin depth determined from microwave $\delta=(2/\mu O \sigma \omega)1/2$ when microwave frequency is 2.45GHz(1.67μm)

Fig. 4

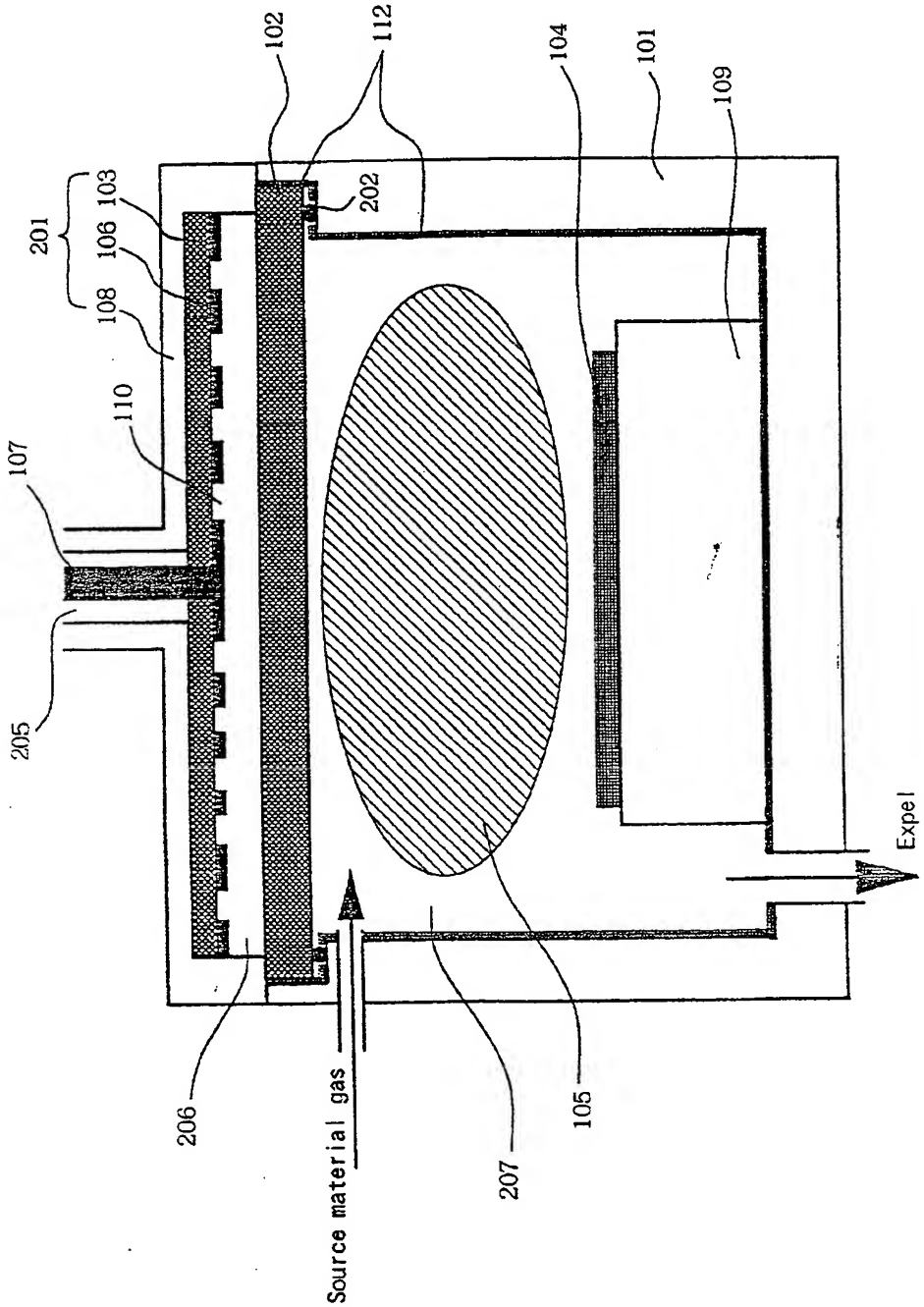
102
112
104
101
109
201
103
106
108
202
110
107
205
206
Source material gas
207
105
Expel

Fig. 5

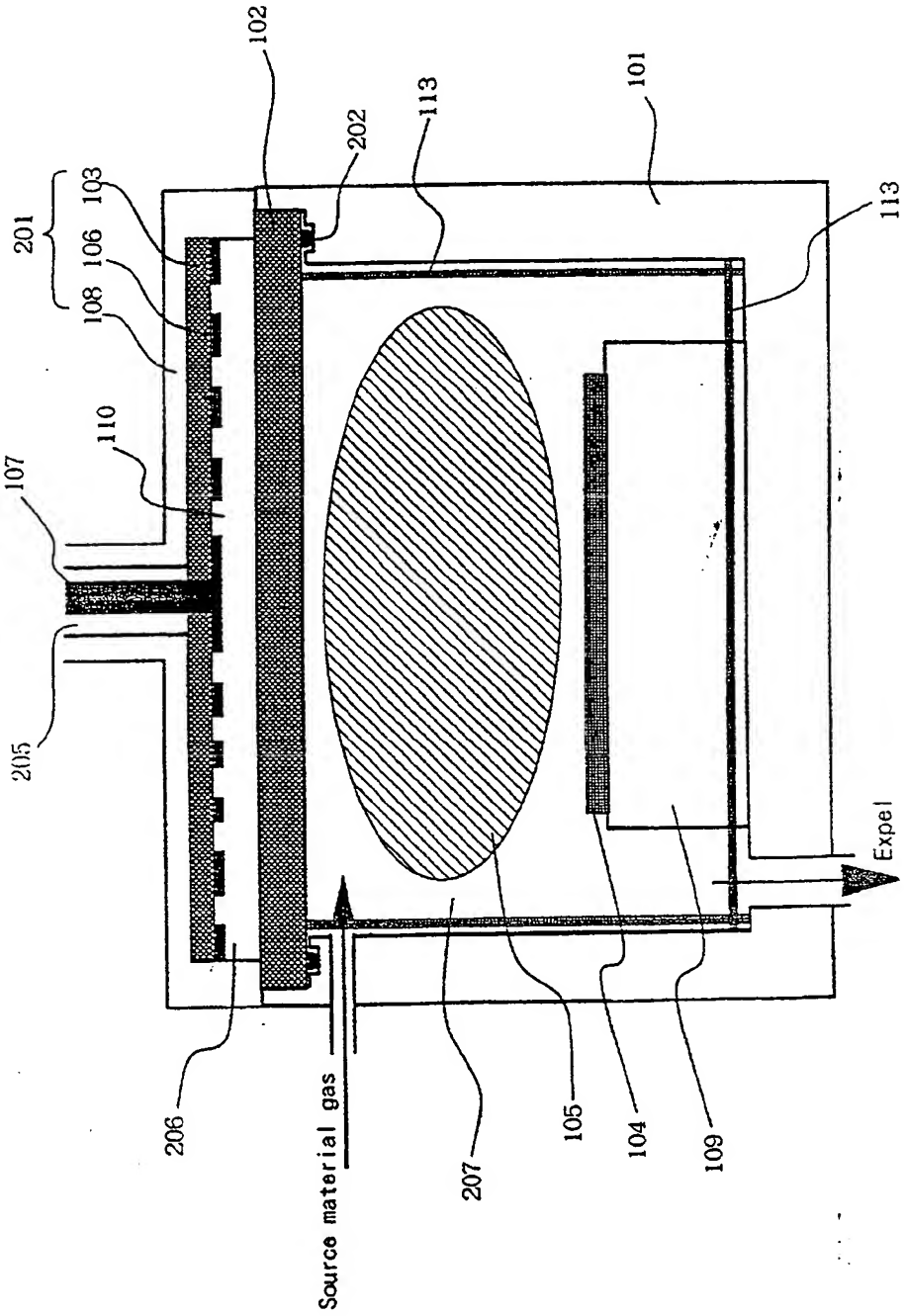
102
202
113
101
113
201
103
106
108
110
107
205
Expel
206
Source material gas
207
105
104
109

Fig. 6

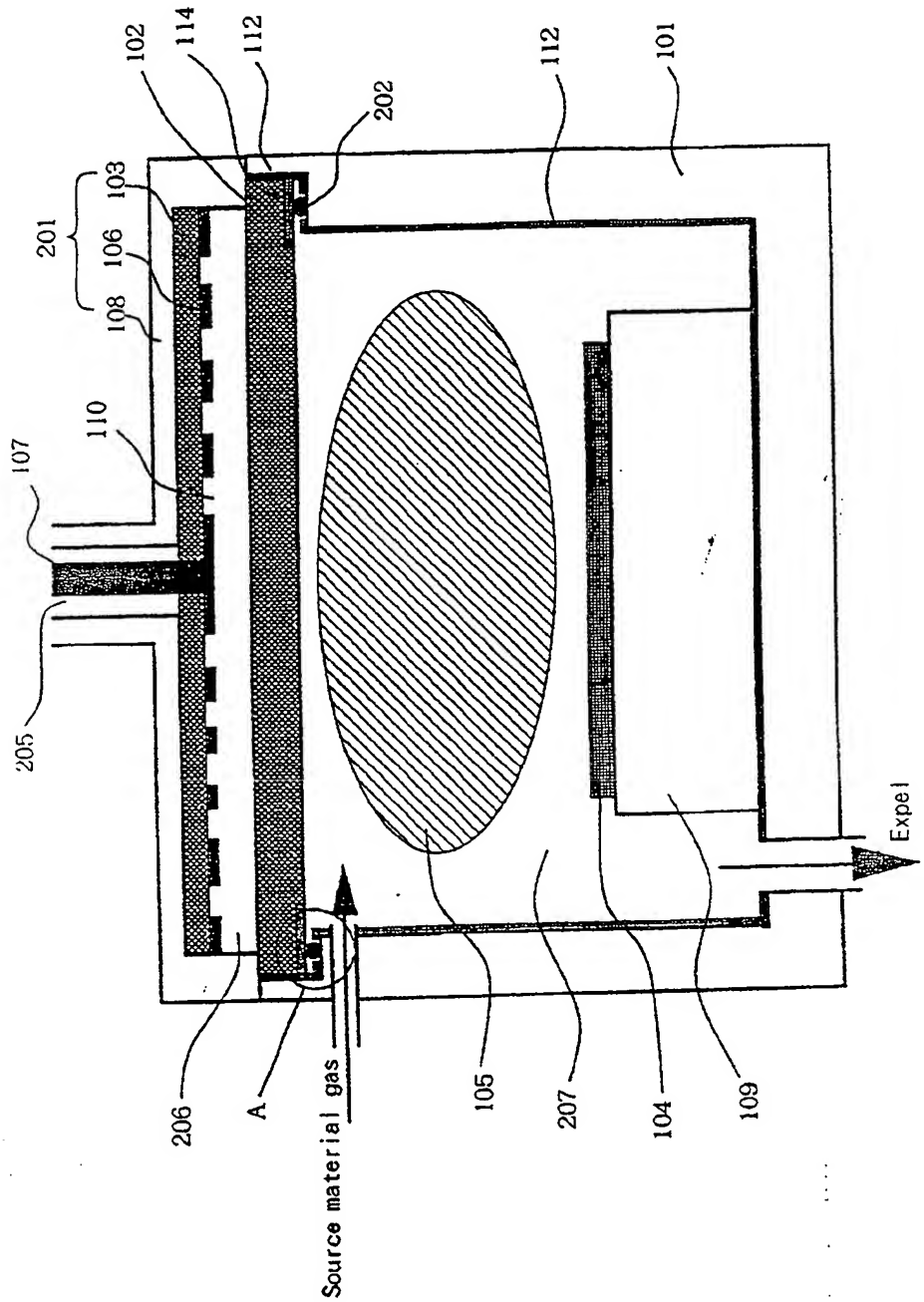
102
114
112
202
112
101
201
103
106
108
110
107
205
206
A
Source material gas
105
207
104
109
Expel

Fig. 7

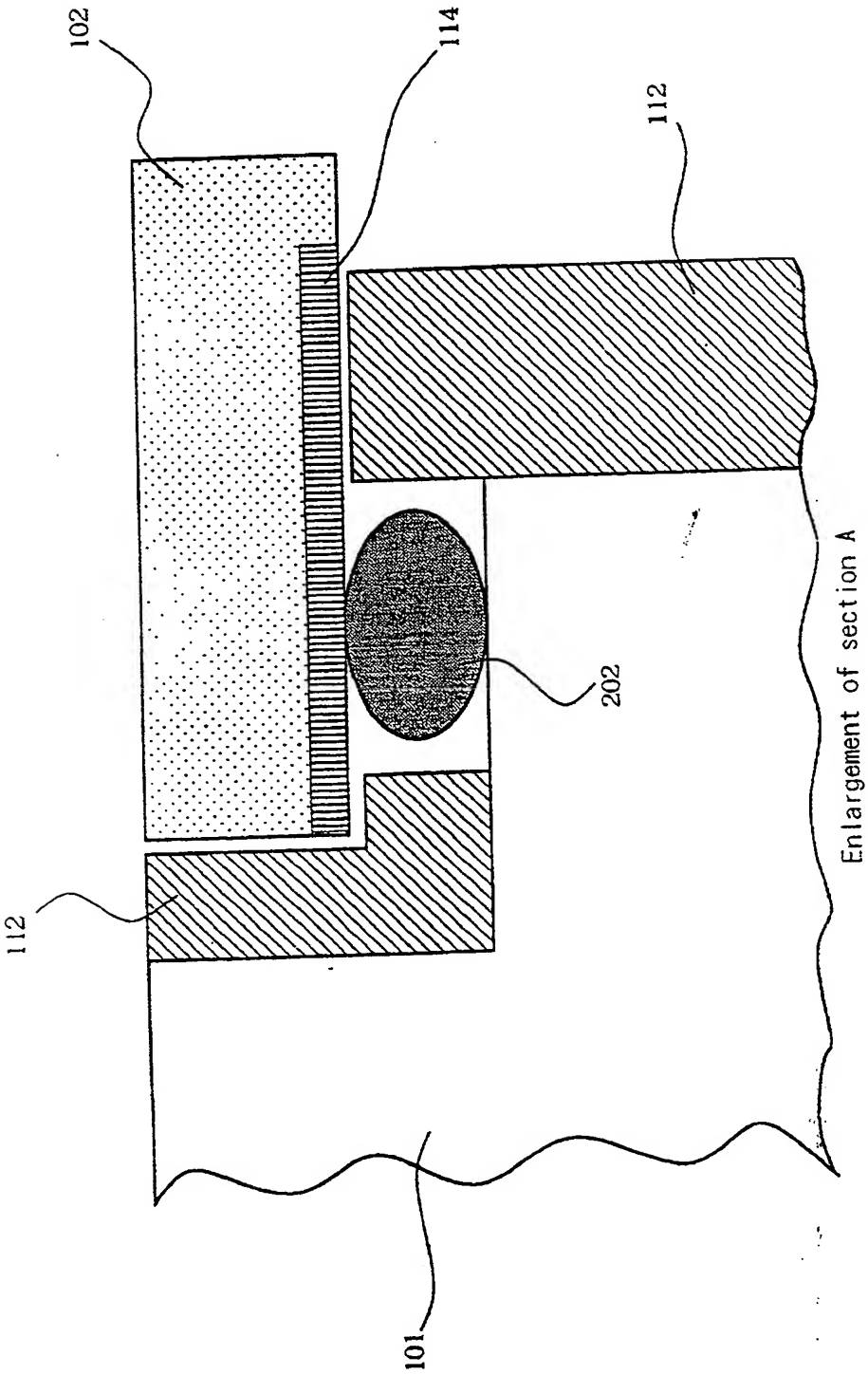

Fig. 8

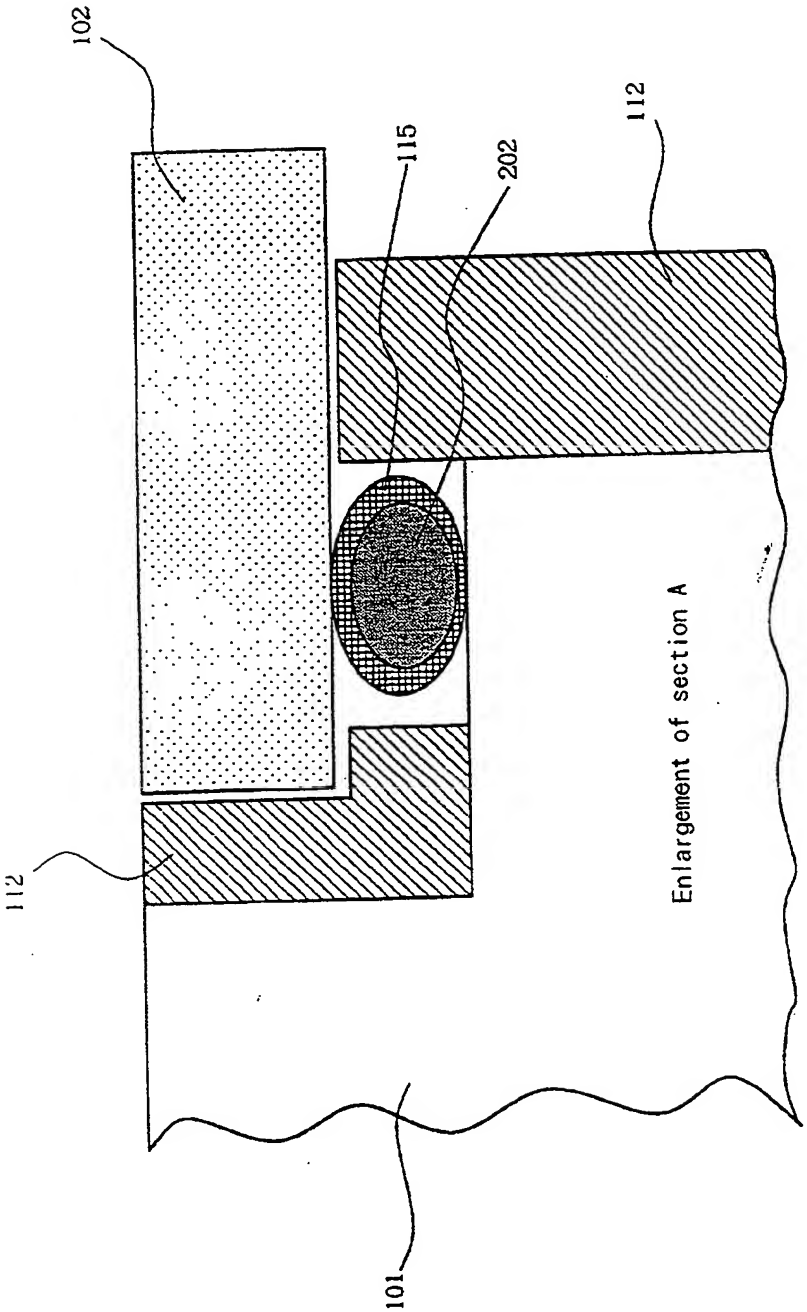

Fig. 9

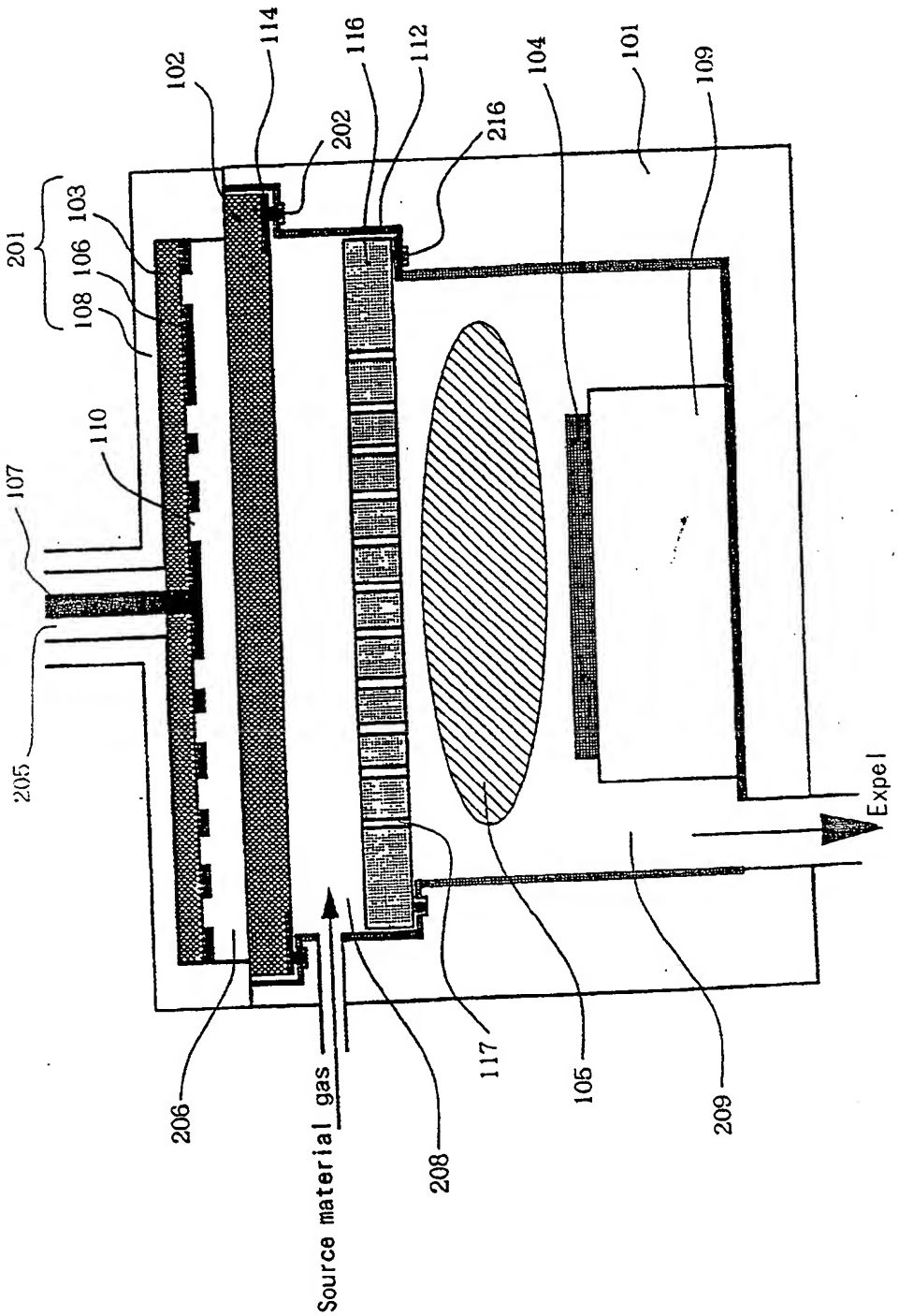
102
114
116
112
104
101
109
202
216
201
103
106
108
110
107
205
Expel
206
Source material gas
208
117
105
209

Fig. 10

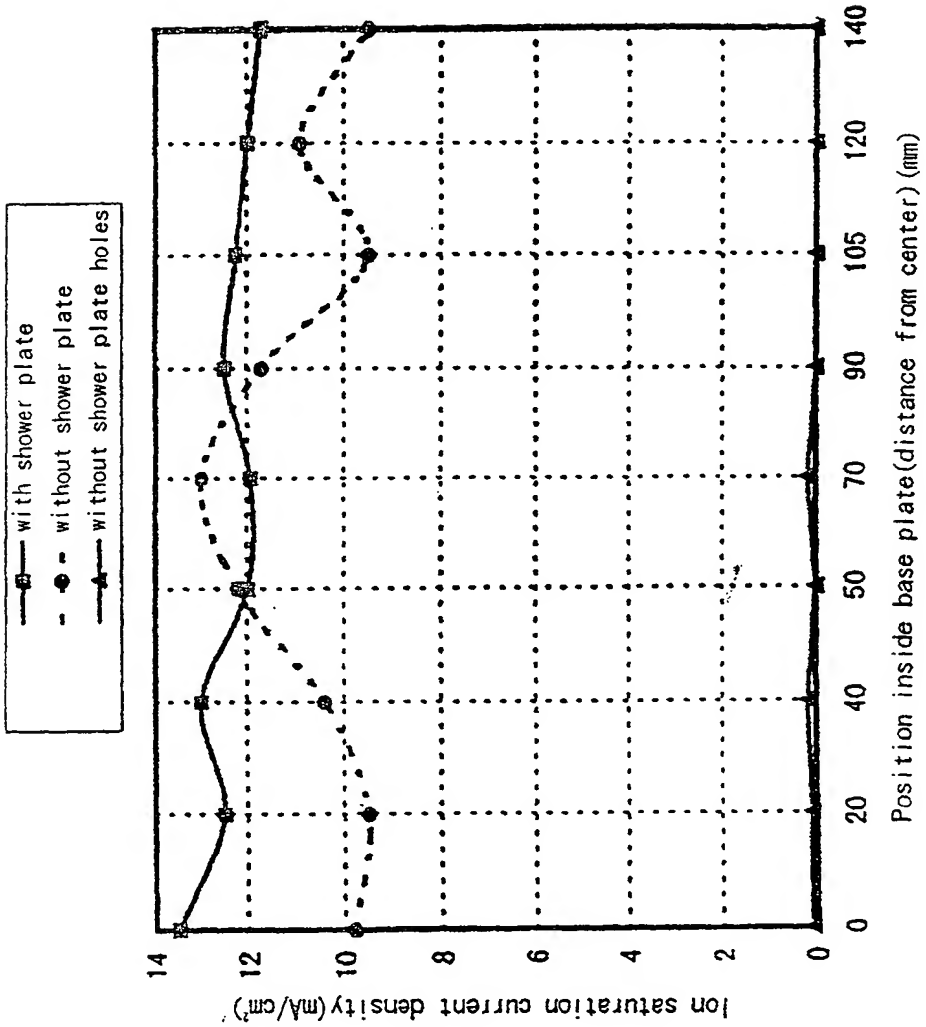
with shower plate
without shower plate
without shower plate holes
ion saturation current density(mA/cm²)
0
2
4
6
8
10
12
14
0
20
40
50
70
90
105
120
140
Position inside base plate(distance from center)(mm)

Fig. 11

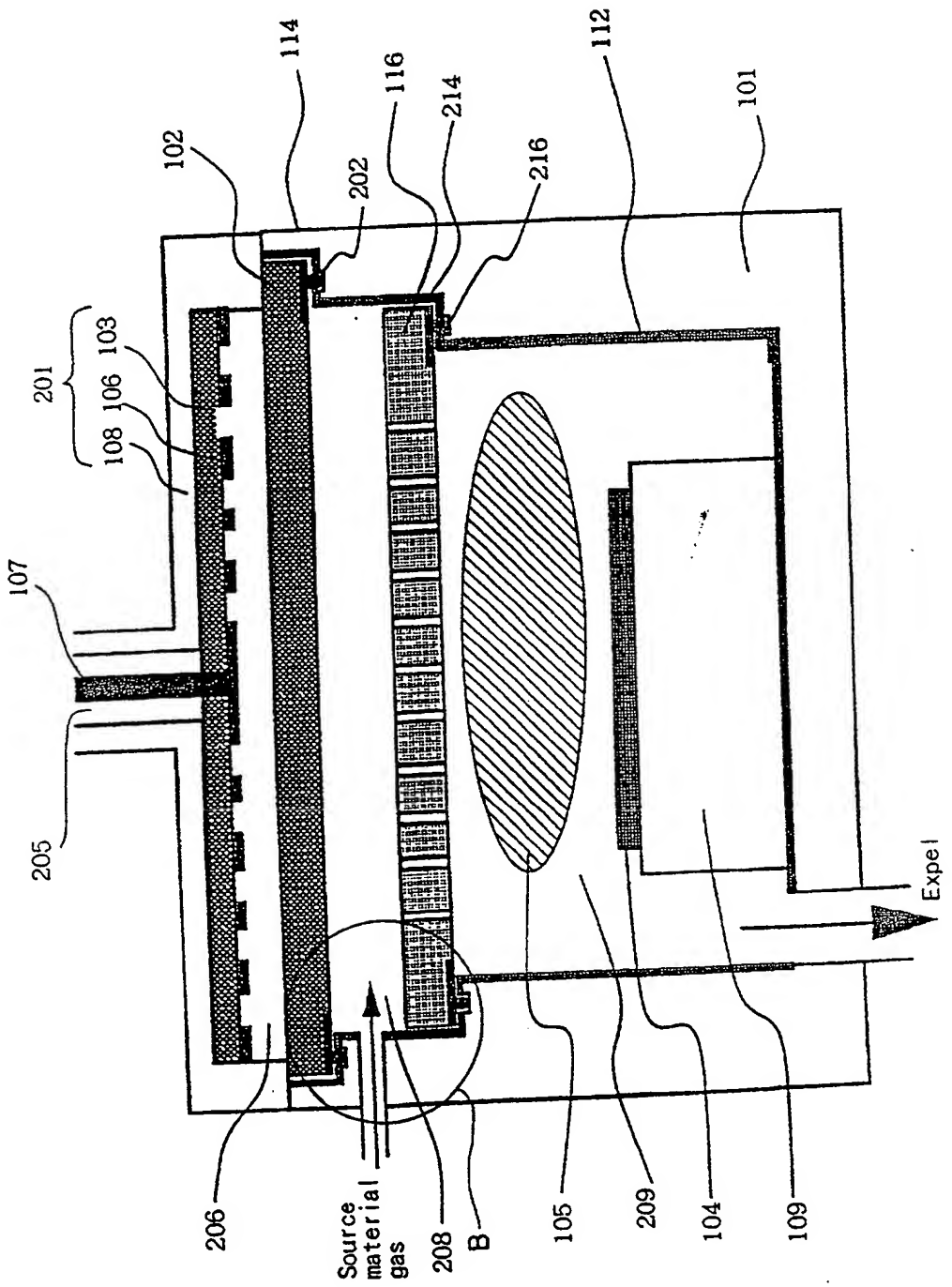
114
116
214
112
101
102
202
216
201
103
106
108
107
205
Expel
206
Source material gas
208
B
105
209
104
109

Fig. 12

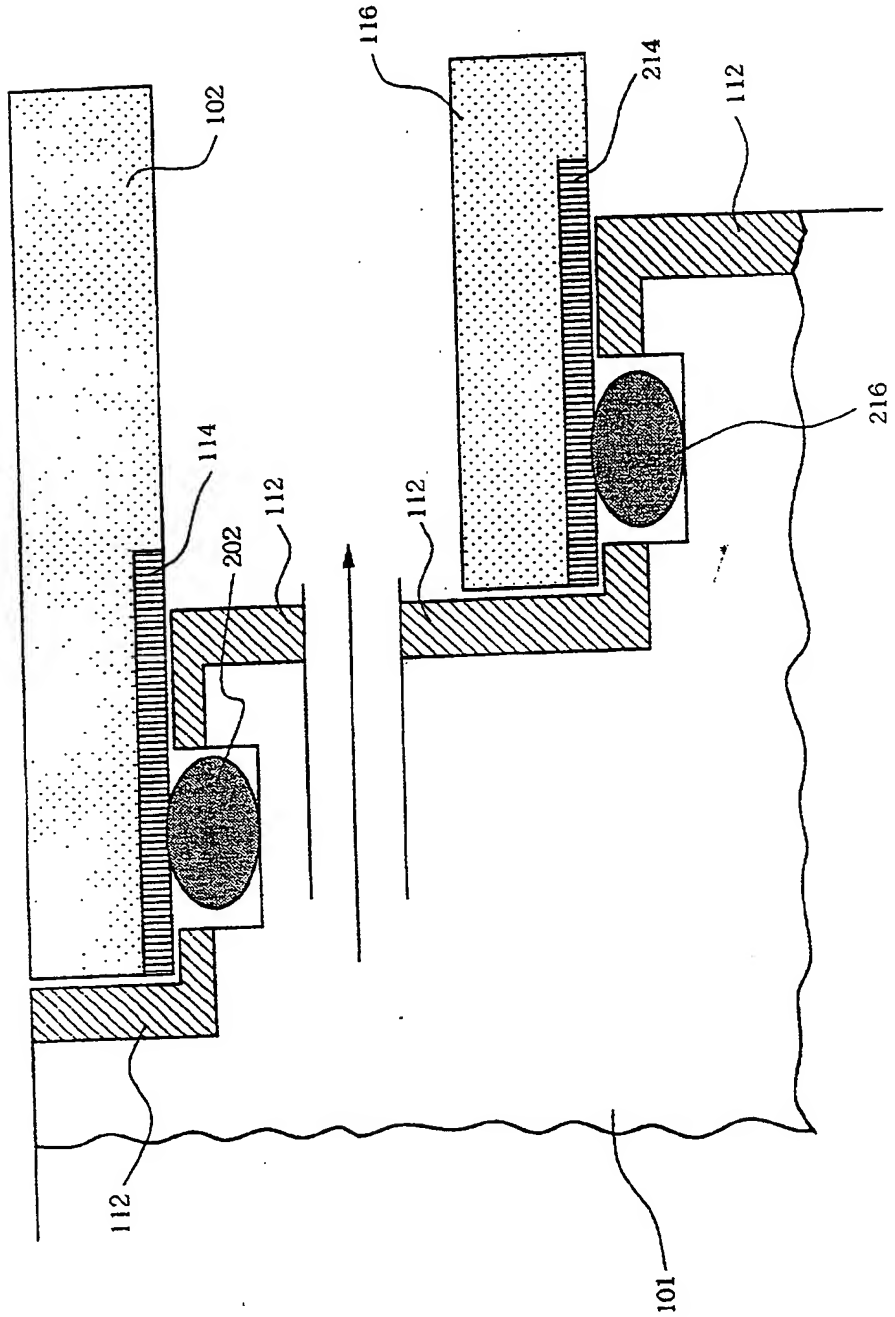

Fig. 13

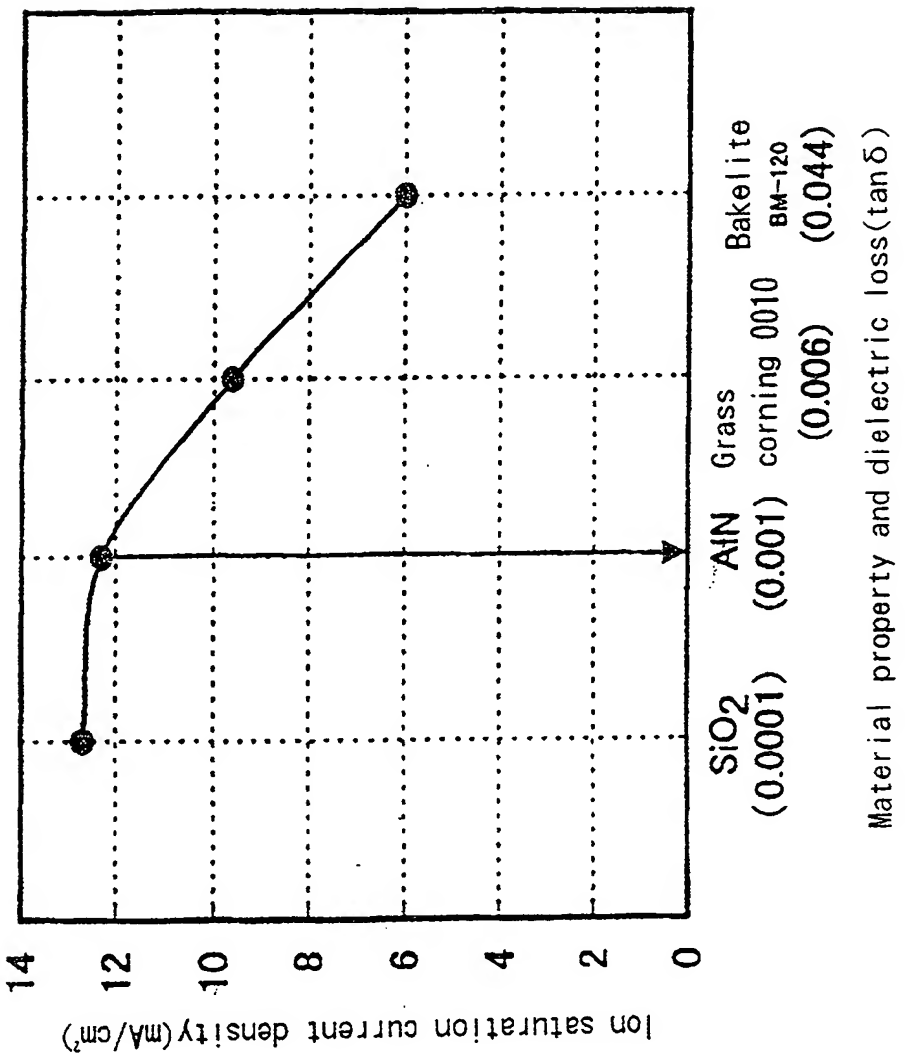
Ion saturation current density(mA/cm²)
14
12
10
8
6
4
2
0
SiO2 (0.0001)
AlN (0.001)
Grass corning 0010 (0.006)
Bakelite BM-120 (0.044)
Material property and dielectric loss(tanδ)

Fig. 14

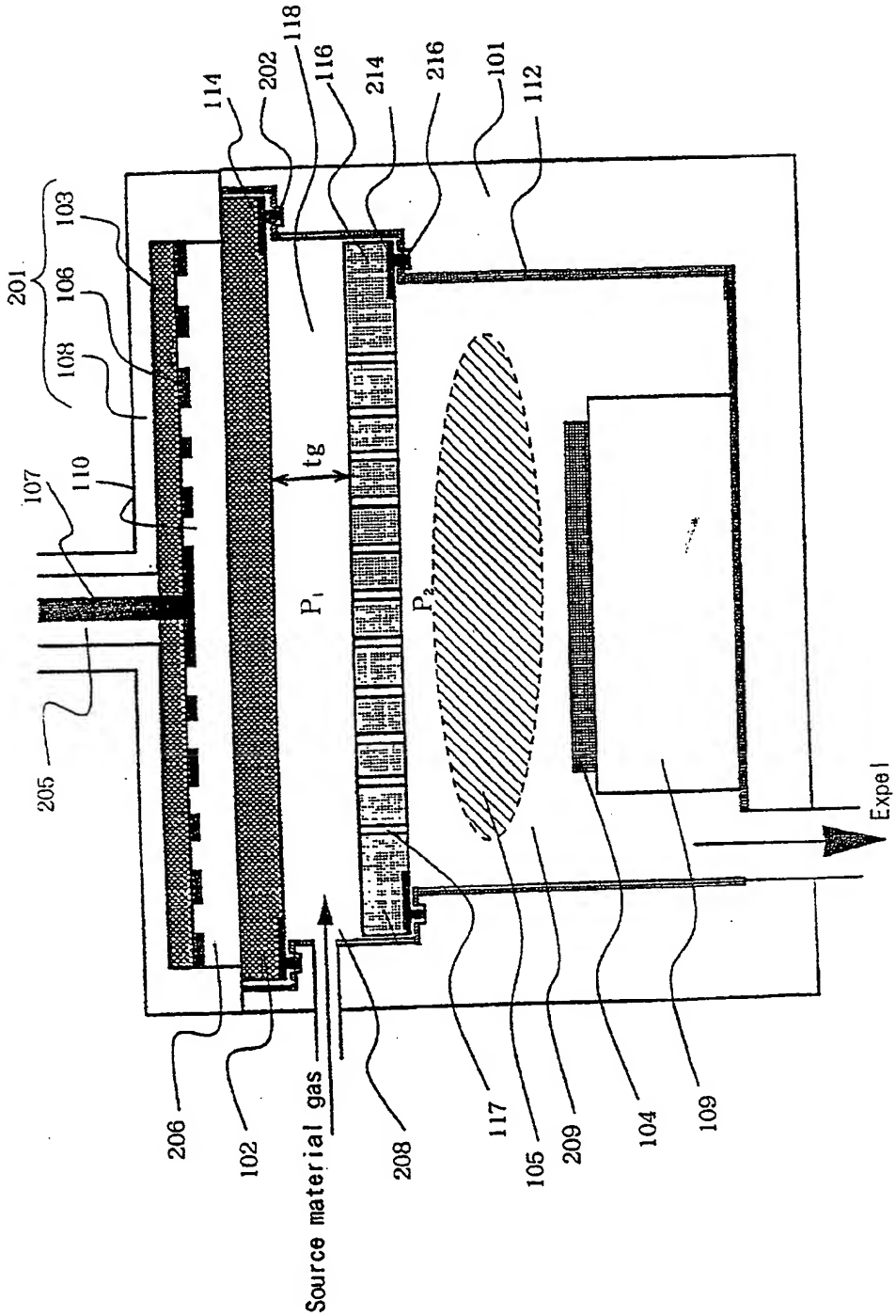
114
202
118
116
214
216
101
112
201
103
106
108
107
110
tg
P1
P2
205
Expel
206
102
Source material gas
208
117
105
209
104
109

Fig. 15

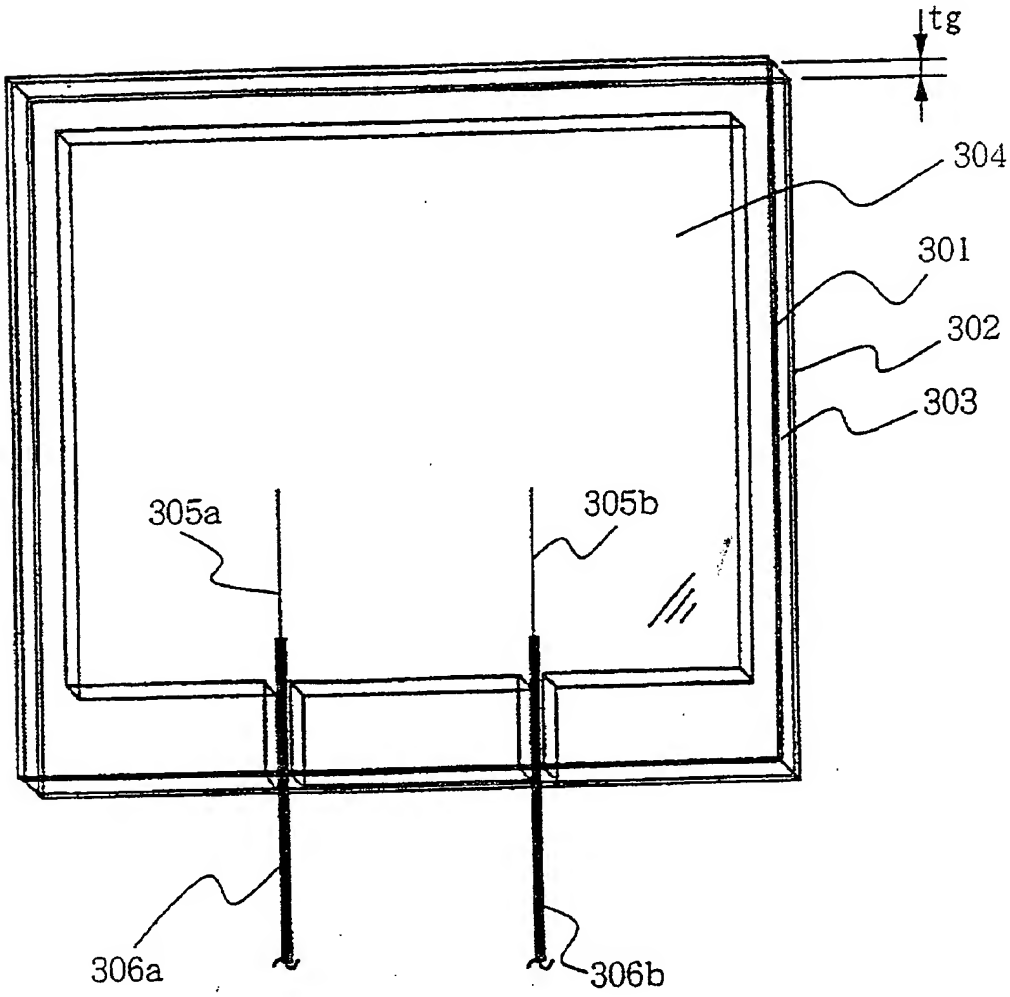

Fig. 16

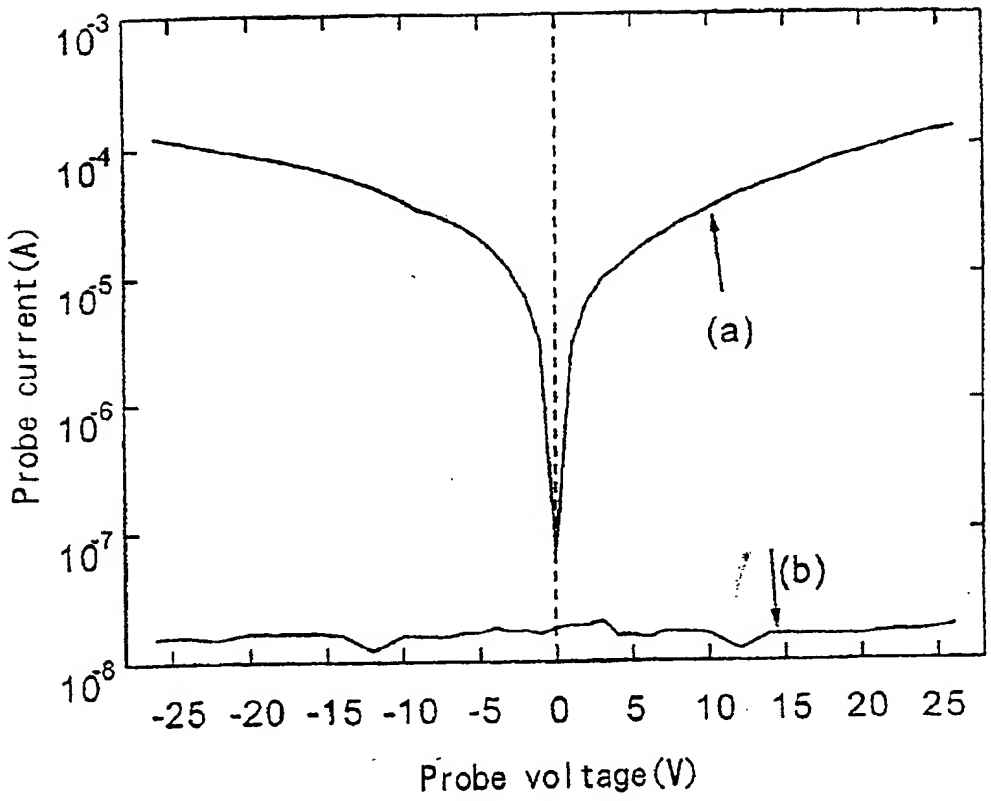
10^{-3}
10^{-4}
10^{-5}
10^{-6}
10^{-7}
10^{-8}
Probe current(A)
(a)
(b)
-25 -20 -15 -10 -5 0 5 10 15 20 25
Probe voltage(V)

Fig. 17

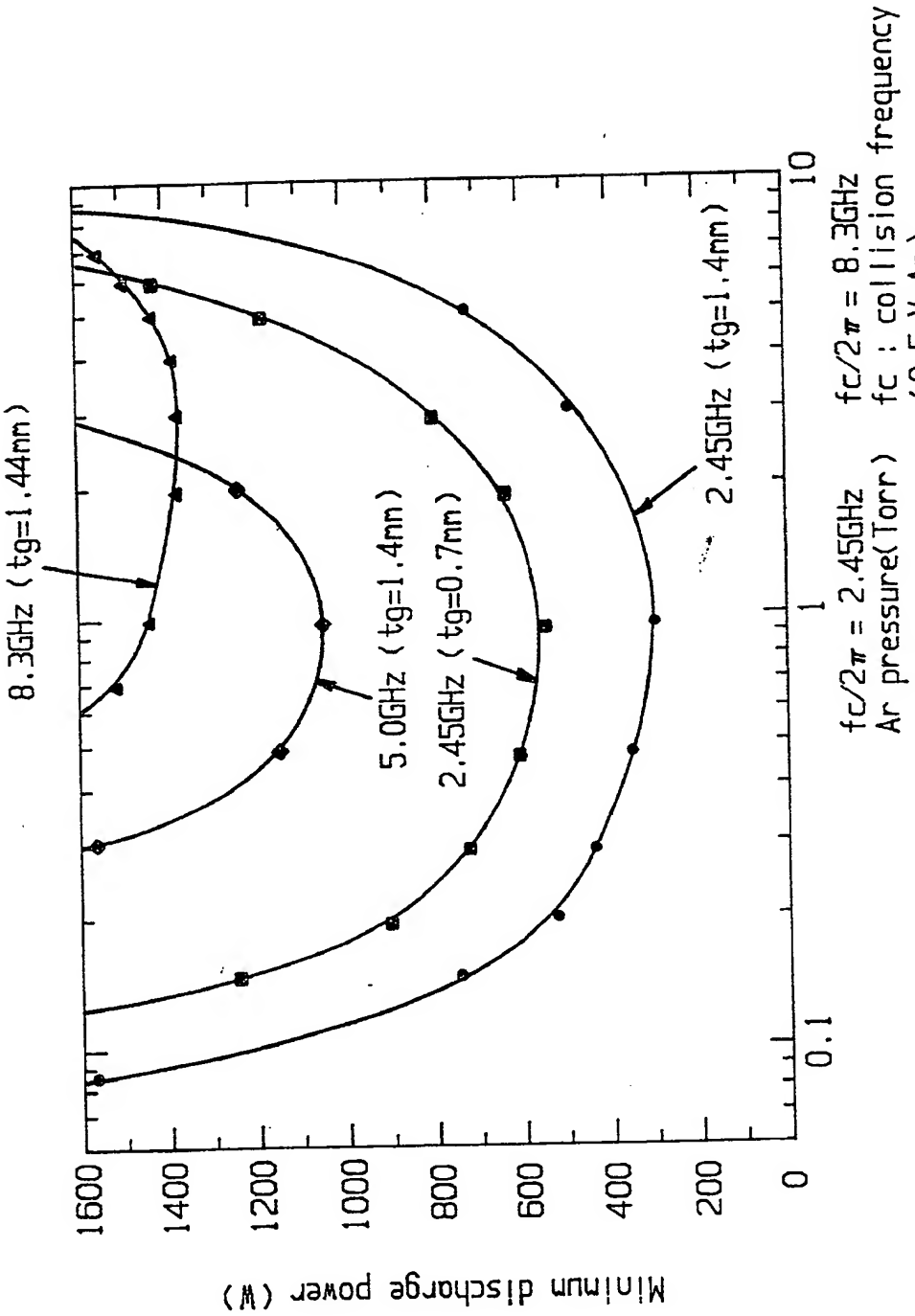
Minimum discharge power (W)
1600
1400
1200
1000
800
600
400
200
0
0.1
1
10
8.3GHz (tg=1.44mm)
5.0GHz (tg=1.4mm)
2.45GHz (tg=0.7mm)
2.45GHz (tg=1.4mm)
fc/2π = 2.45GHz
Ar pressure(Torr)
fc/2π = 8.3GHz
fc : collision frequency
(0.5eV,Ar)

Fig. 18

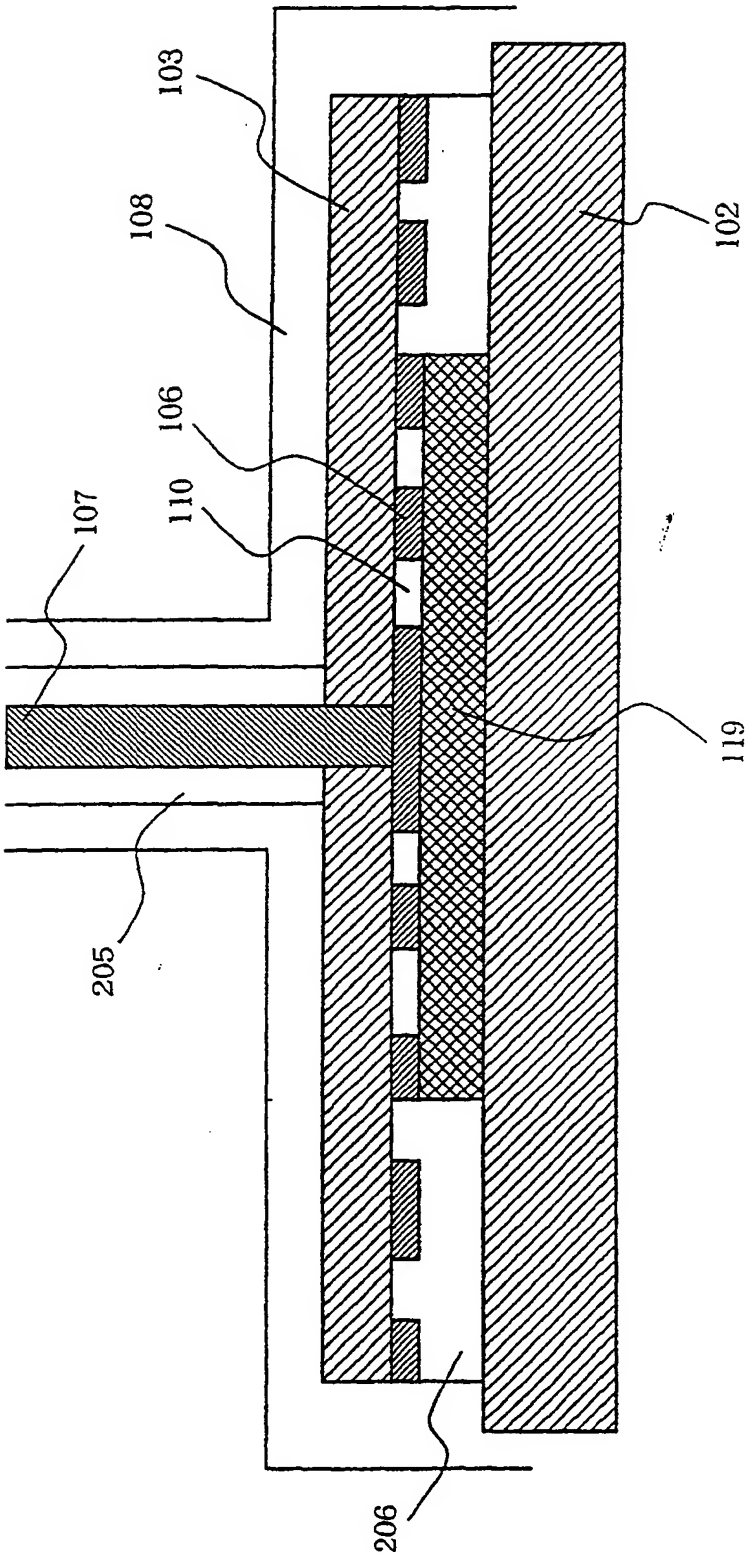

Fig. 19

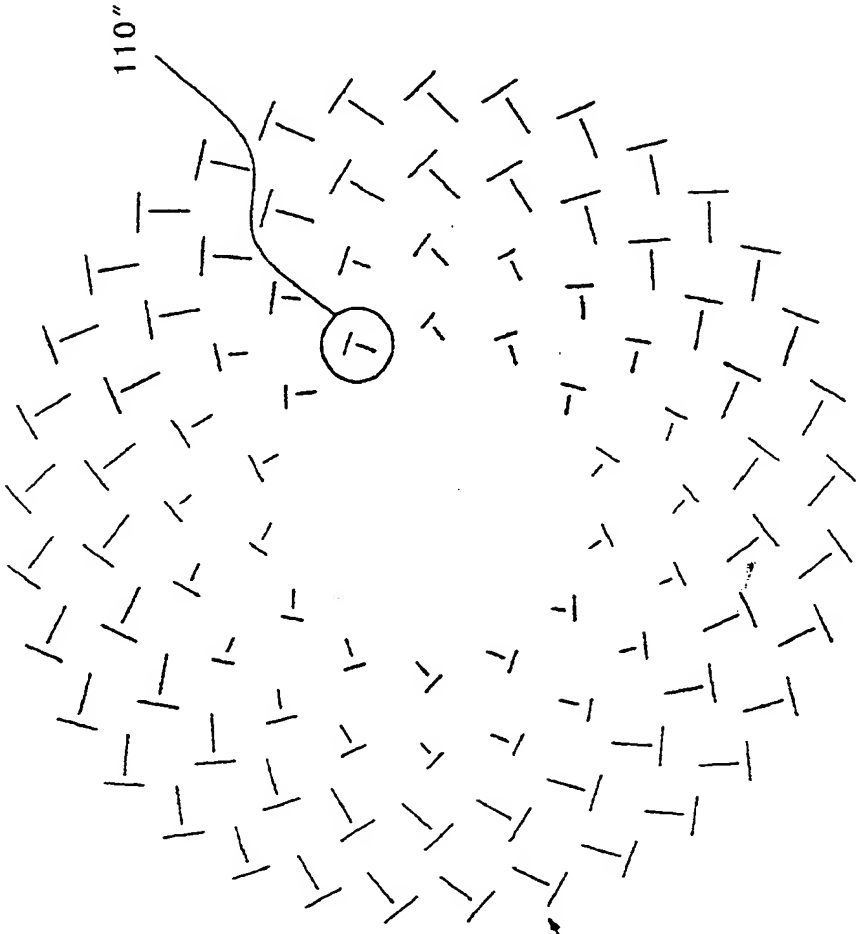

Fig. 20B

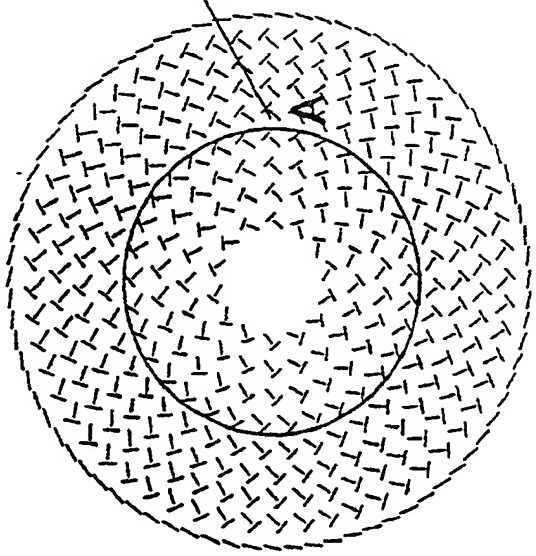

Fig. 20A

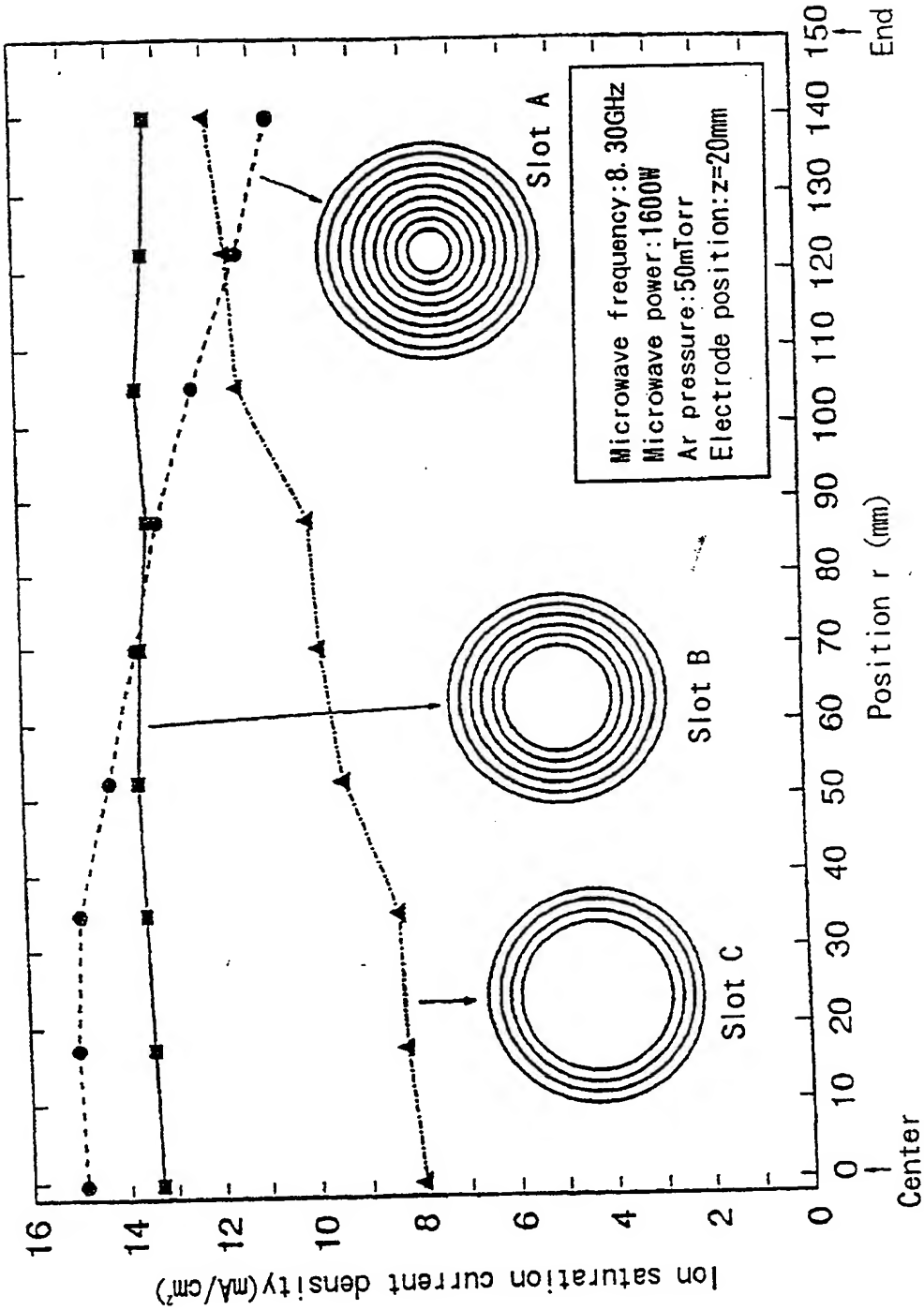
Ion saturation current density(mA/cm²)
16
14
12
10
8
6
4
2
0
Center
0
10
20
30
40
50
60
70
80
90
100
110
120
130
140
150
End
Position r (mm)
Microwave frequency:8.30GHz
Microwave power:1600W
Ar pressure:50mTorr
Electrode position:z=20mm
Slot A
Slot B
Slot C

Fig. 21

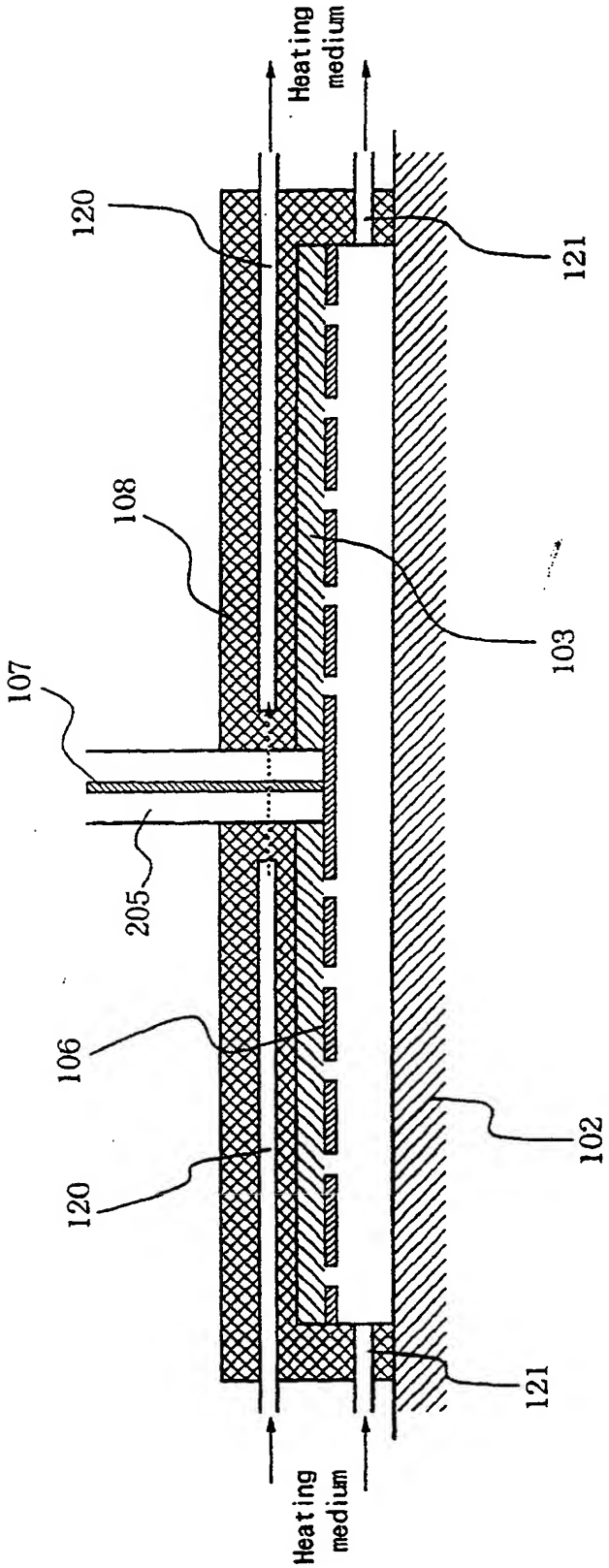
Heating medium
120
121
108
103
107
205
106
102
120
121
Heating medium

Fig. 22

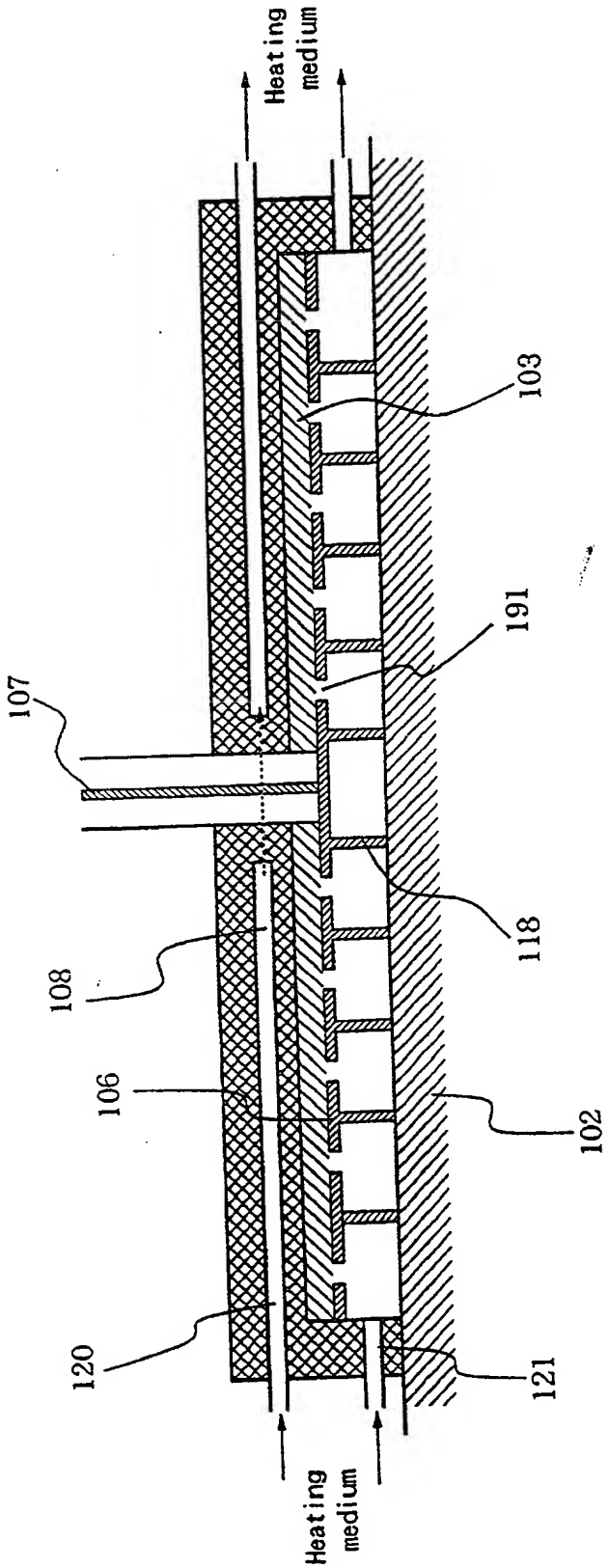
Heating medium
103
191
107
118
108
106
102
120
121
Heating medium

Fig. 23

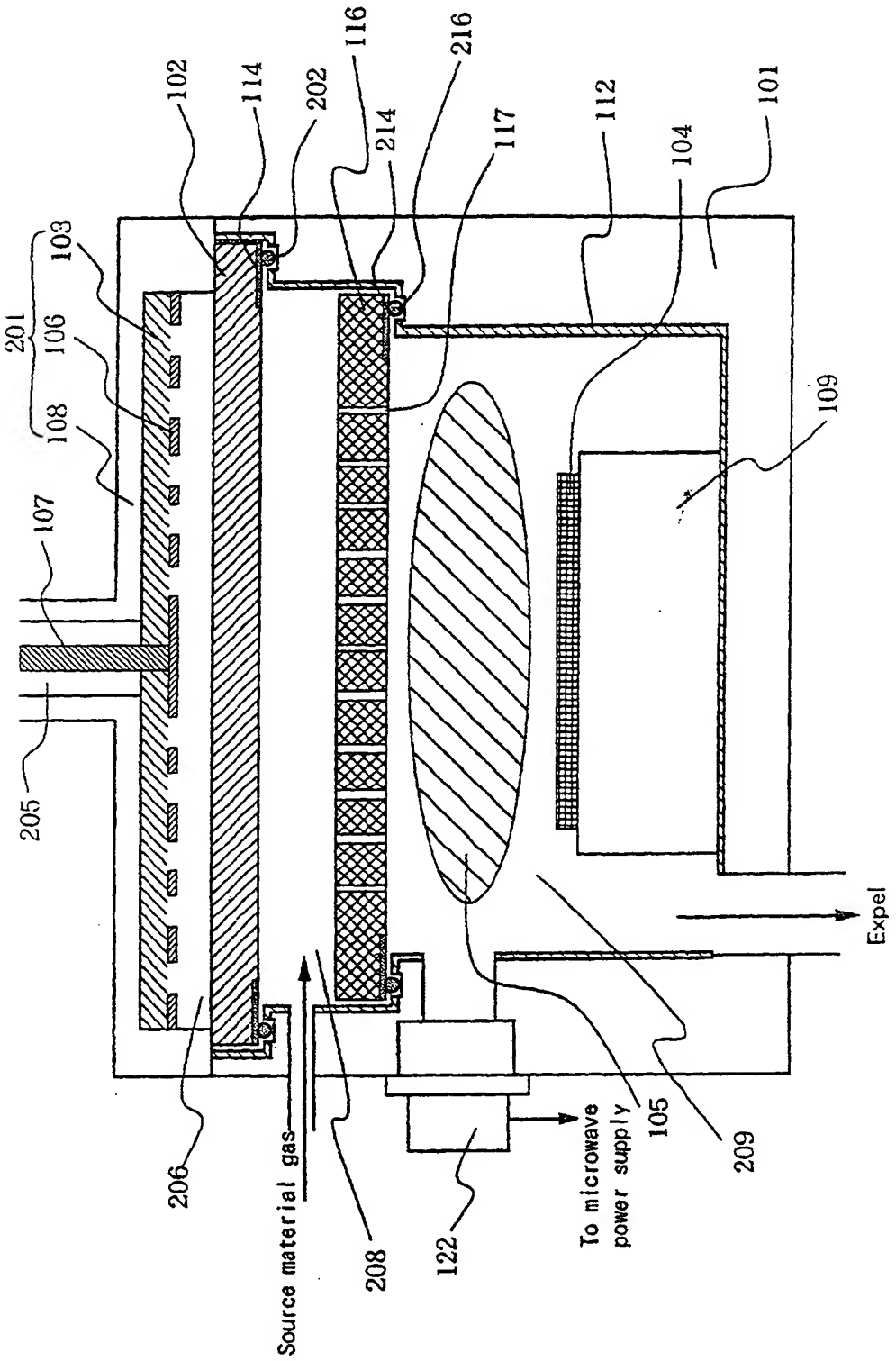
102
114
202
116
214
216
117
112
104
101
103
201
106
108
107
205
109
206
Source material gas
208
122
To microwave power supply
105
209
Expel

Fig. 24

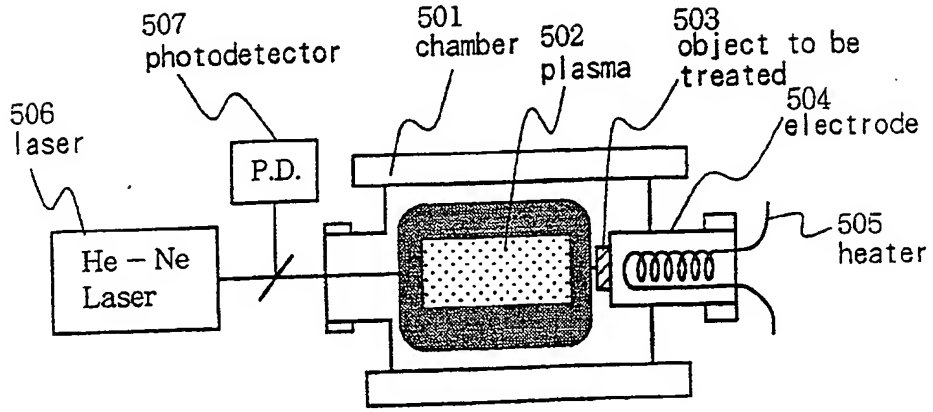
507
photodetector
501
chamber
502
plasma
503
object to be
treated
504
electrode
506
laser
P.D.
505
heater
He – Ne
Laser

Fig. 25

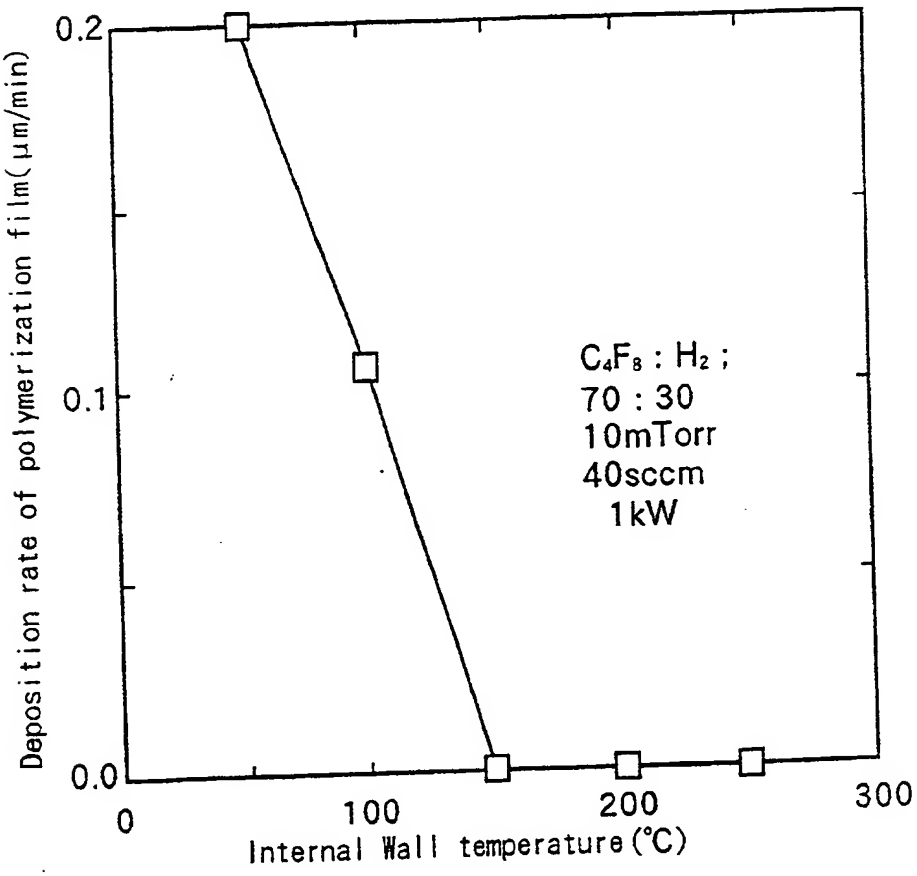
0.2
0.1
0.0
0
100
200
300
Deposition rate of polymerization film(μm/min)
Internal Wall temperature(℃)
C4F8 : H2 ;
70 : 30
10mTorr
40sccm
1kW

Fig. 26

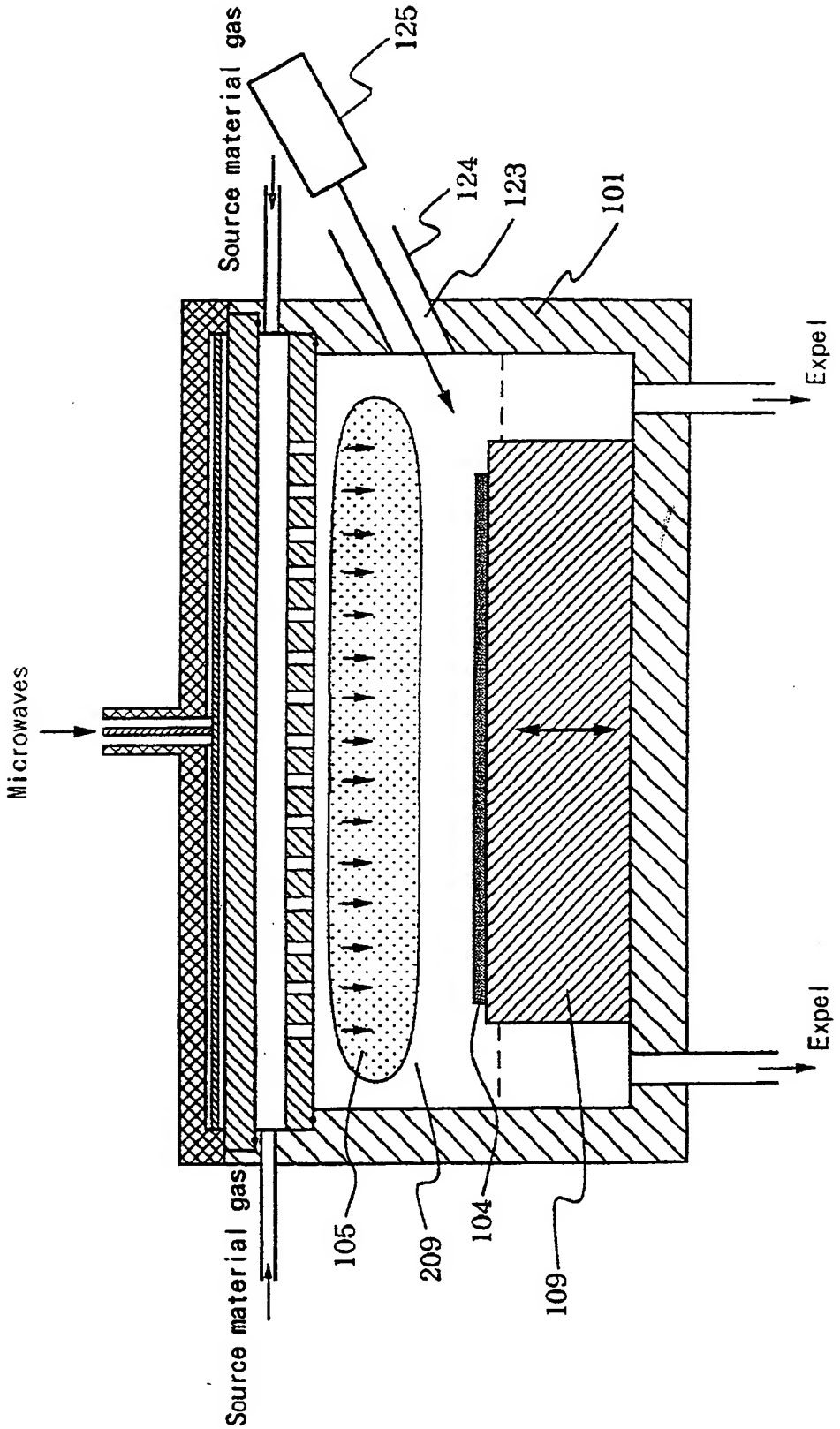
Source material gas
125
124
123
101
Expel
Microwaves
Expel
Source material gas
105
209
104
109

Fig. 27

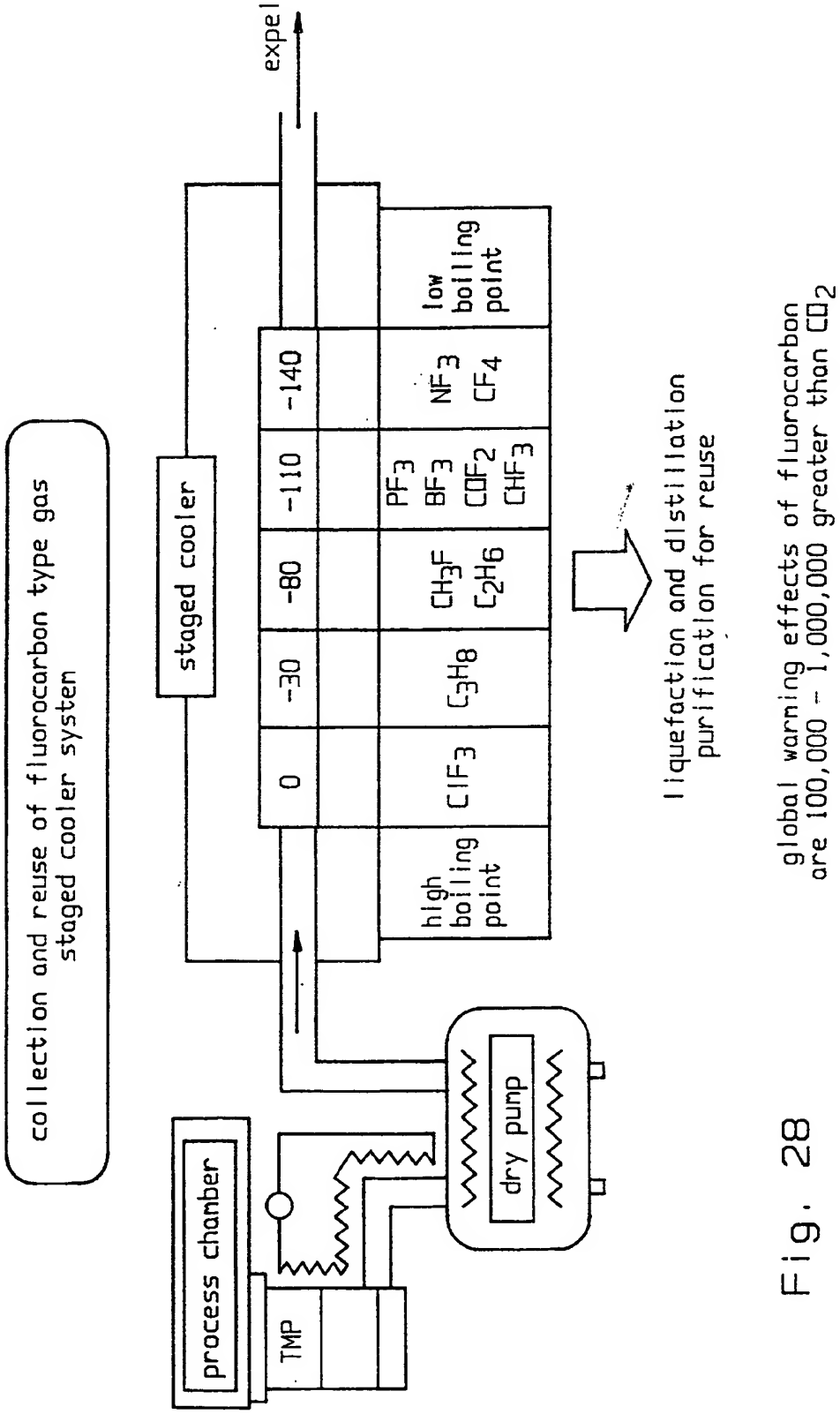

Fig. 28

global warming effects of fluorocarbon are 100,000 - 1,000,000 greater than CO_2

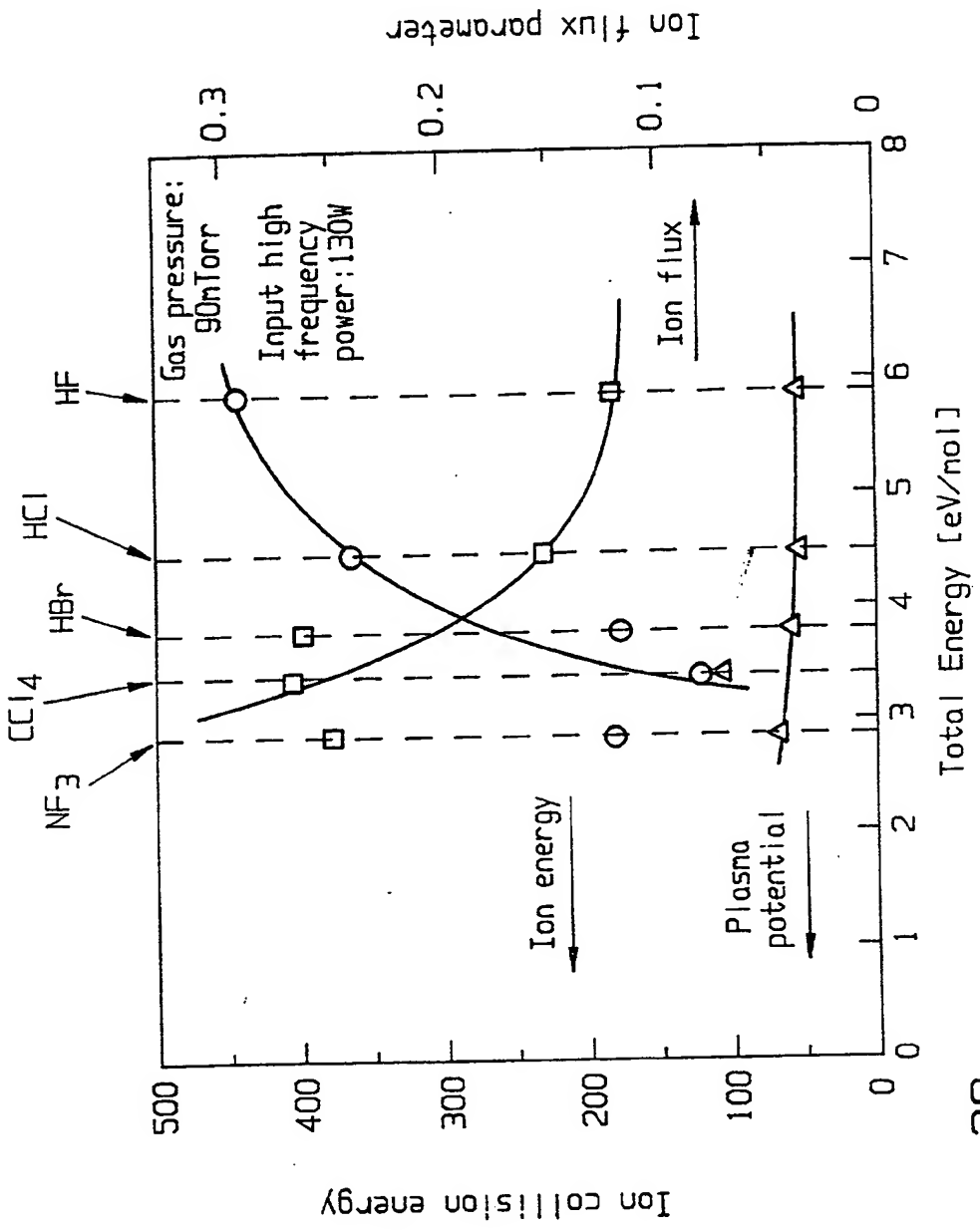
Ion flux parameter
0.3
0.2
0.1
0
Gas pressure: 90mTorr
Input high frequency power:130W
Ion flux
HF
HCl
HBr
CCl4
NF3
Ion energy
Plasma potential
Ion collision energy
500
400
300
200
100
0
0
1
2
3
4
5
6
7
8
Total Energy [eV/mol]

Fig. 29

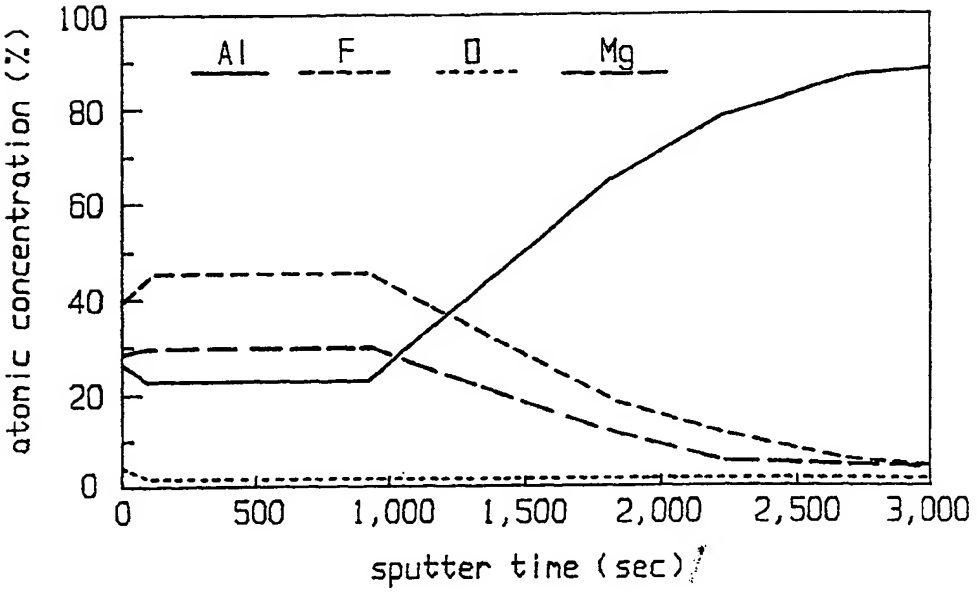

Fig. 30A

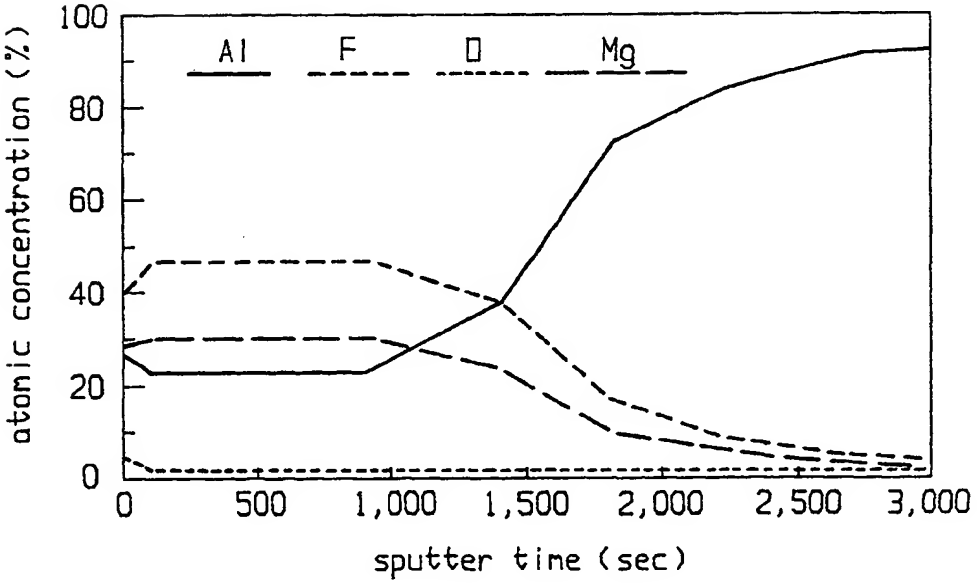

Fig. 30B

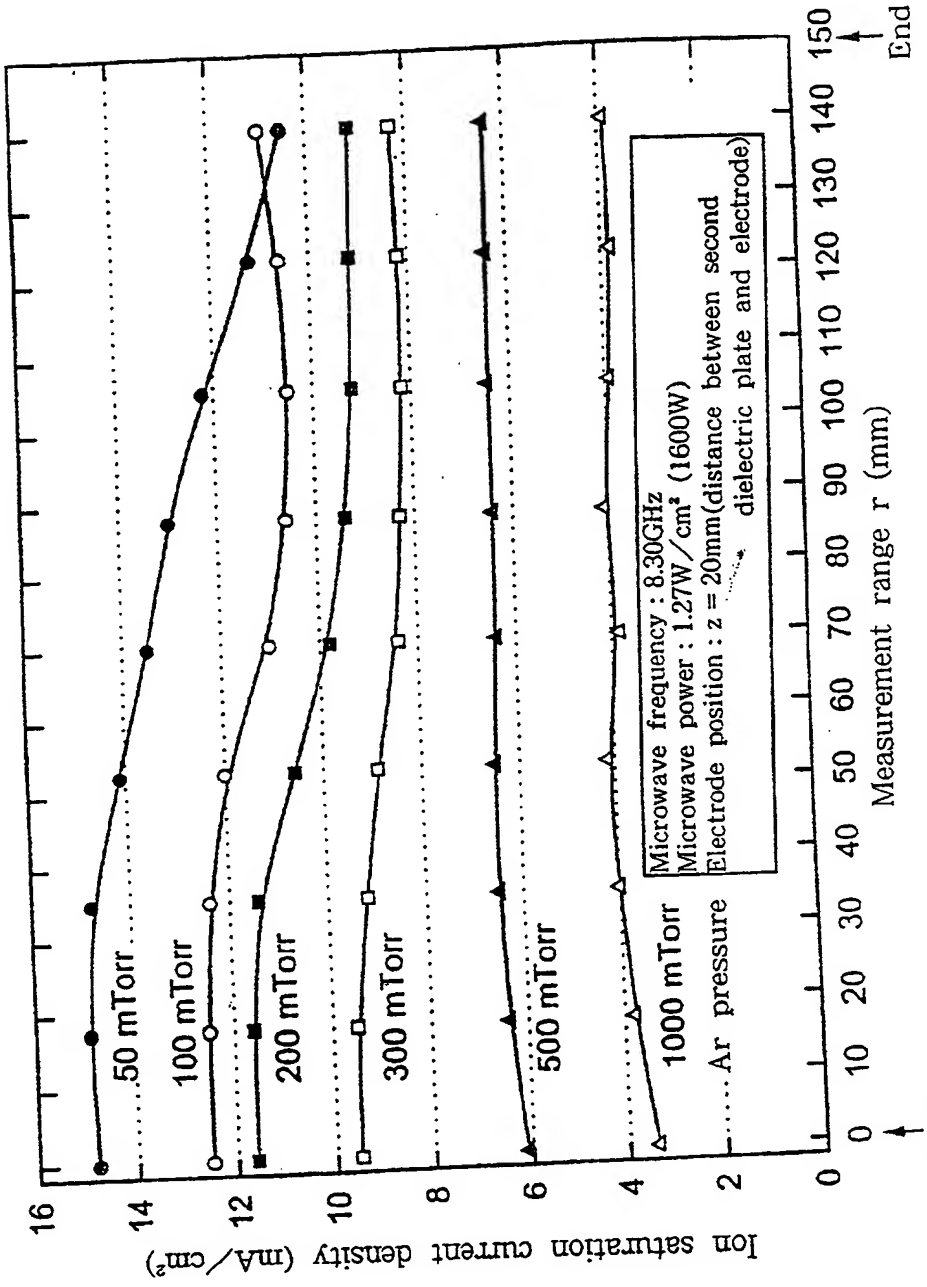
Ion saturation current density (mA/cm²)
16
14
12
10
8
6
4
2
0
0 10 20 30 40 50 60 70 80 90 100 110 120 130 140 150
Center
End
Measurement range r (mm)
50 mTorr
100 mTorr
200 mTorr
300 mTorr
500 mTorr
1000 mTorr
Ar pressure
Microwave frequency : 8.30GHz
Microwave power : 1.27W/cm² (1600W)
Electrode position : z = 20mm(distance between second dielectric plate and electrode)

Fig. 31

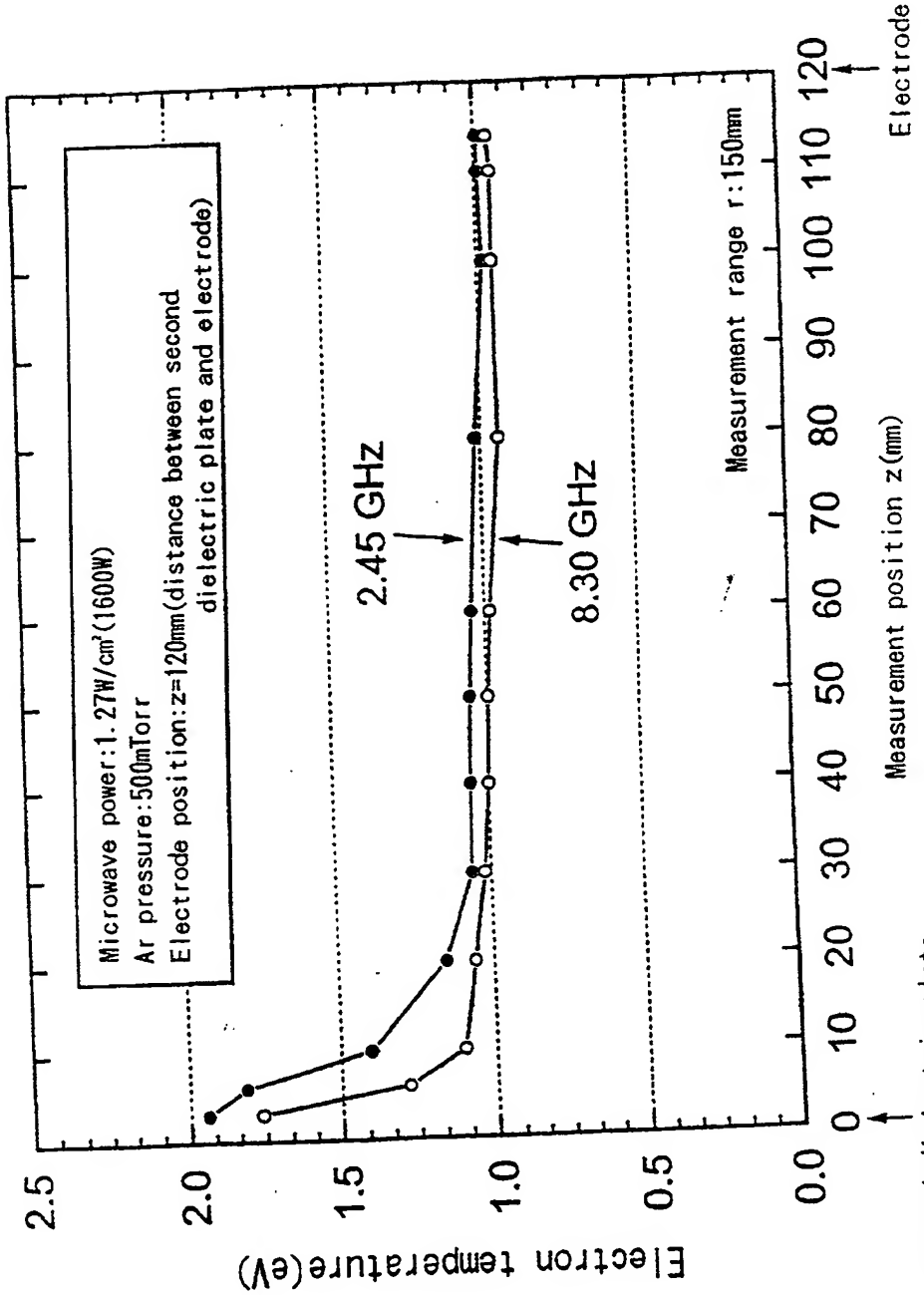
Microwave power:1.27W/cm²(1600W)
Ar pressure:500mTorr
Electrode position:z=120mm(distance between second dielectric plate and electrode)
2.45 GHz
8.30 GHz
Measurement range r:150mm
Electron temperature(eV)
Measurement position z(mm)
Second dielectric plate
Electrode
2.5
2.0
1.5
1.0
0.5
0.0
0
10
20
30
40
50
60
70
80
90
100
110
120

Fig. 32

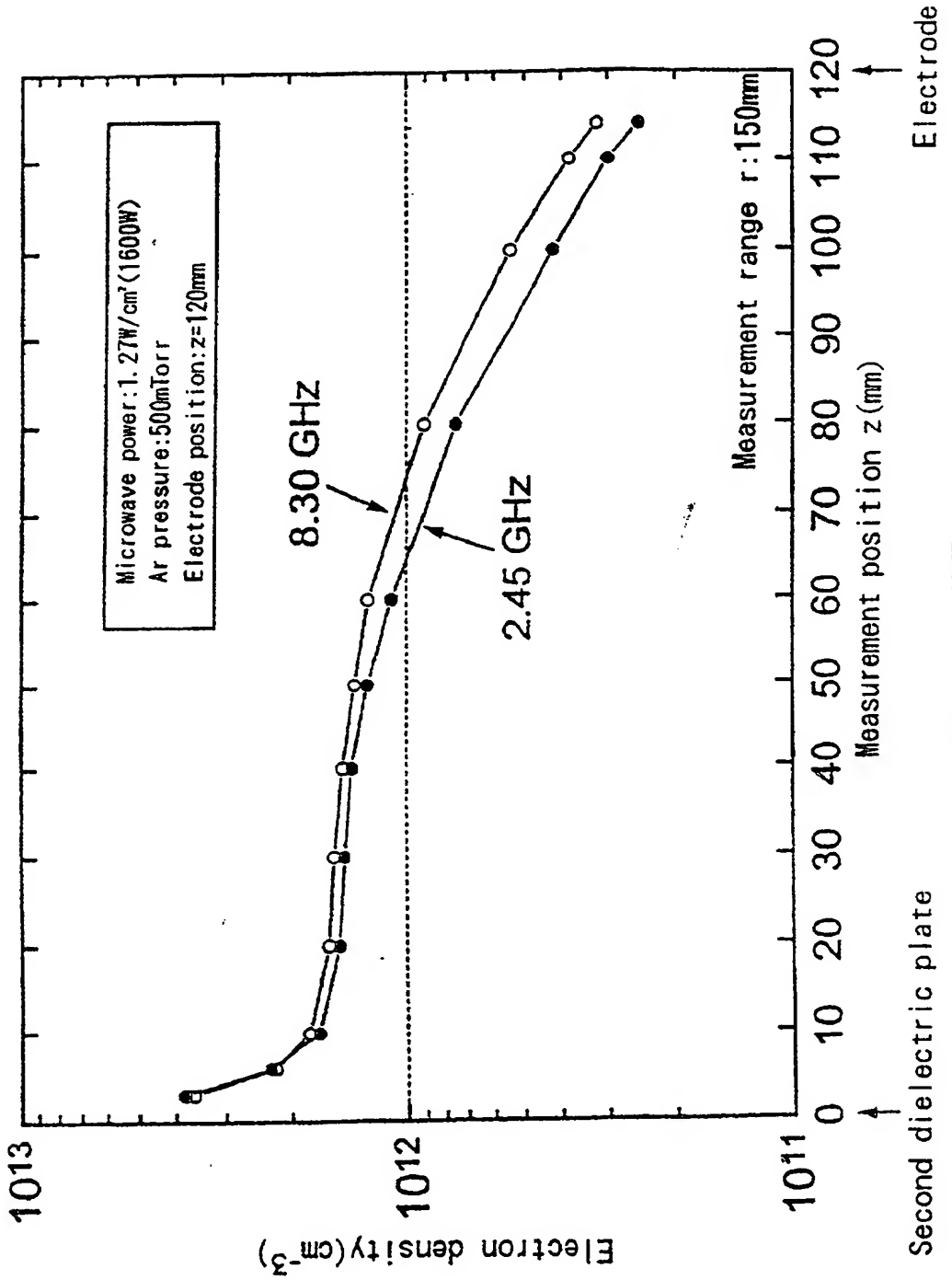
Microwave power:1.27W/cm²(1600W)
Ar pressure:500mTorr
Electrode position:z=120mm
8.30 GHz
2.45 GHz
Measurement range r:150mm
Electron density(cm⁻³)
10¹³
10¹²
10¹¹
0 10 20 30 40 50 60 70 80 90 100 110 120
Measurement position z(mm)
Second dielectric plate
Electrode

Fig. 33

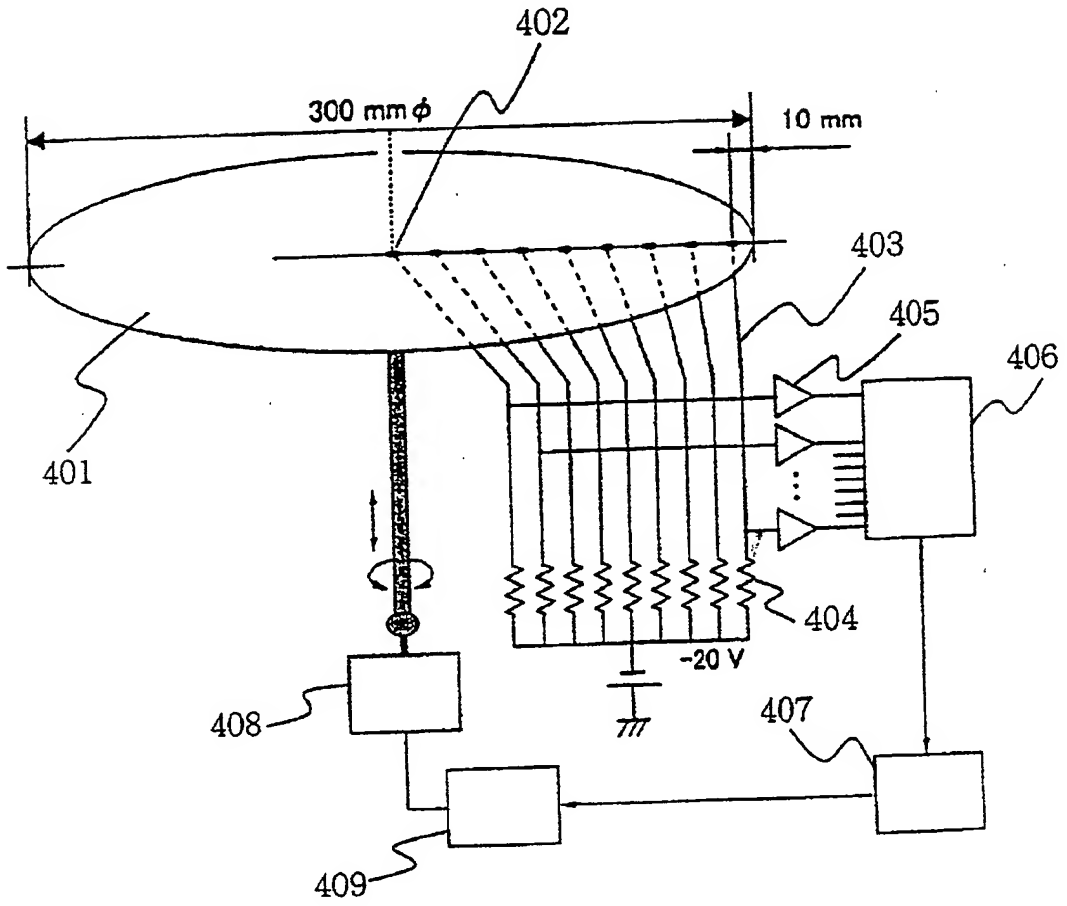

Fig. 34

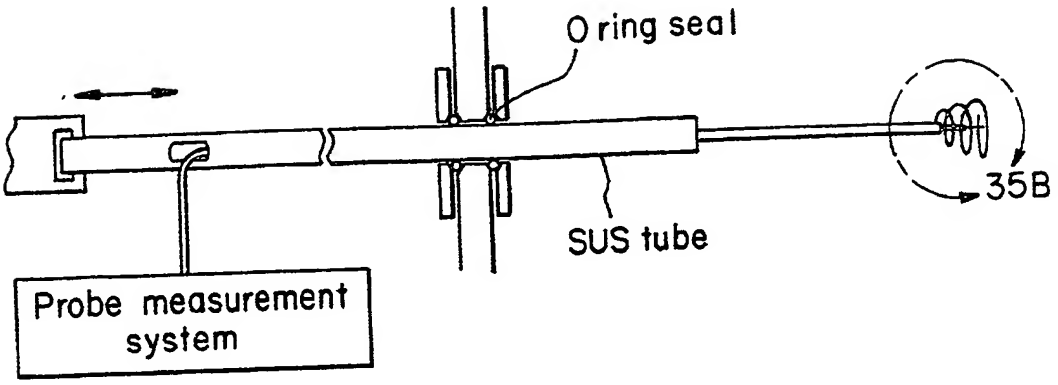

Fig. 35A

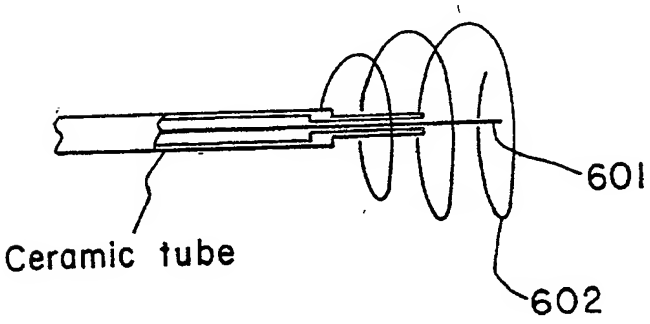

Fig. 35B

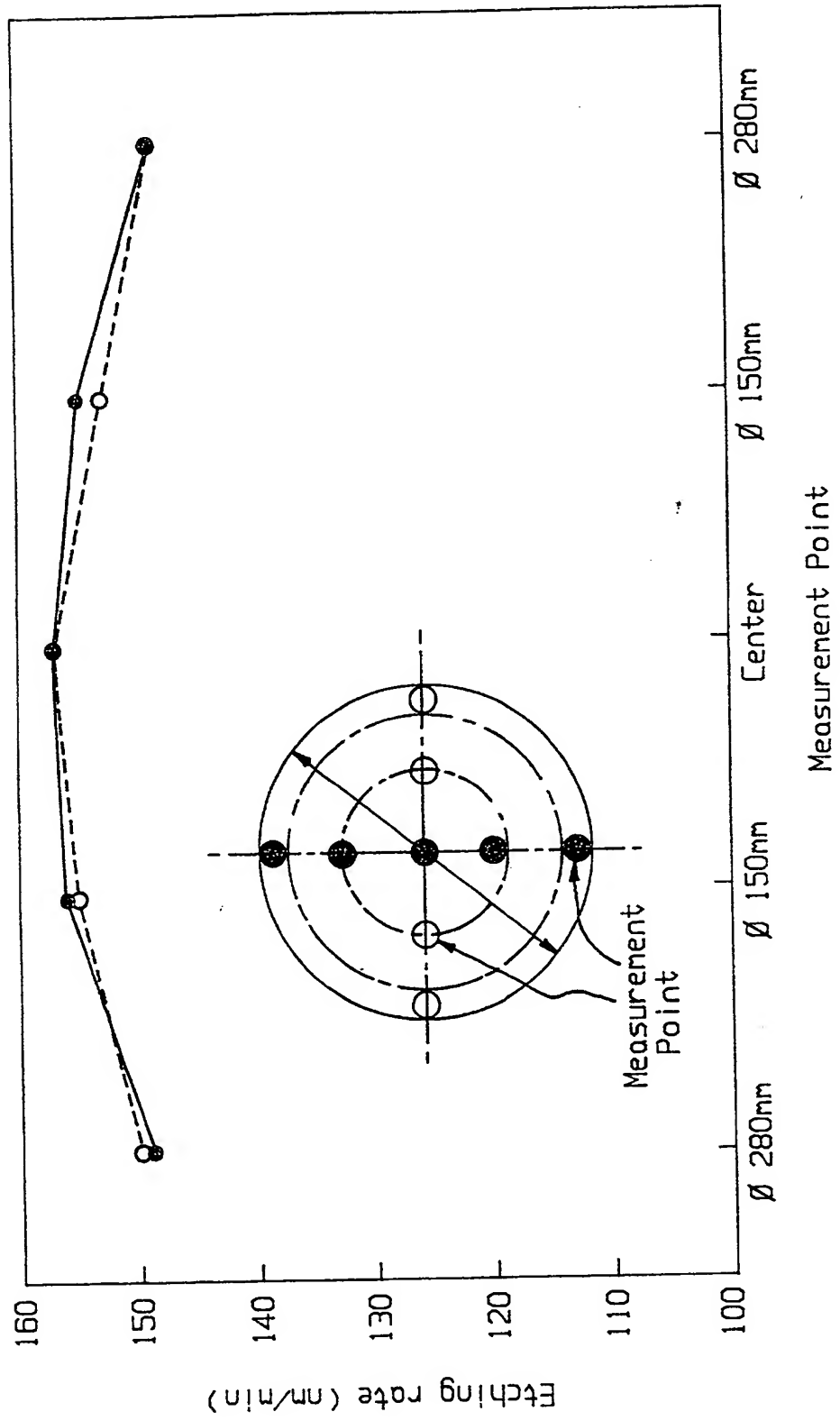
Etching rate (nm/min)
160
150
140
130
120
110
100
Ø 280mm
Ø 150mm
Center
Ø 150mm
Ø 280mm
Measurement Point
Measurement Point

Fig. 36

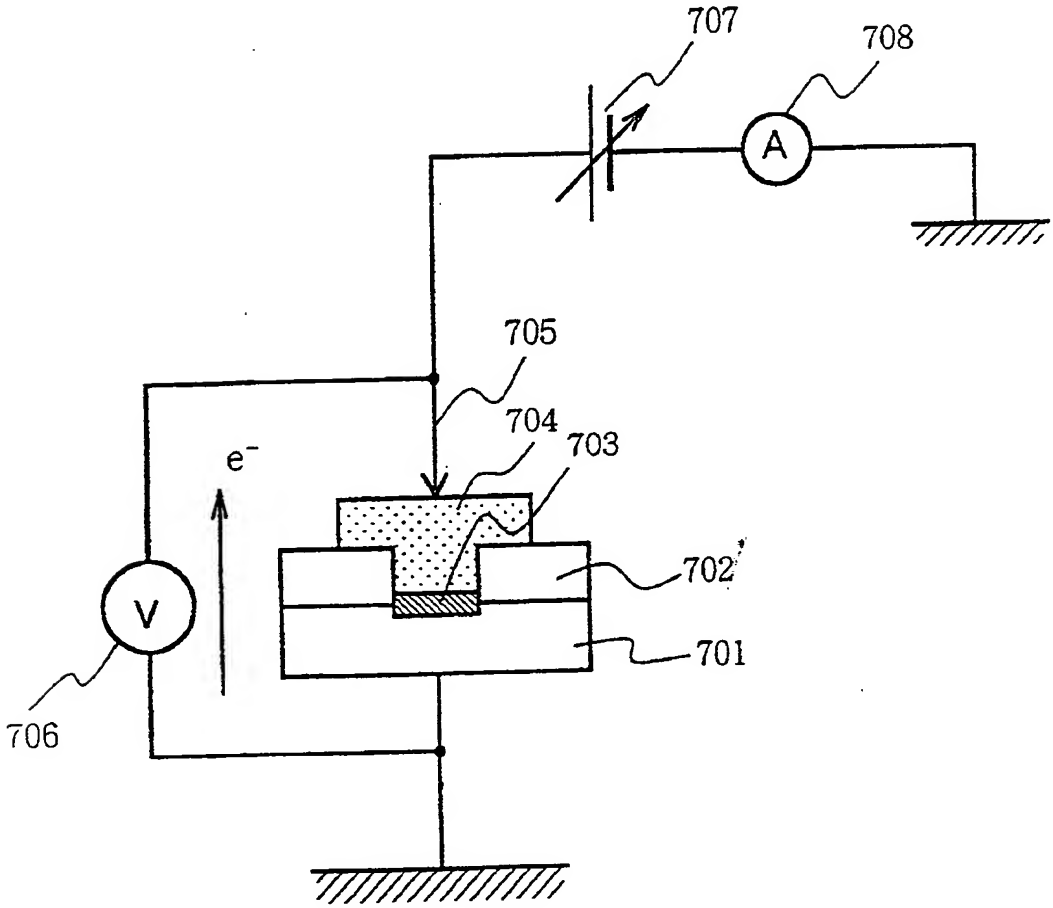

Fig. 37

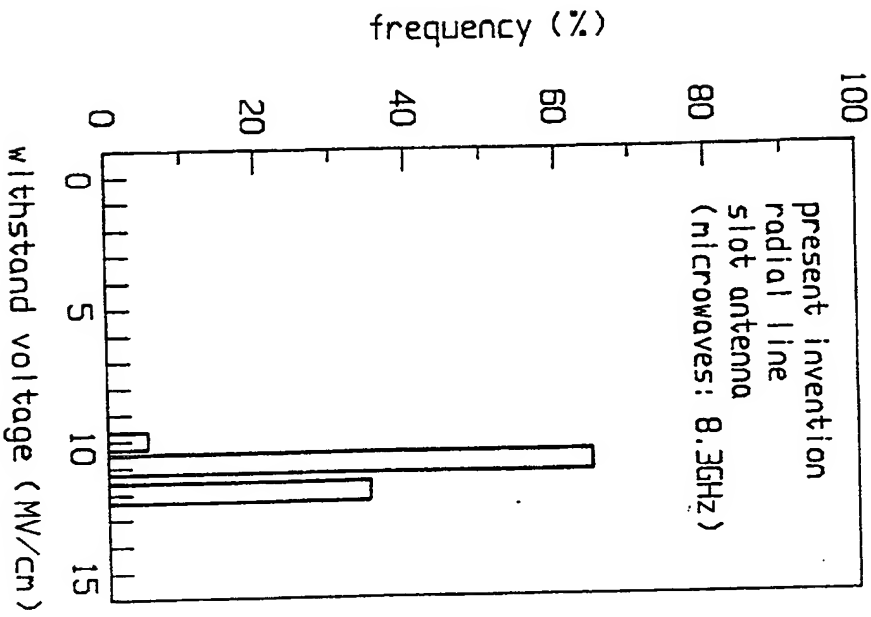

Fig. 38A

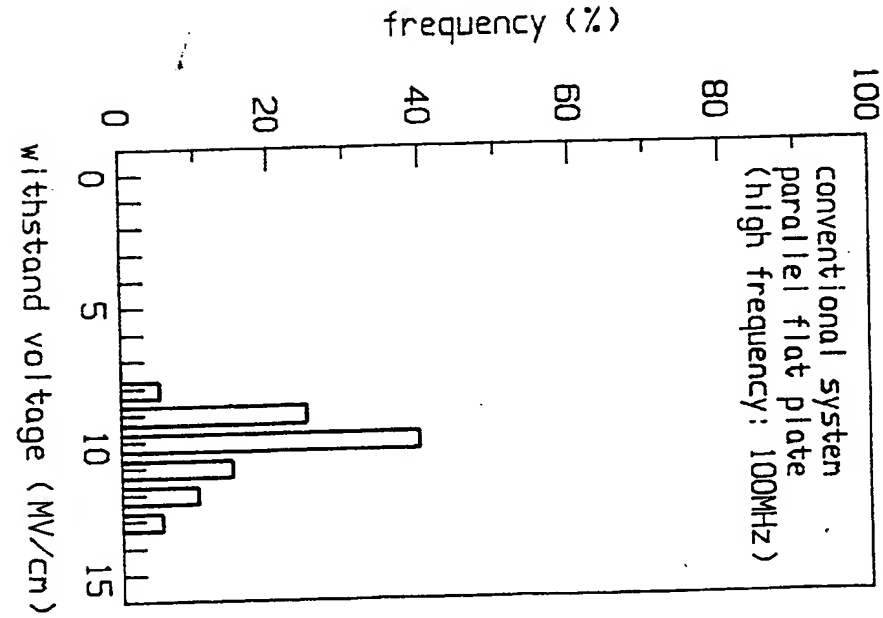

Fig. 38B

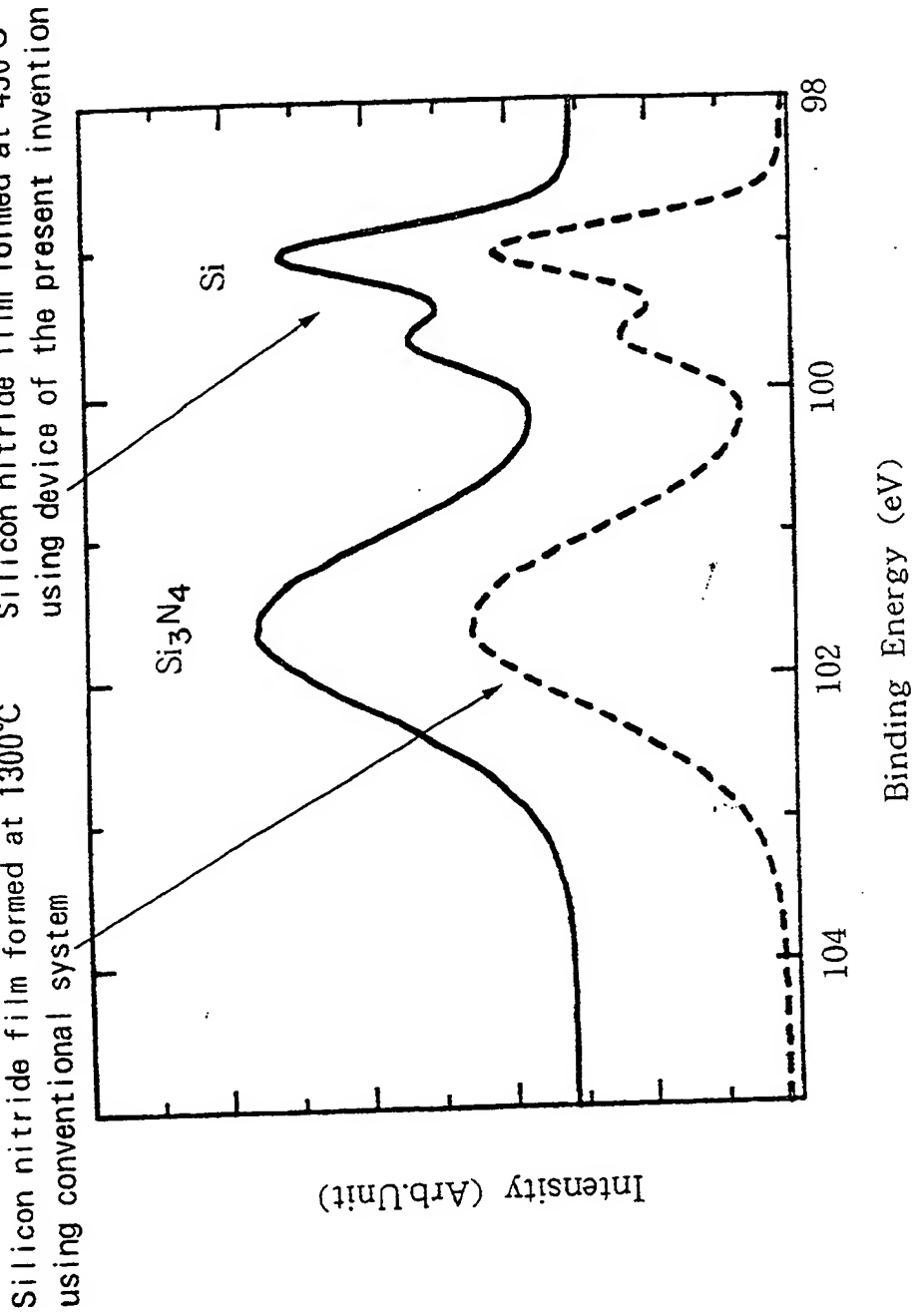
Silicon nitride film formed at 450°C
using device of the present invention
Silicon nitride film formed at 1300°C
using conventional system
Si
Si_3N_4
Intensity (Arb.Unit)
98
100
102
104
Binding Energy (eV)

Fig. 39

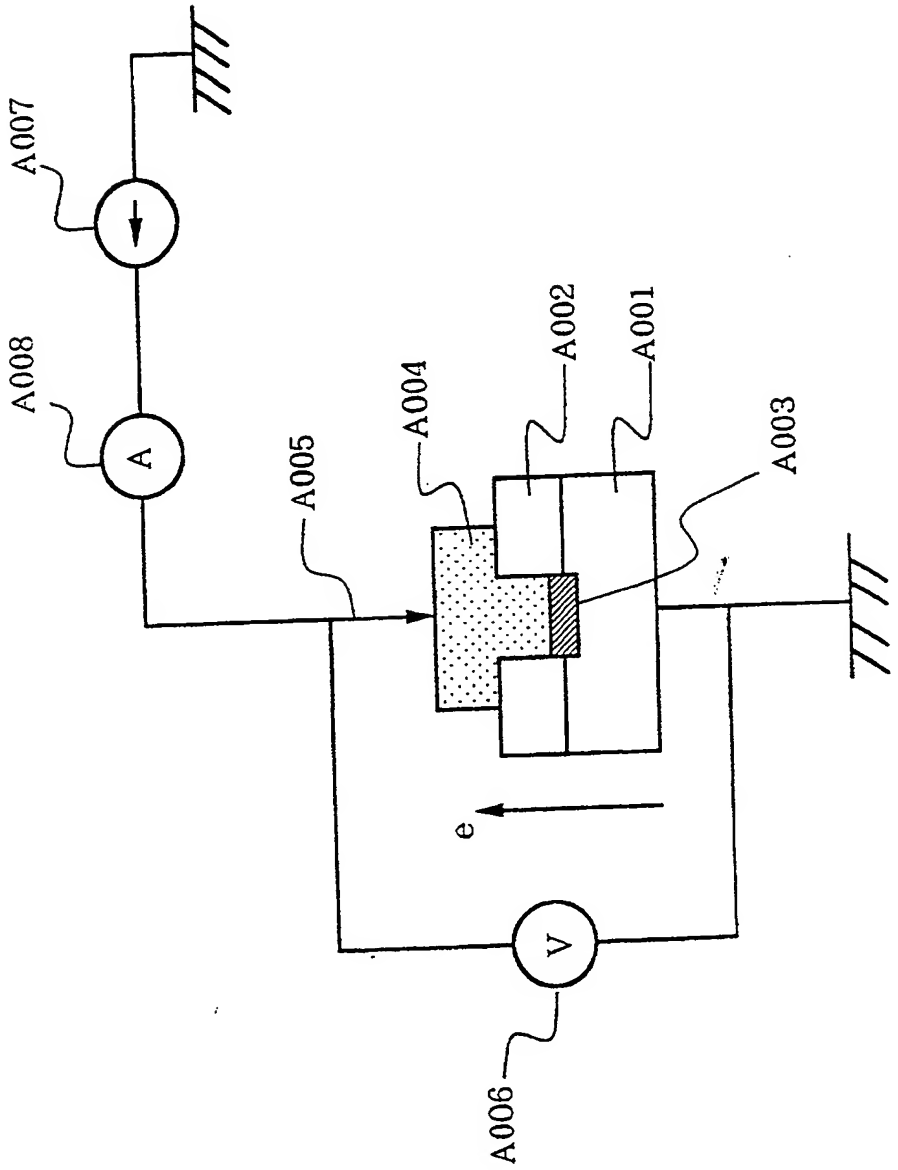

Fig. 40

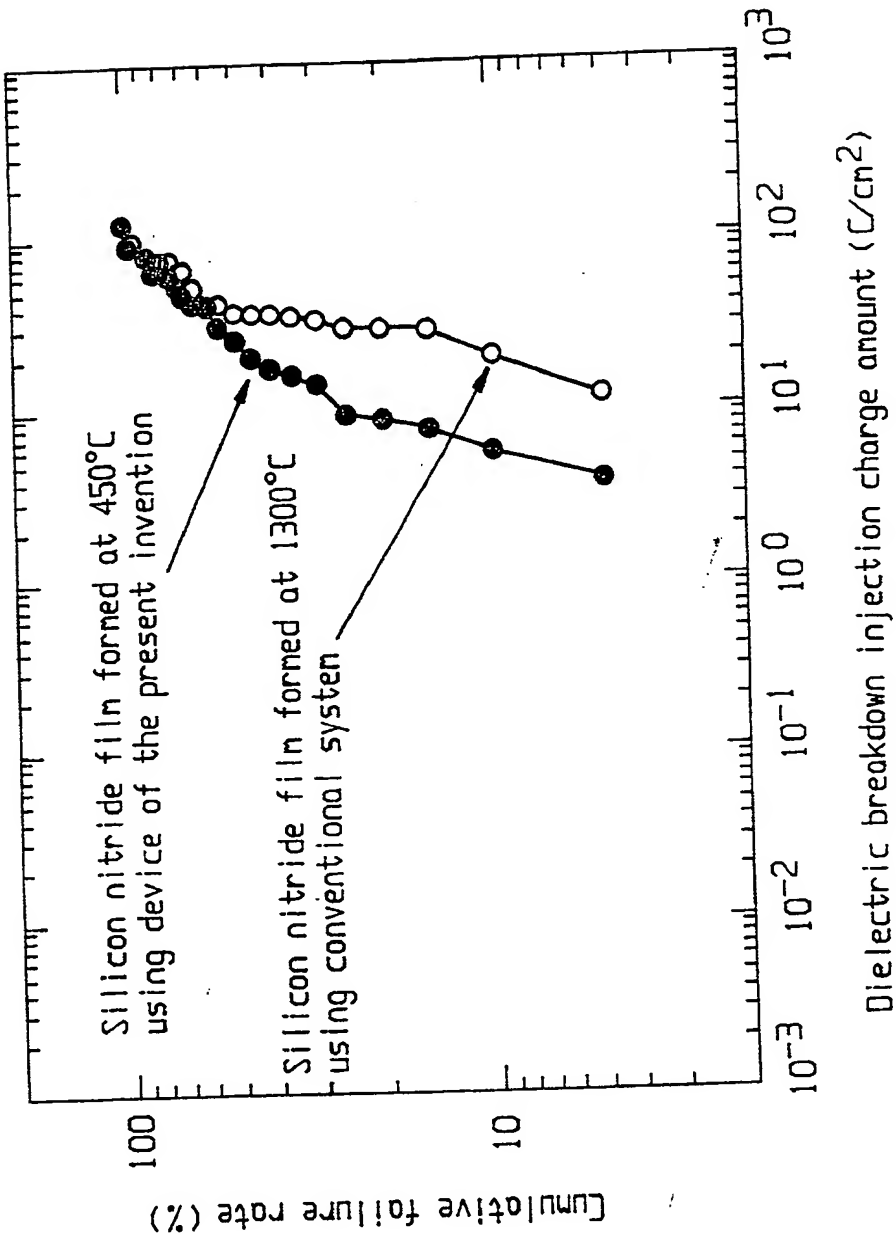
Silicon nitride film formed at 450°C
using device of the present invention
Silicon nitride film formed at 1300°C
using conventional system
Cumulative failure rate (%)
100
10
10^{-3}
10^{-2}
10^{-1}
10^{0}
10^{1}
10^{2}
10^{3}
Dielectric breakdown injection charge amount (C/cm^2)

Fig. 41

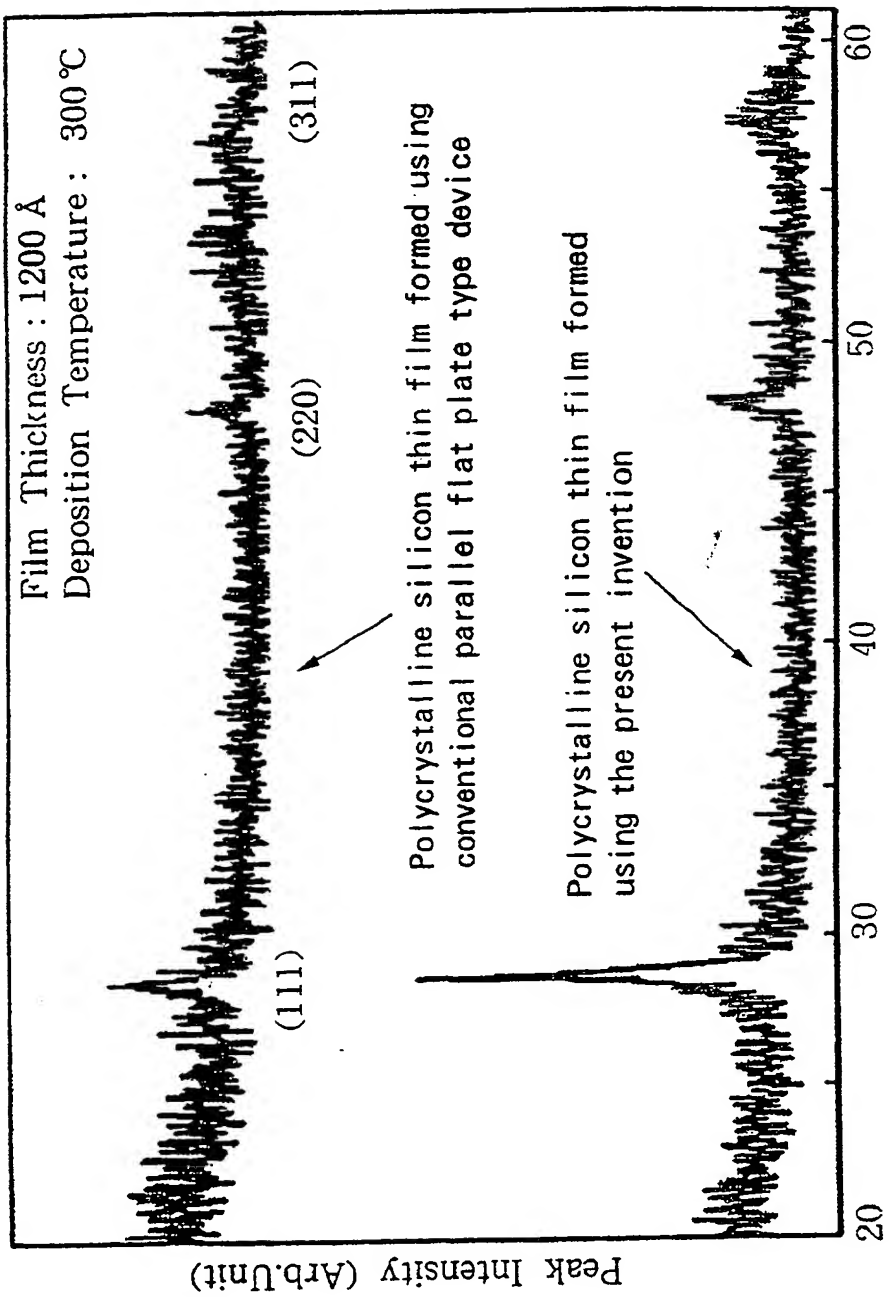
Film Thickness : 1200 Å
Deposition Temperature : 300 ℃
(111)
(220)
(311)
Polycrystalline silicon thin film formed using conventional parallel flat plate type device
Polycrystalline silicon thin film formed using the present invention
Peak Intensity (Arb.Unit)
20
30
40
50
60
2θ (°)

Fig. 42

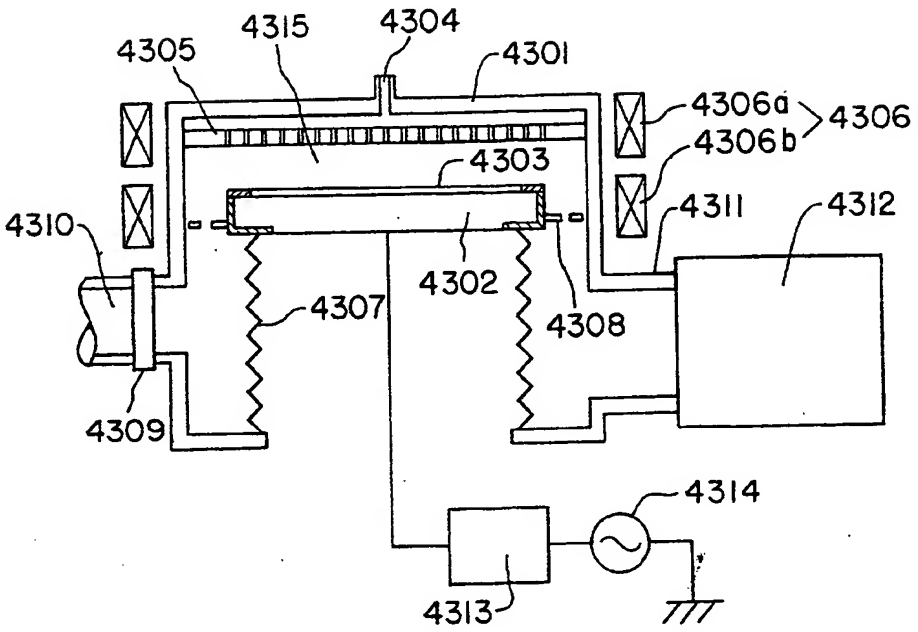

PRIOR ART

Fig. 43A

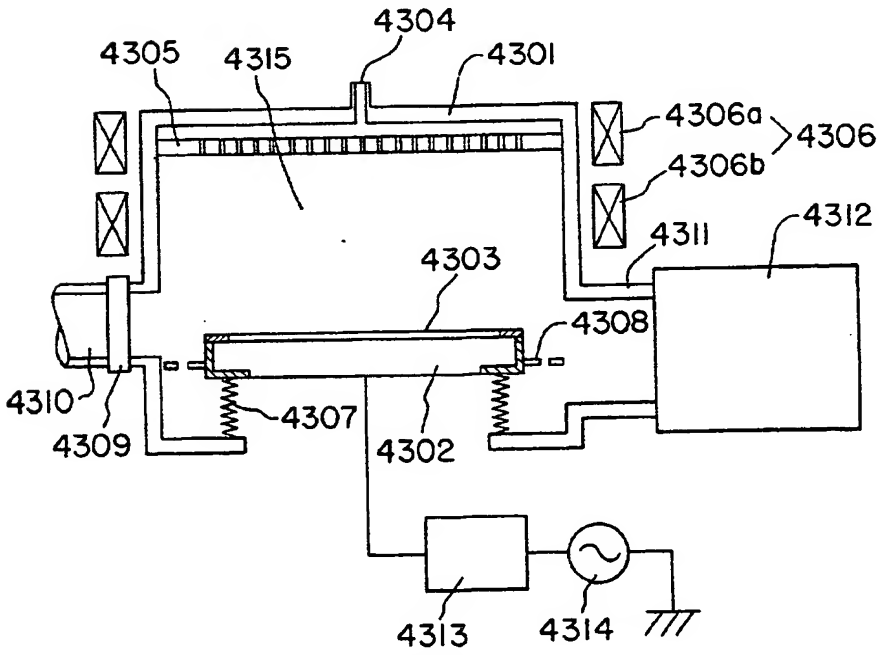

PRIOR ART

Fig. 43B

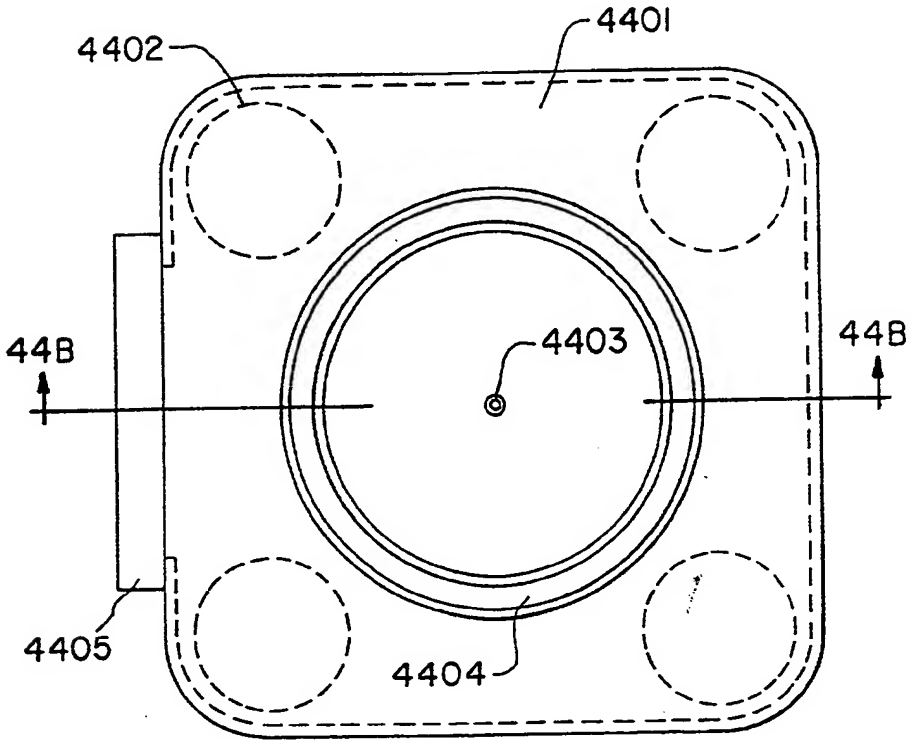

Fig. 44A

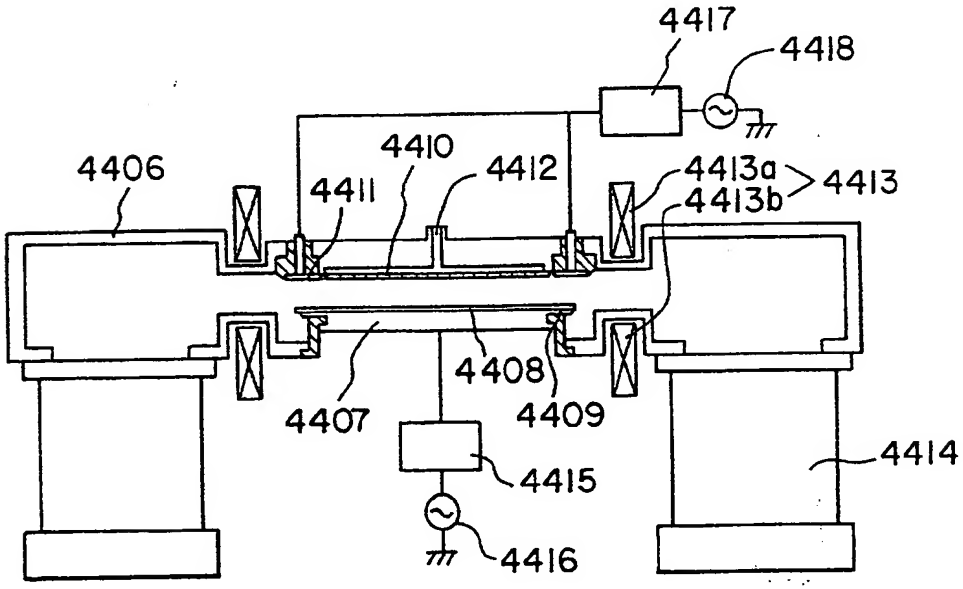

Fig. 44B

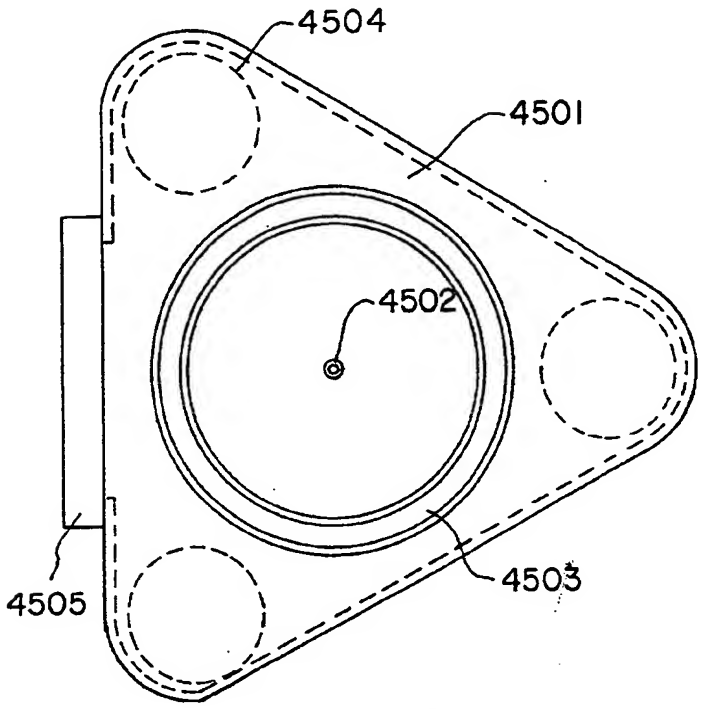

Fig. 45

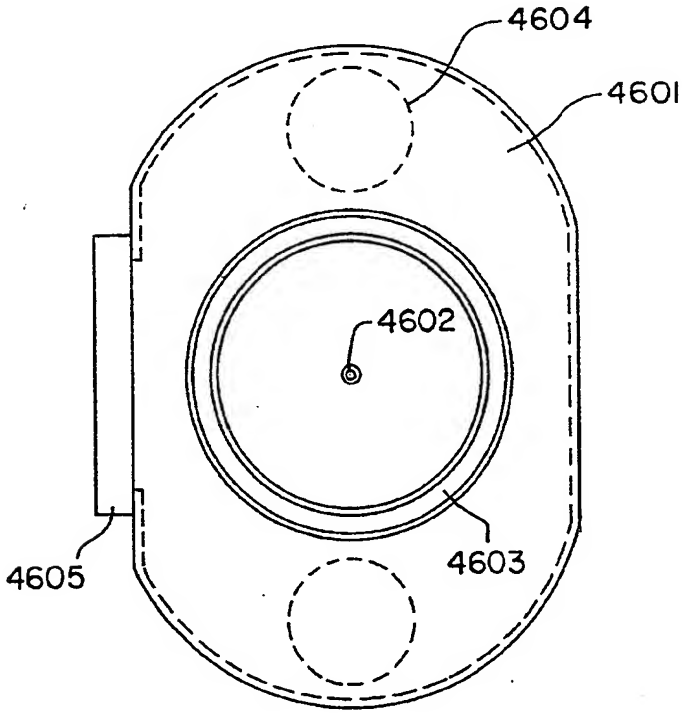

Fig. 46

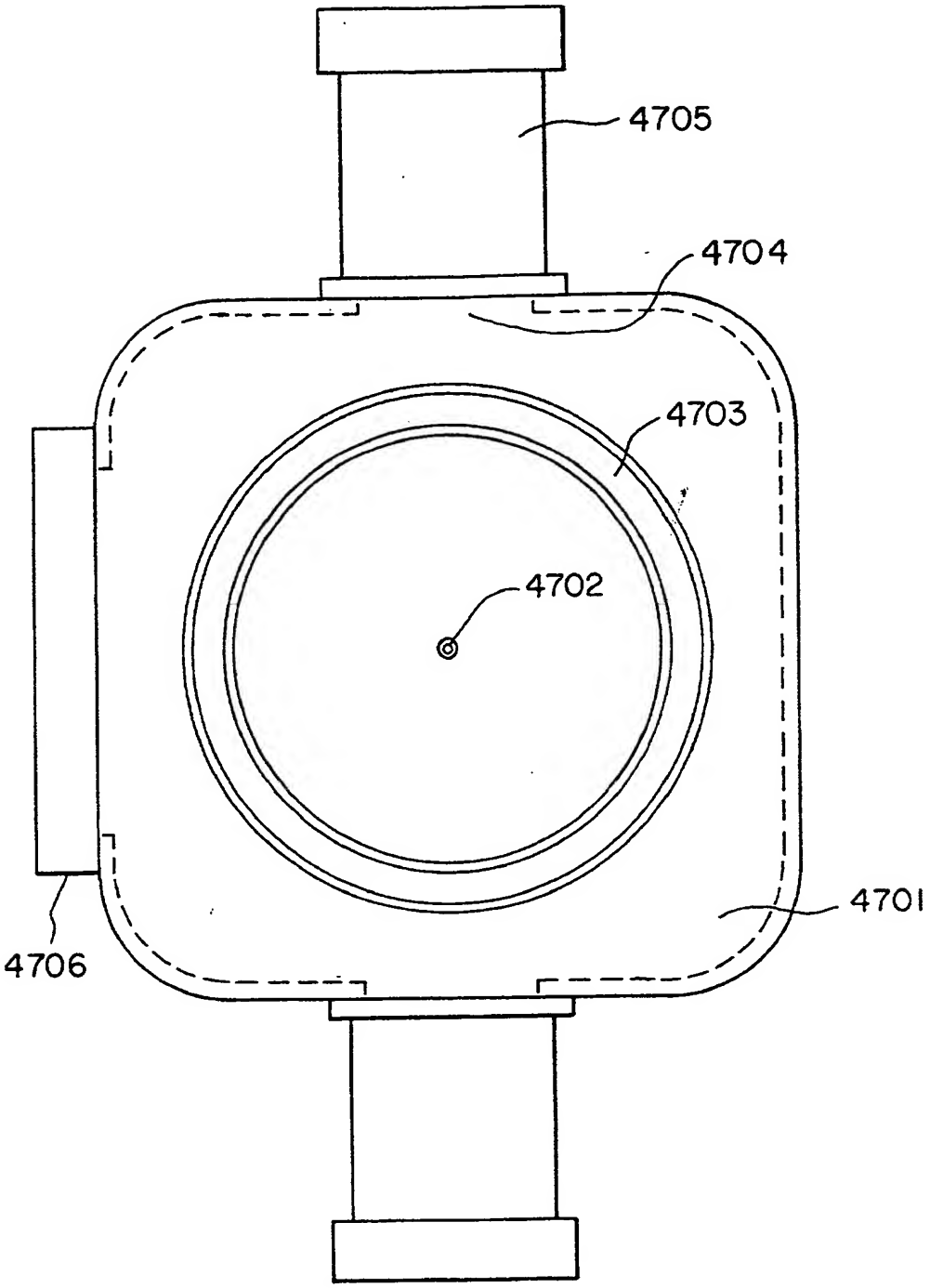

Fig. 47

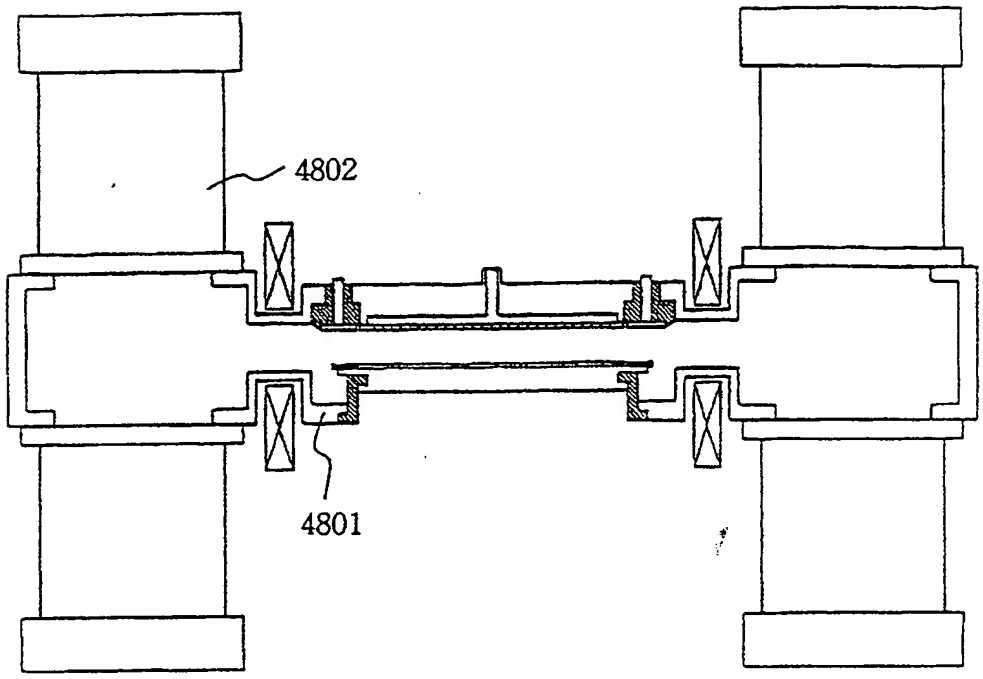

Fig. 48

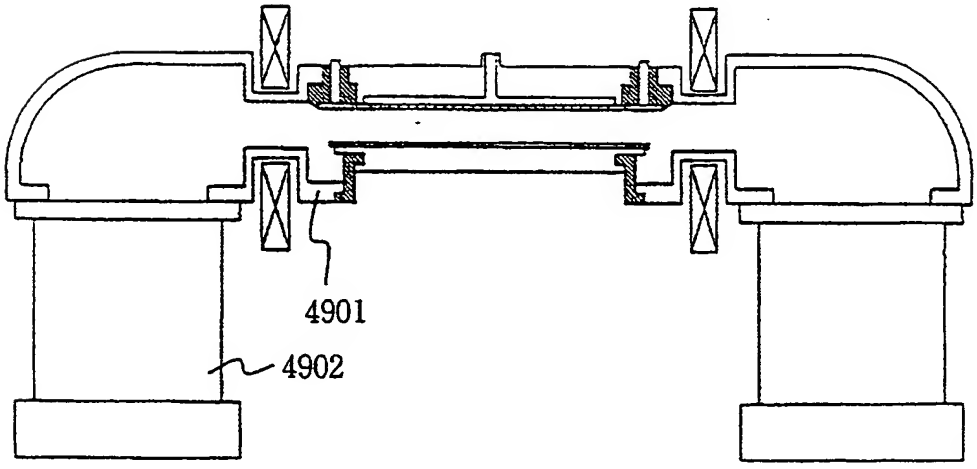

Fig. 49

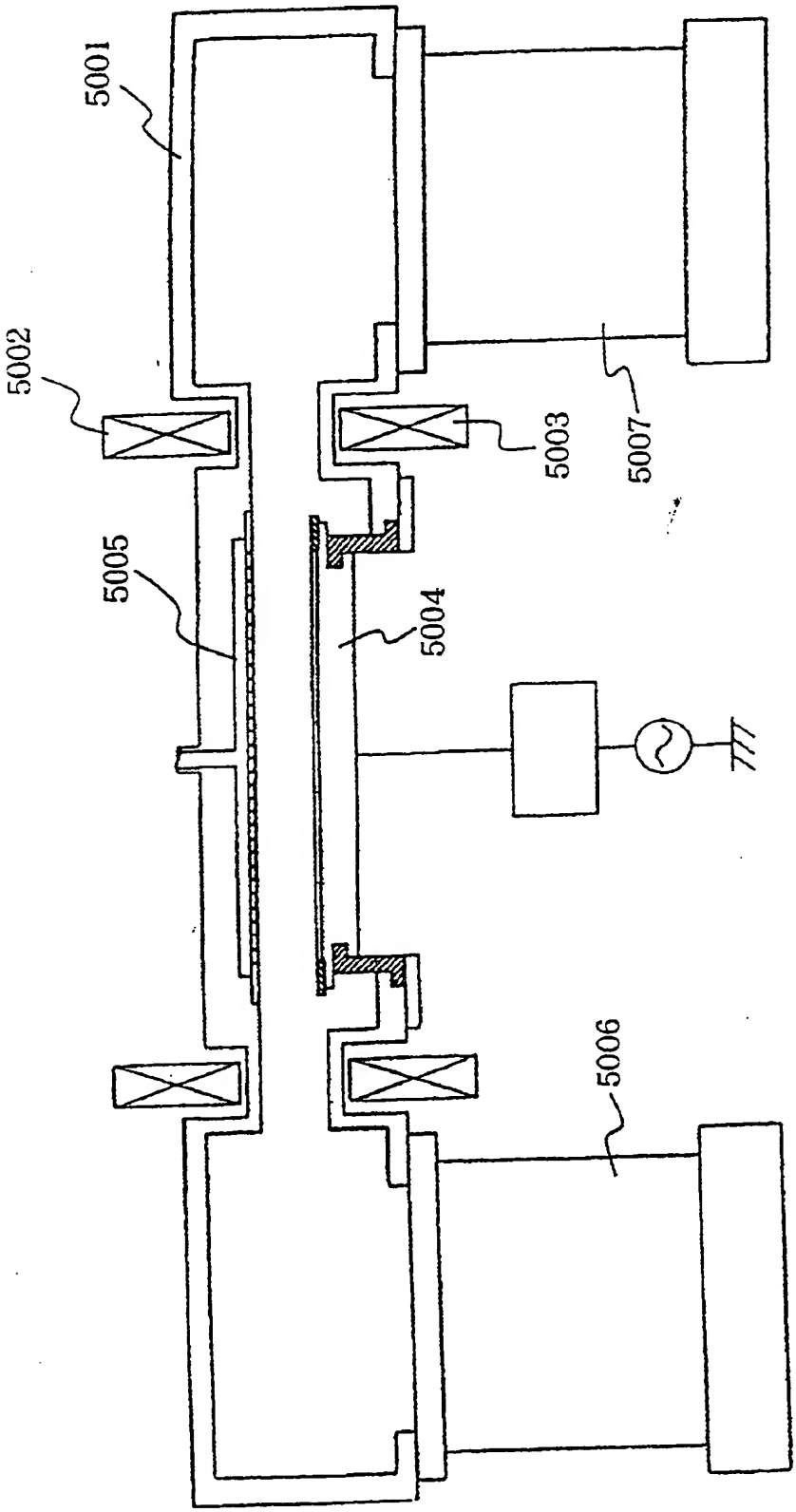

Fig. 50

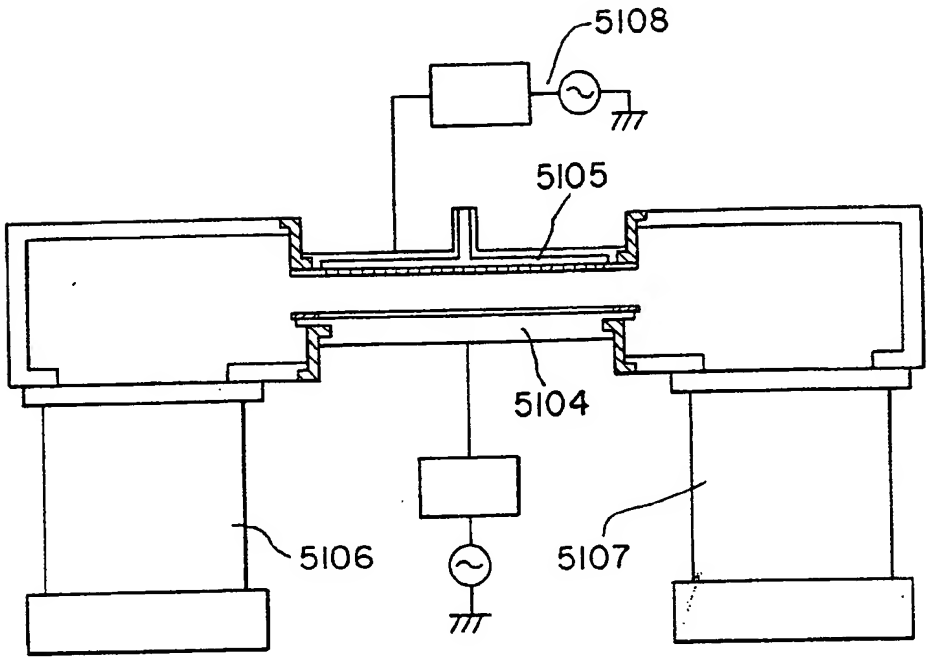

Fig. 51

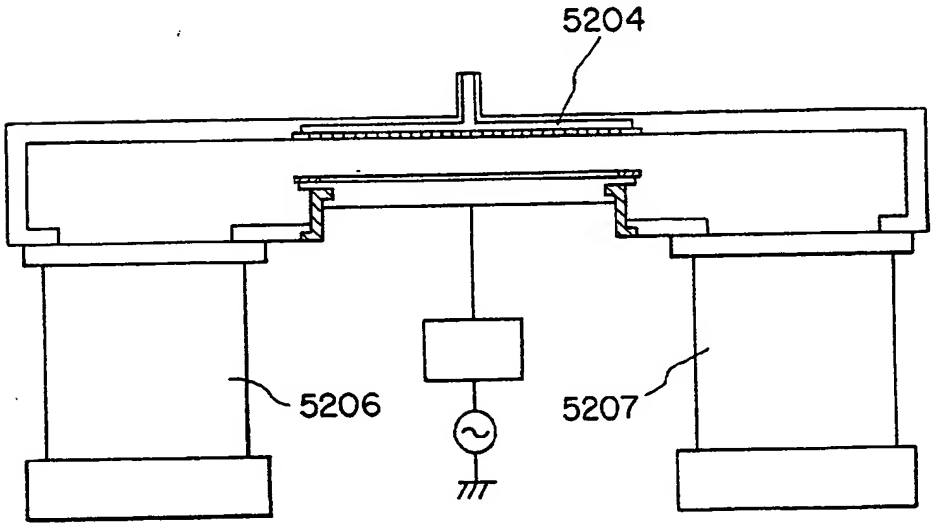

Fig. 52

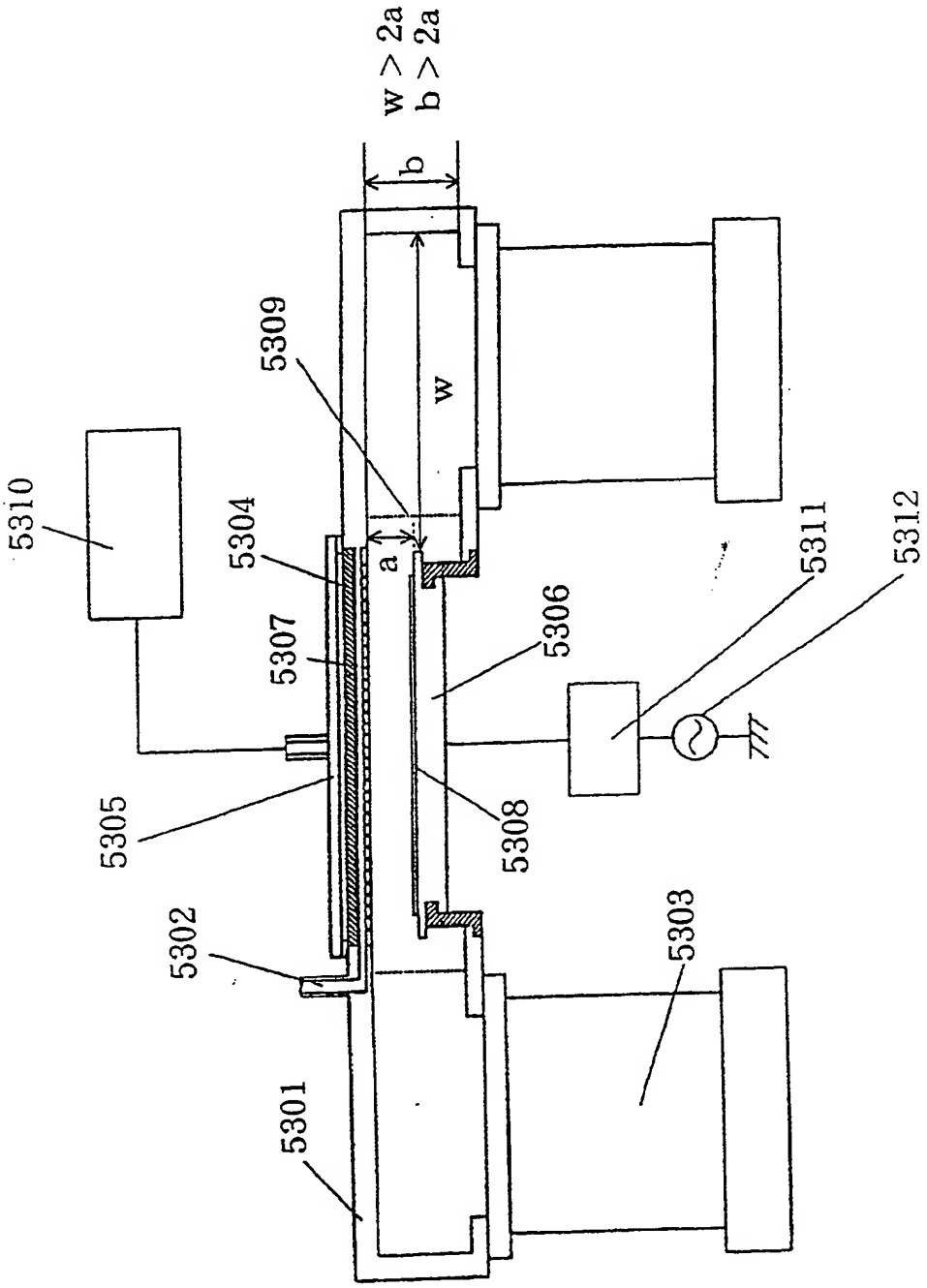
w > 2a
b > 2a
b
w
a
5309
5310
5304
5307
5306
5311
5312
5305
5308
5302
5303
5301

Fig. 53

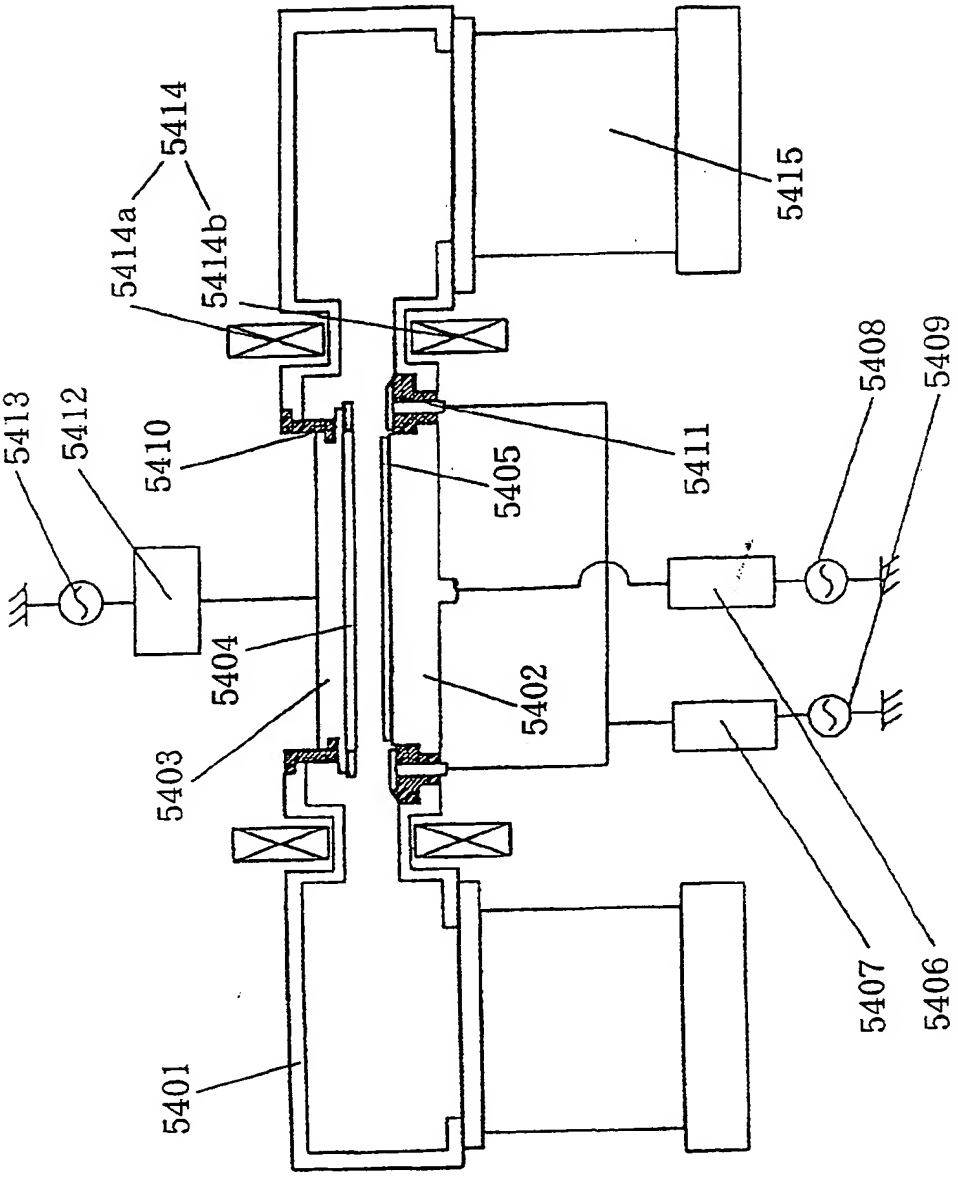
5414
5414a
5414b
5415
5413
5412
5410
5405
5411
5408
5409
5404
5402
5403
5407
5406
5401

Fig. 54

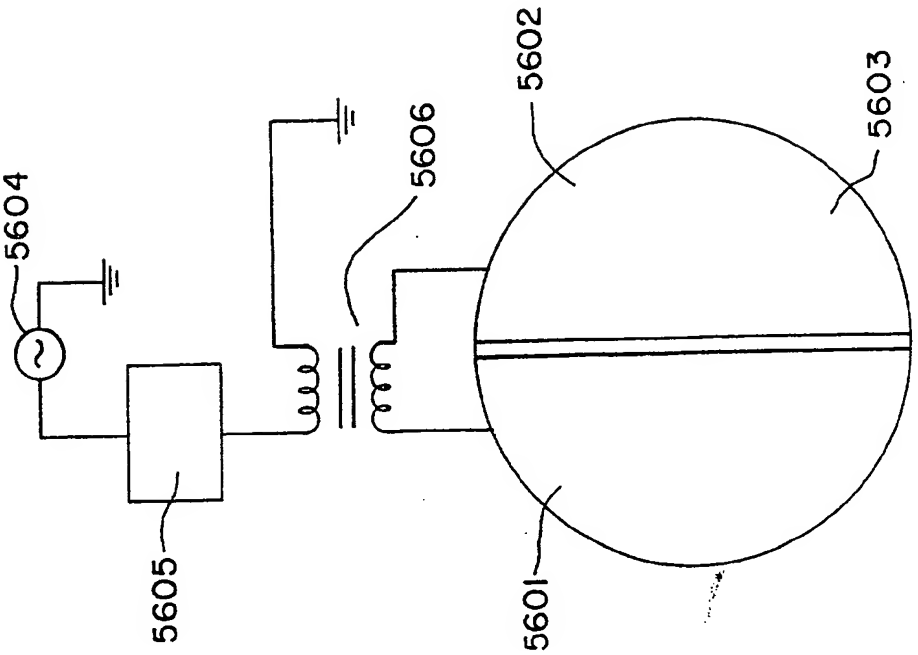
5604
5606
5602
5603
5605
5601

Fig. 56

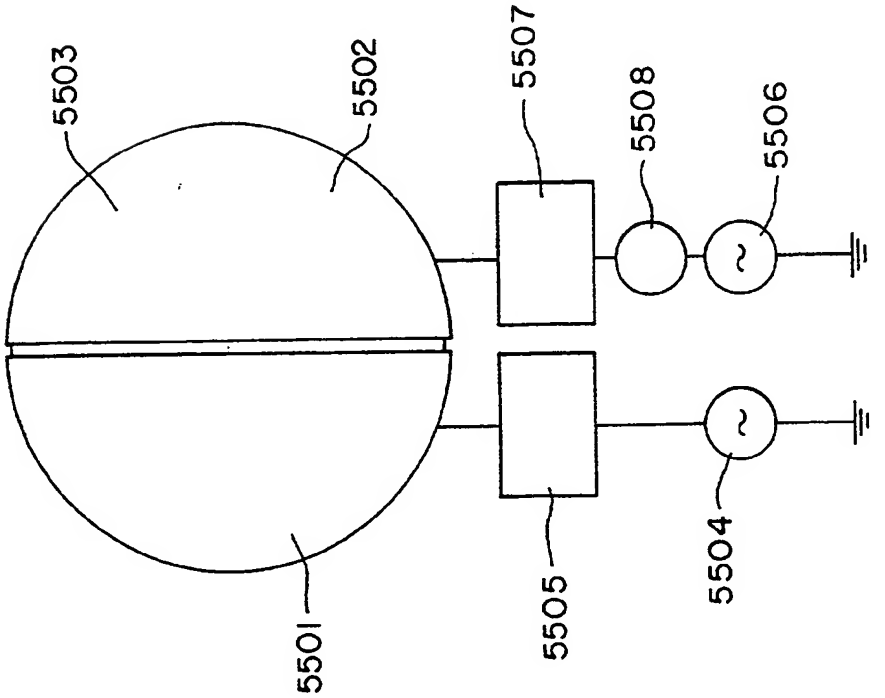
5503
5502
5507
5508
5506
5501
5505
5504

Fig. 55

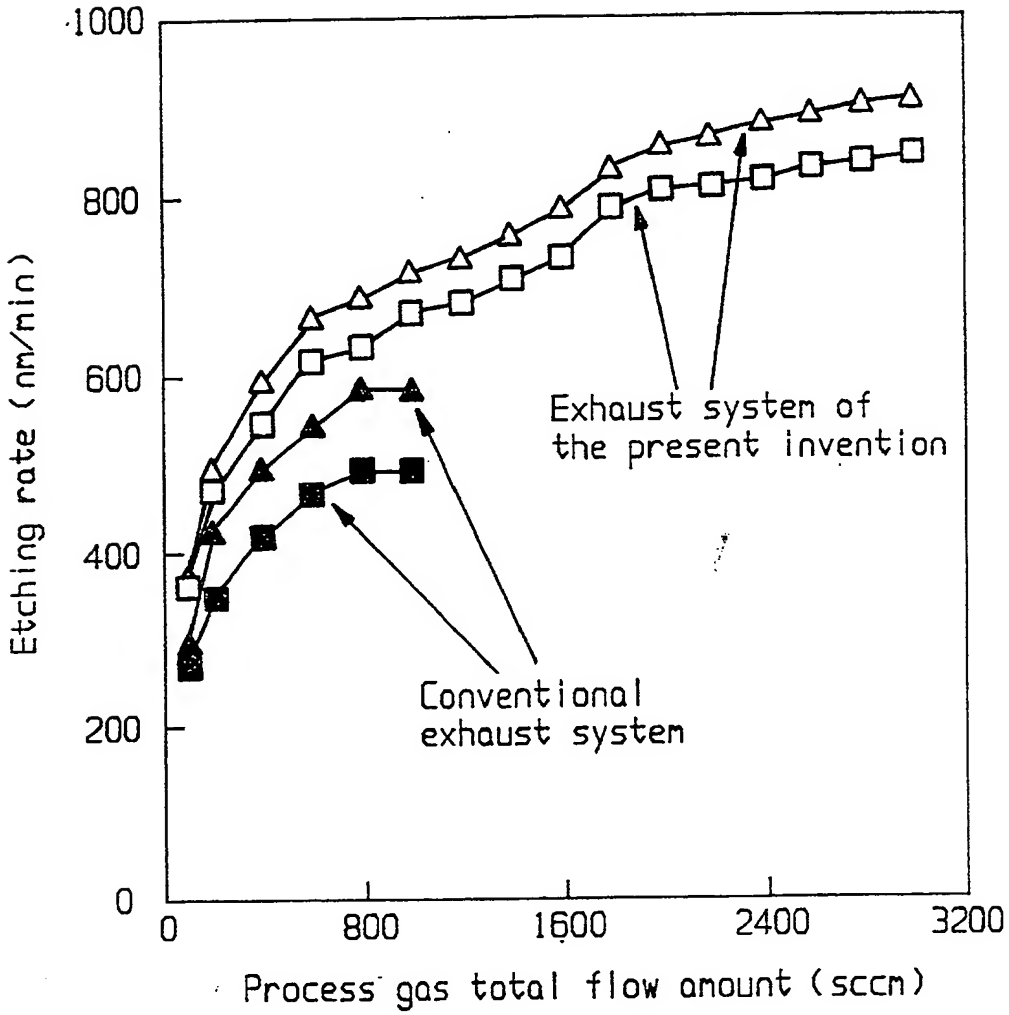
1000
800
600
400
200
0
Etching rate (nm/min)
0
800
1600
2400
3200
Process gas total flow amount (sccm)
Exhaust system of
the present invention
Conventional
exhaust system

Fig. 57

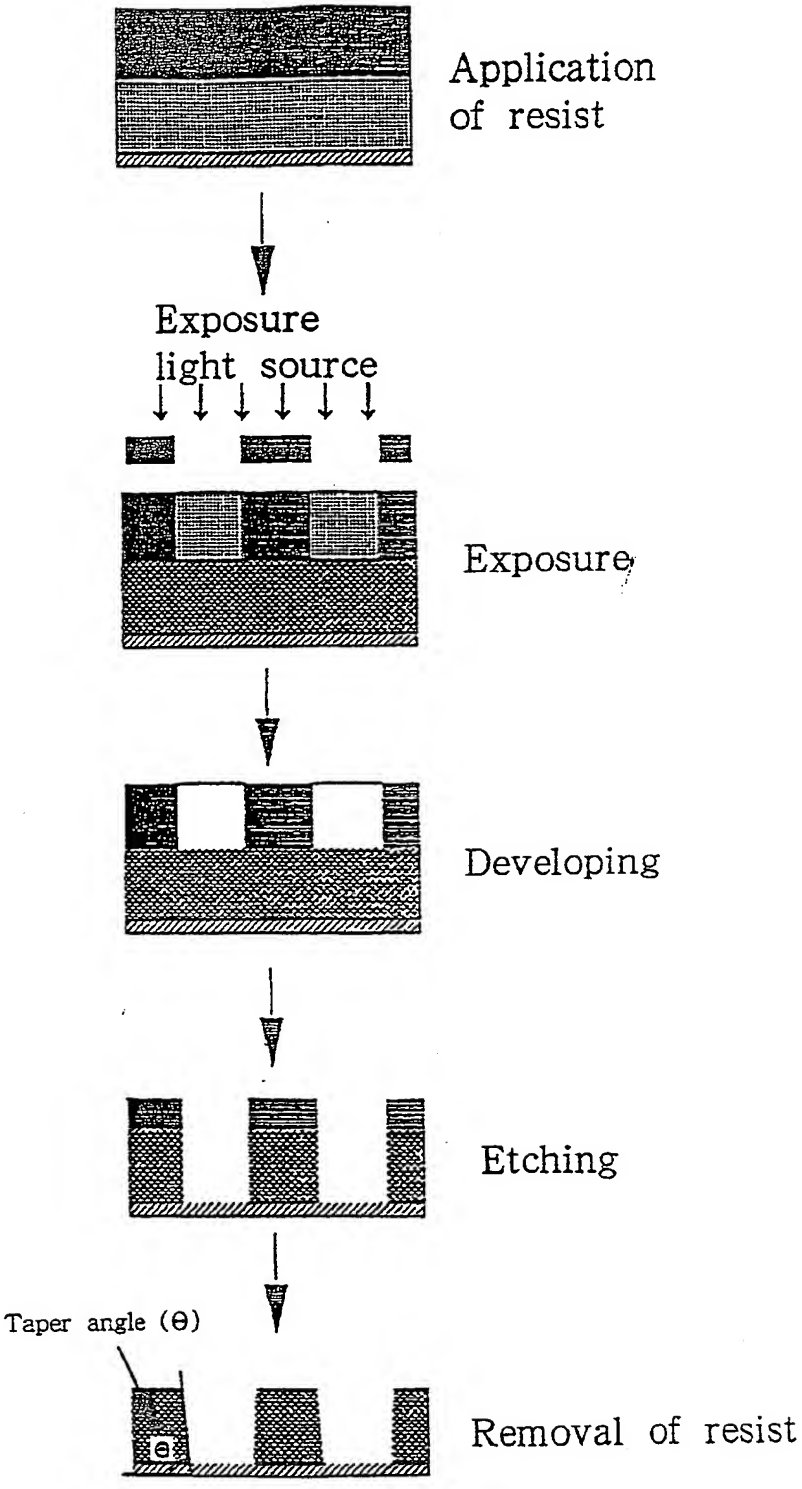
Application
of resist
Exposure
light source
Exposure
Developing
Etching
Taper angle (θ)
θ
Removal of resist

Fig. 58

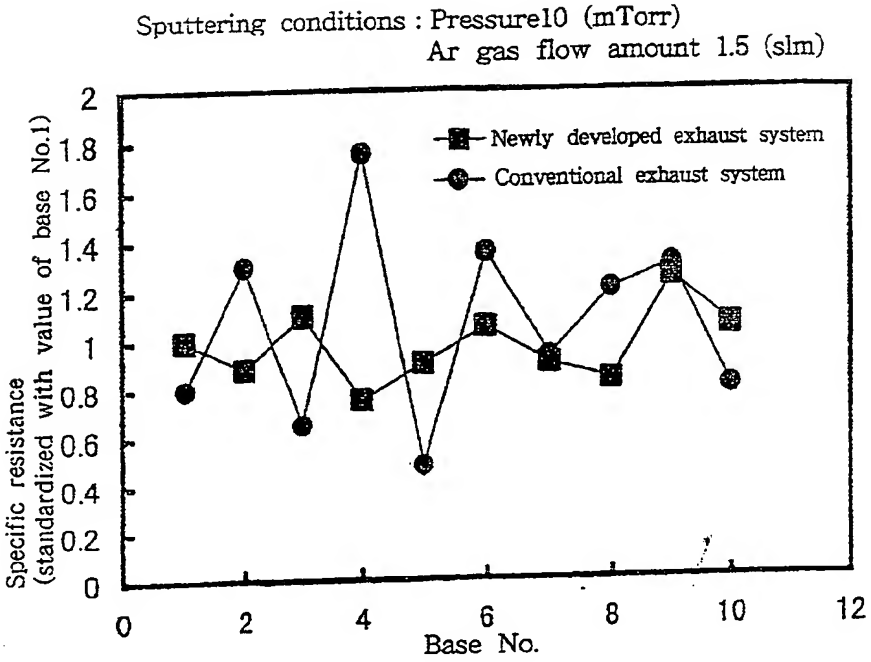
Sputtering conditions : Pressure10 (mTorr)
Ar gas flow amount 1.5 (slm)
Newly developed exhaust system
Conventional exhaust system
Specific resistance (standardized with value of base No.1)
Base No.
0
0.2
0.4
0.6
0.8
1
1.2
1.4
1.6
1.8
2
0
2
4
6
8
10
12

Fig. 59

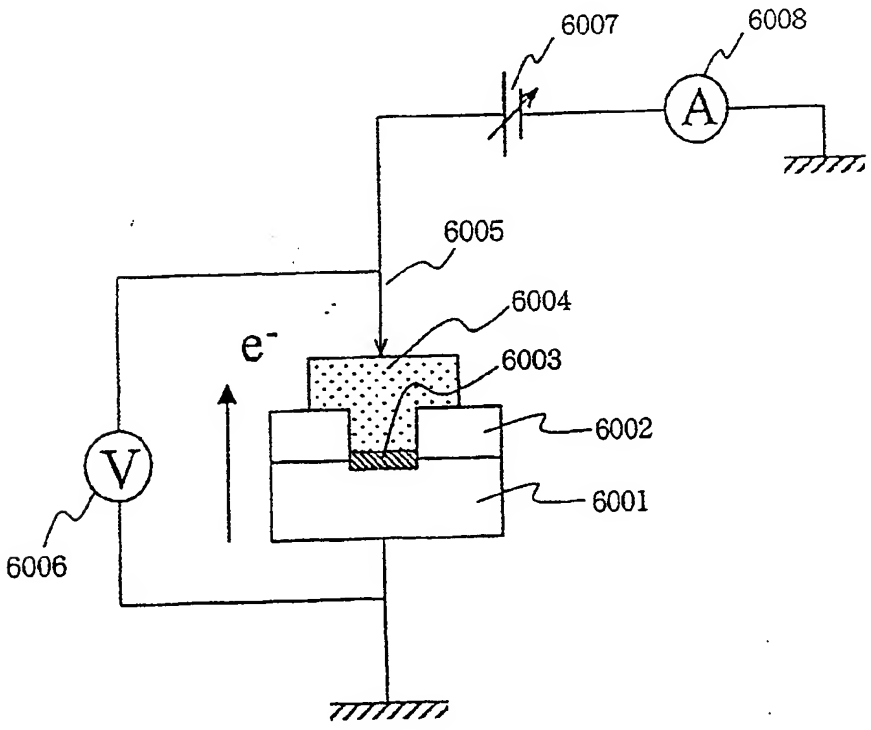
6007
6008
A
6005
6004
e-
6003
6002
6001
V
6006

Fig. 60

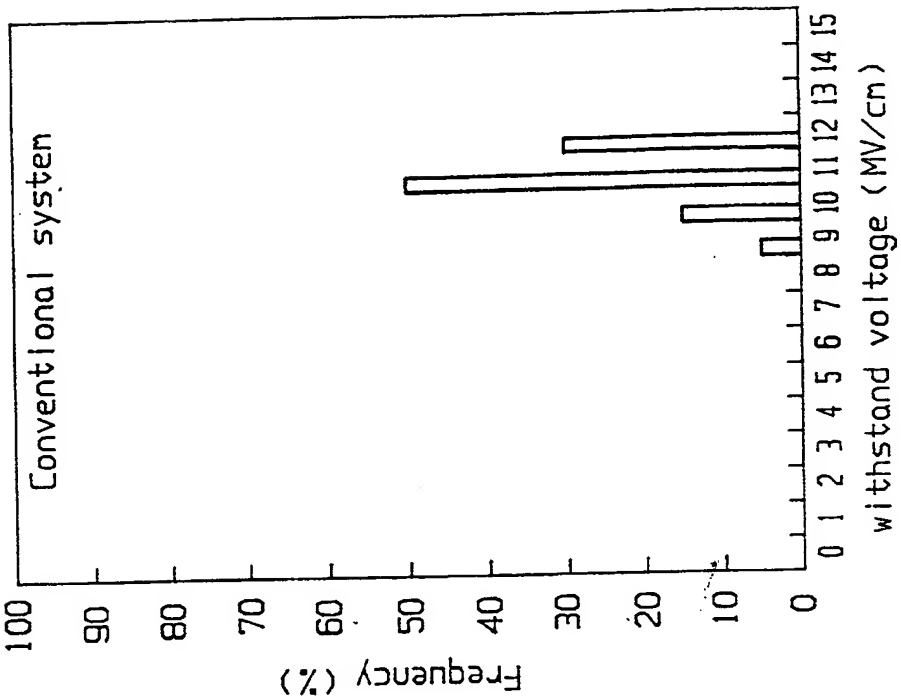

Fig. 61B

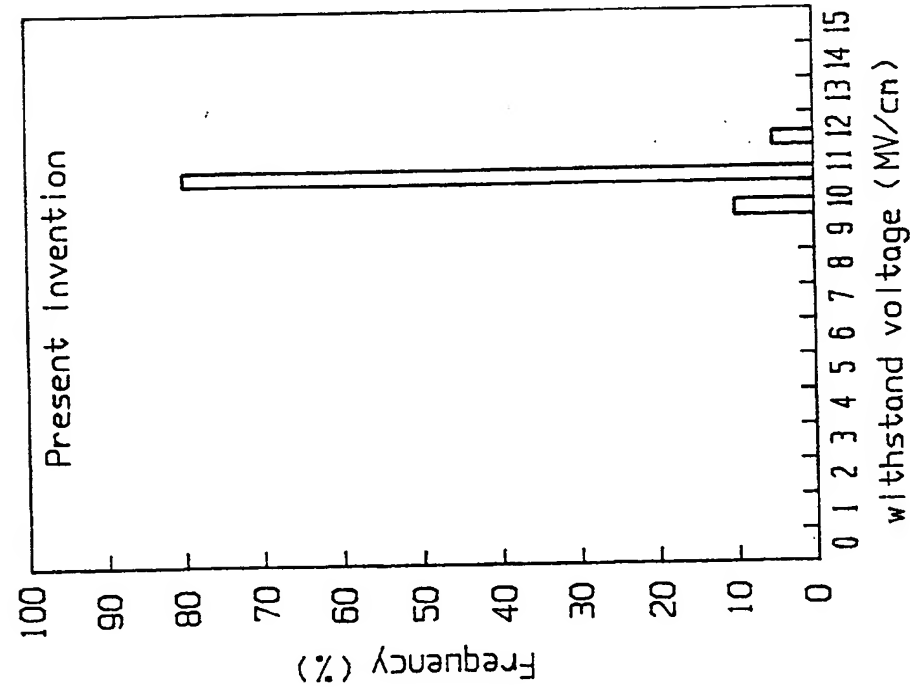

Fig. 61A

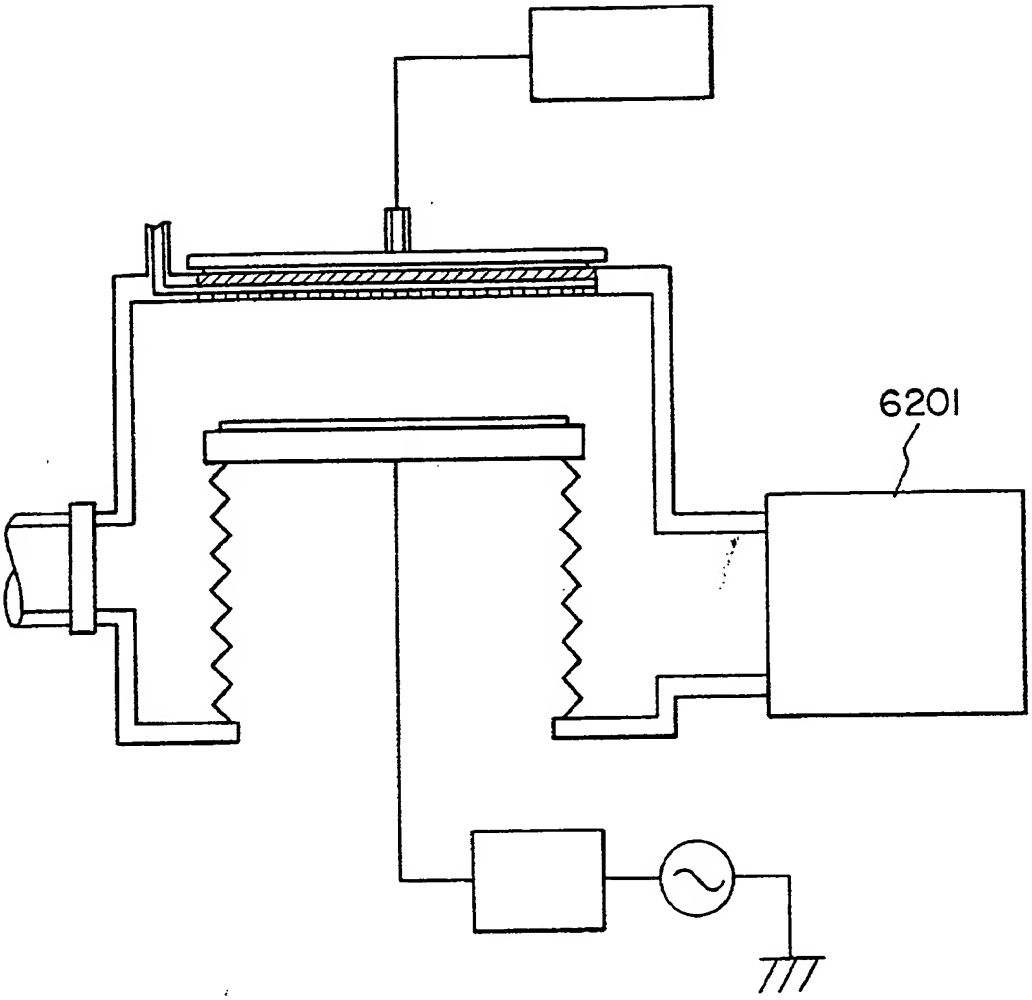

Fig. 62

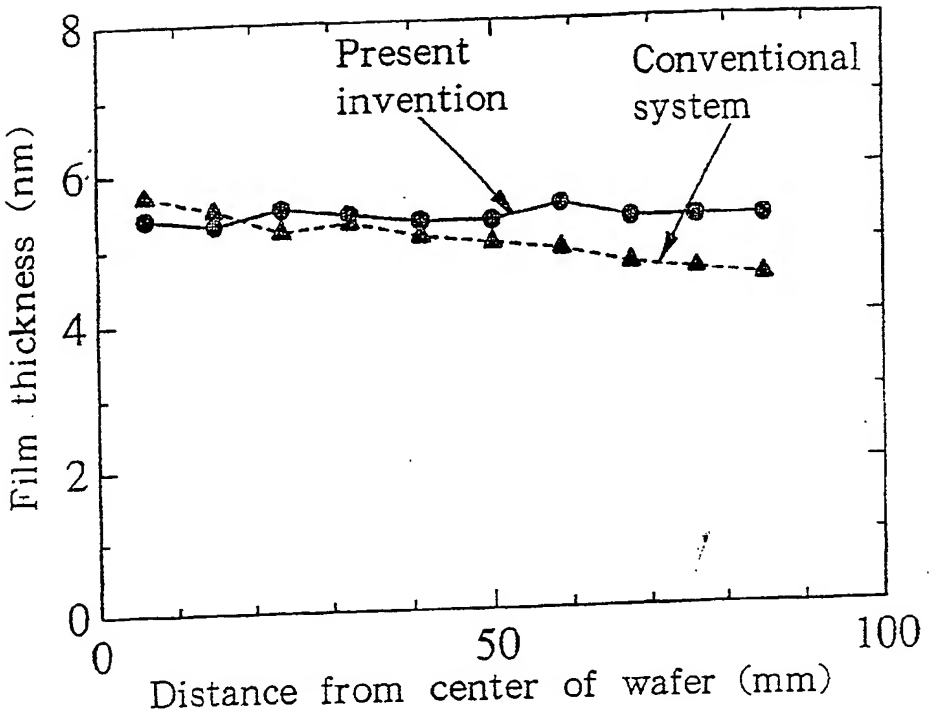
Present invention
Conventional system
Film thickness (nm)
8
6
4
2
0
0
50
100
Distance from center of wafer (mm)

Fig. 63

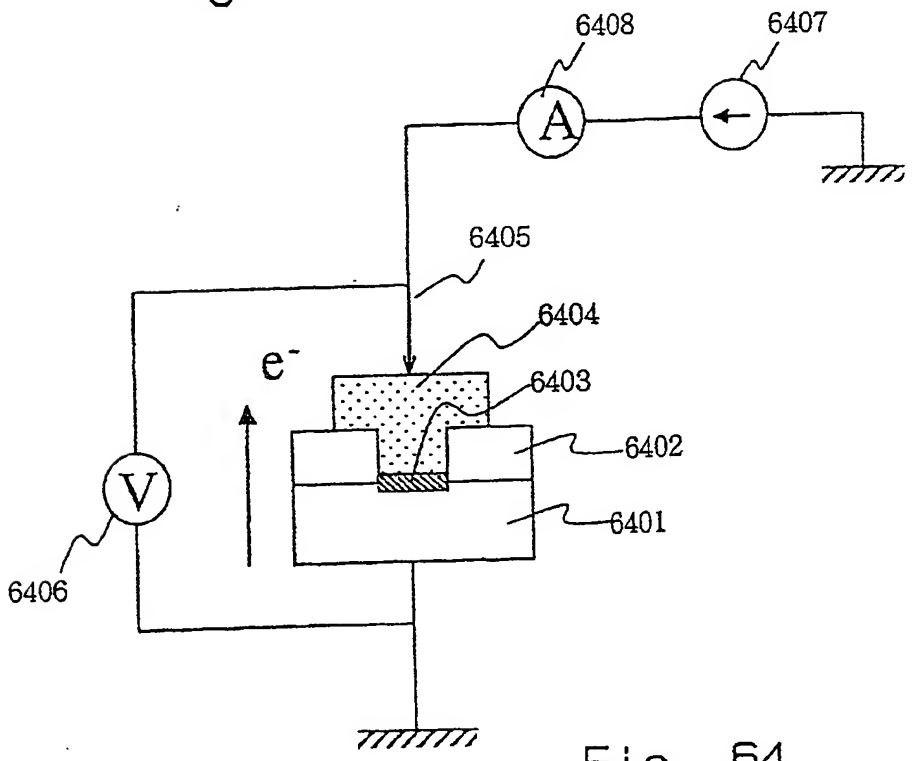
6408
6407
A
6405
6404
e⁻
6403
6402
6401
V
6406

Fig. 64

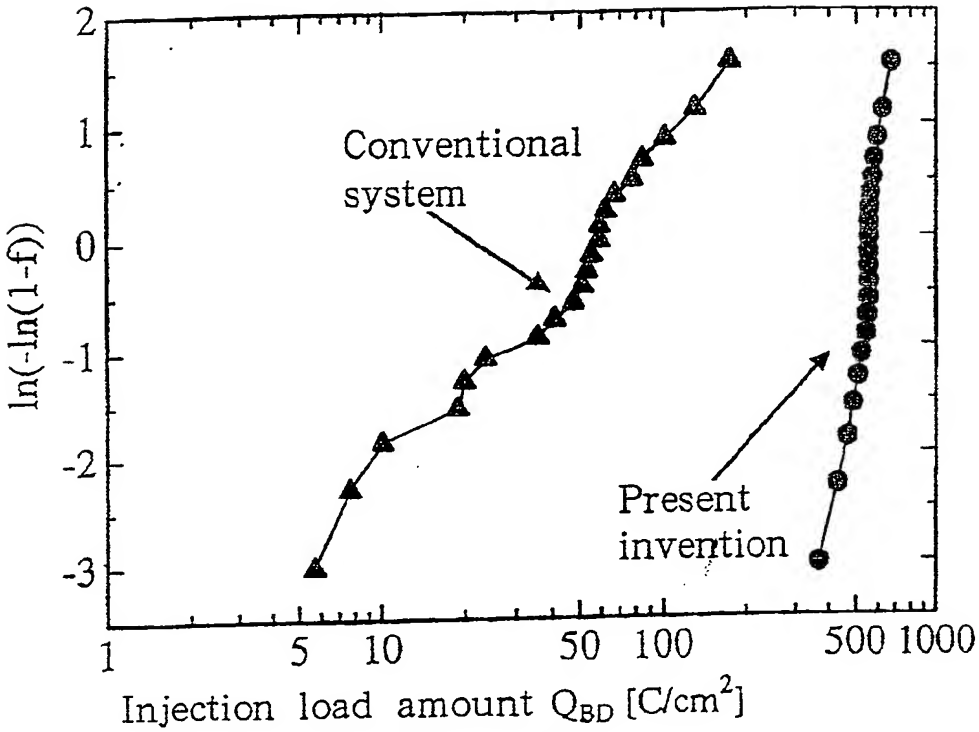
2
1
0
-1
-2
-3
ln(-ln(1-f))
Conventional system
Present invention
1
5
10
50
100
500
1000
Injection load amount Q_{BD} [C/cm^2]

Fig. 65

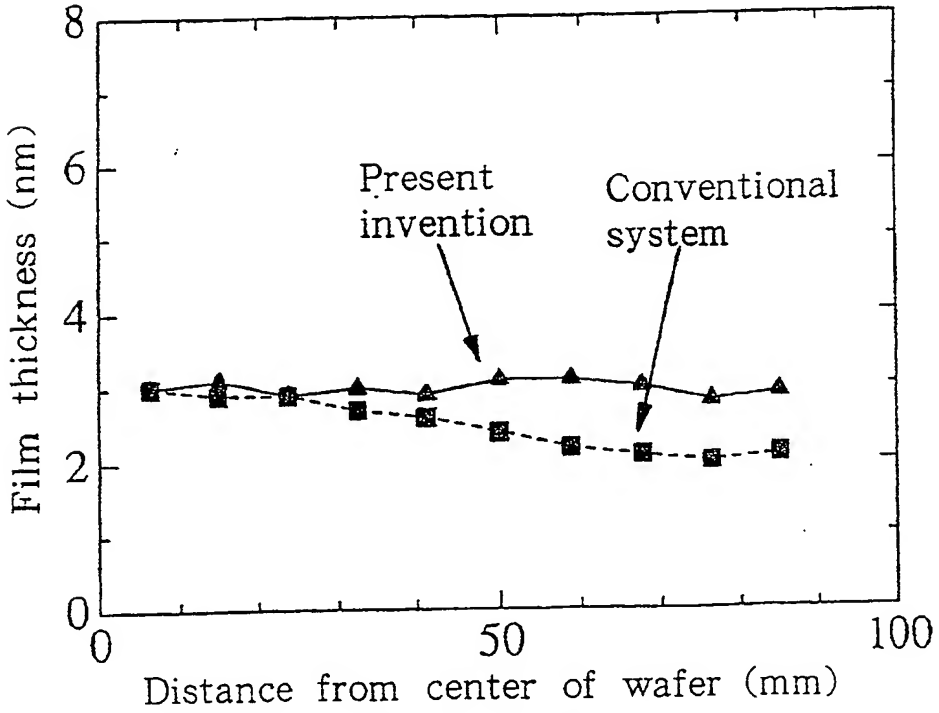
8
6
4
2
0
Film thickness (nm)
Present invention
Conventional system
0
50
100
Distance from center of wafer (mm)

Fig. 66

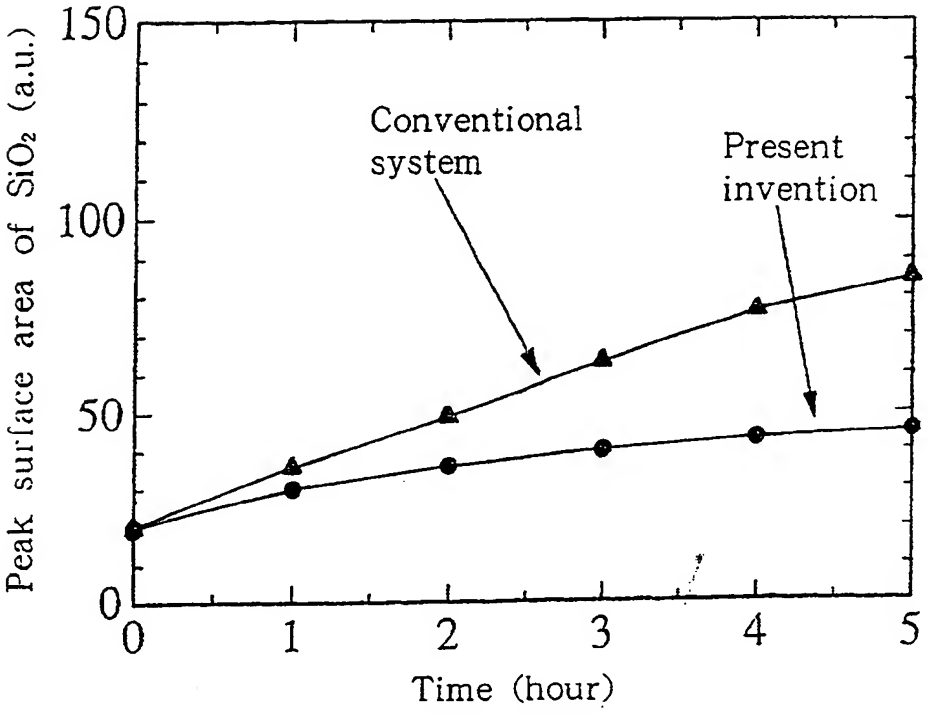
150
100
50
0
0
1
2
3
4
5
Peak surface area of SiO_2 (a.u.)
Time (hour)
Conventional system
Present invention

Fig. 67

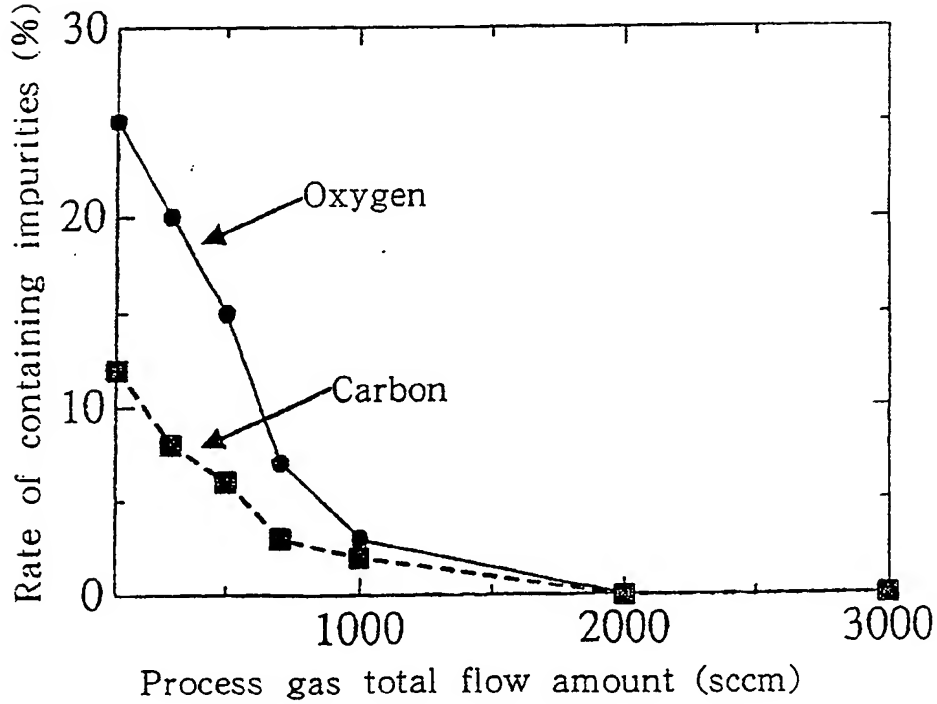
30
20
10
0
1000
2000
3000
Rate of containing impurities (%)
Process gas total flow amount (sccm)
Oxygen
Carbon

Fig. 68

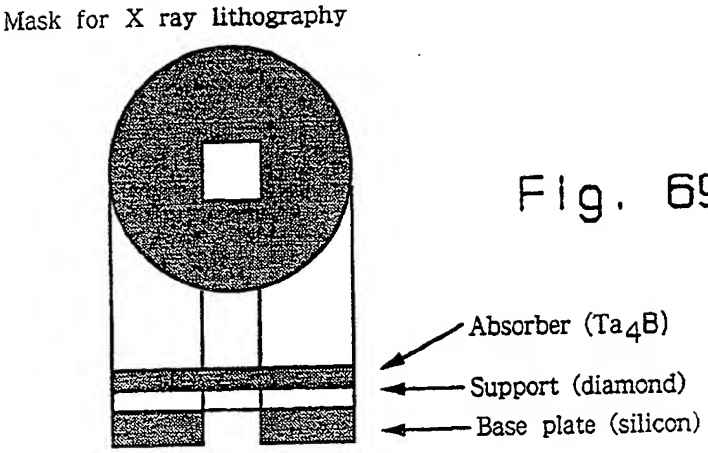

Fig. 69

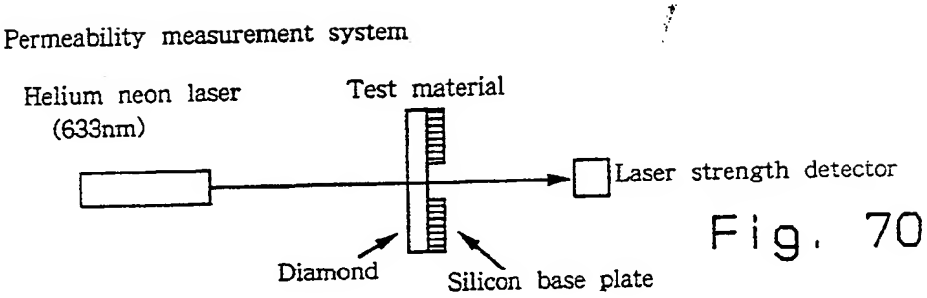

Fig. 70

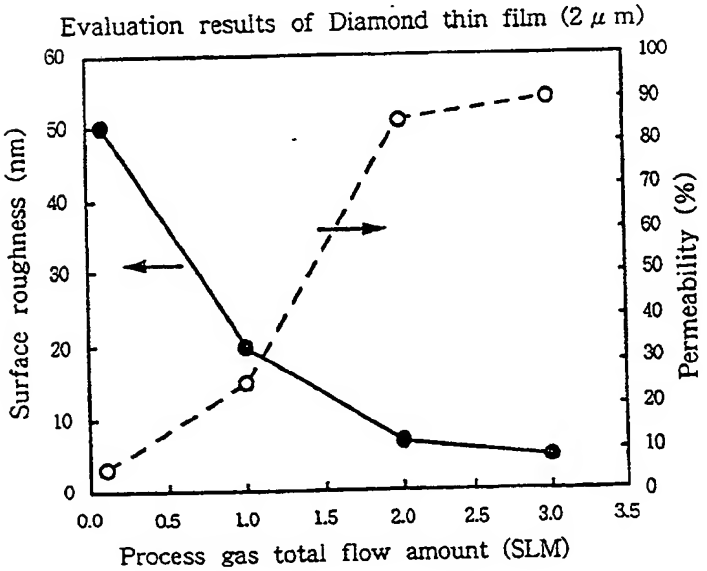

Fig. 71

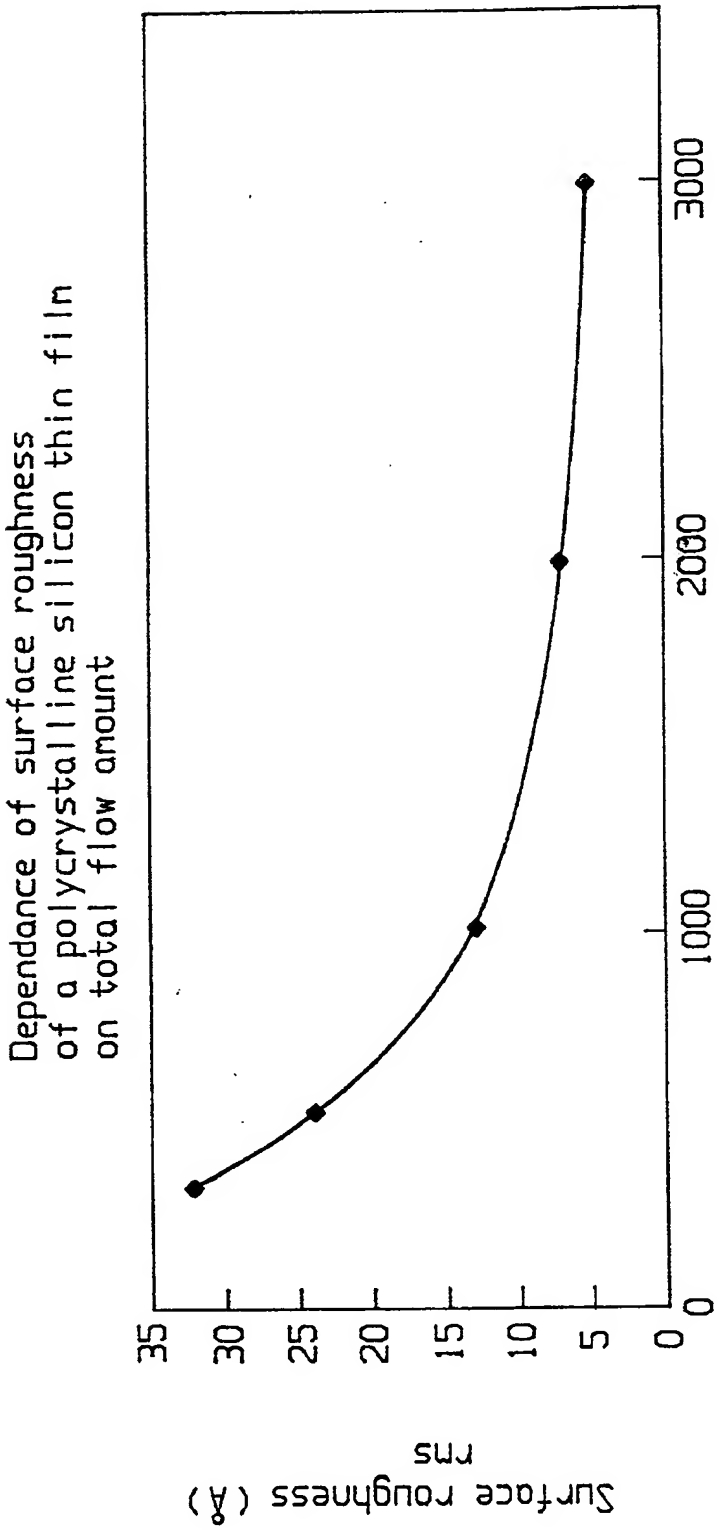
Dependance of surface roughness
of a polycrystalline silicon thin film
on total flow amount
Surface roughness (Å)
rms
0
5
10
15
20
25
30
35
1000
2000
3000
Total gas flow amount (sccm)

Fig. 72

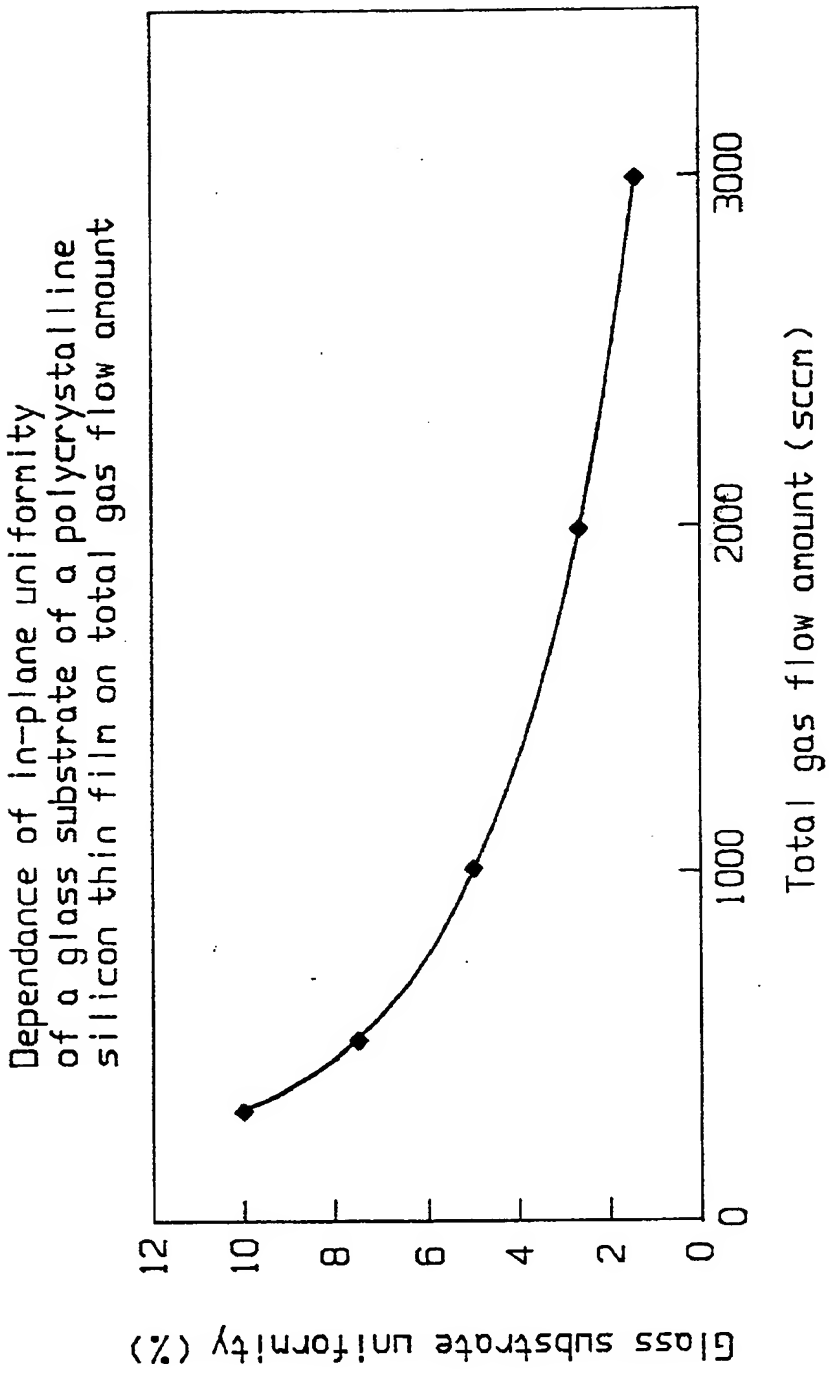
Dependance of in-plane uniformity
of a glass substrate of a polycrystalline
silicon thin film on total gas flow amount
Glass substrate uniformity (%)
0
2
4
6
8
10
12
0
1000
2000
3000
Total gas flow amount (sccm)

Fig. 73

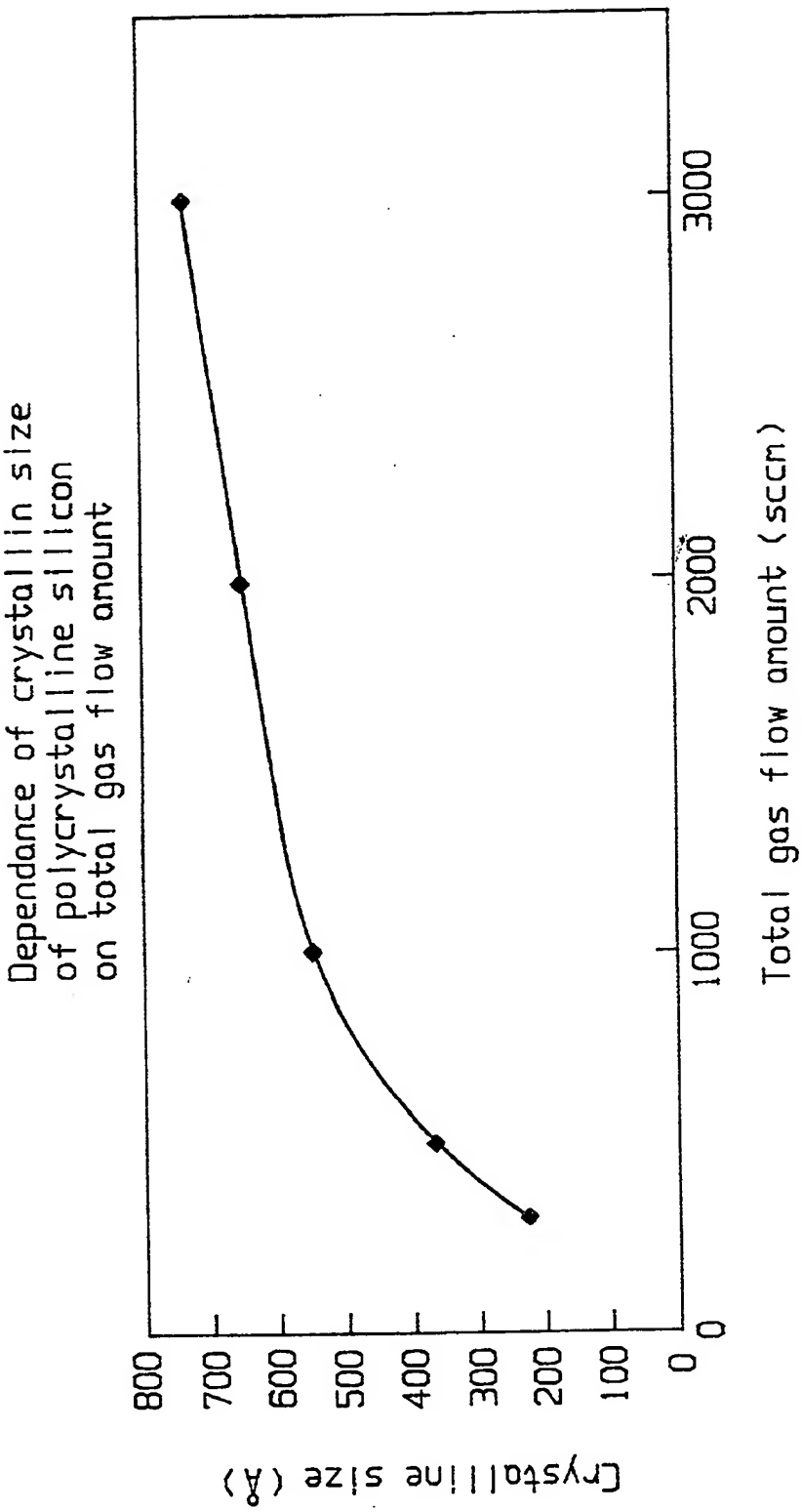
Dependance of crystallin size
of polycrystalline silicon
on total gas flow amount
Crystalline size (Å)
800
700
600
500
400
300
200
100
0
0
1000
2000
3000
Total gas flow amount (sccm)

Fig. 74

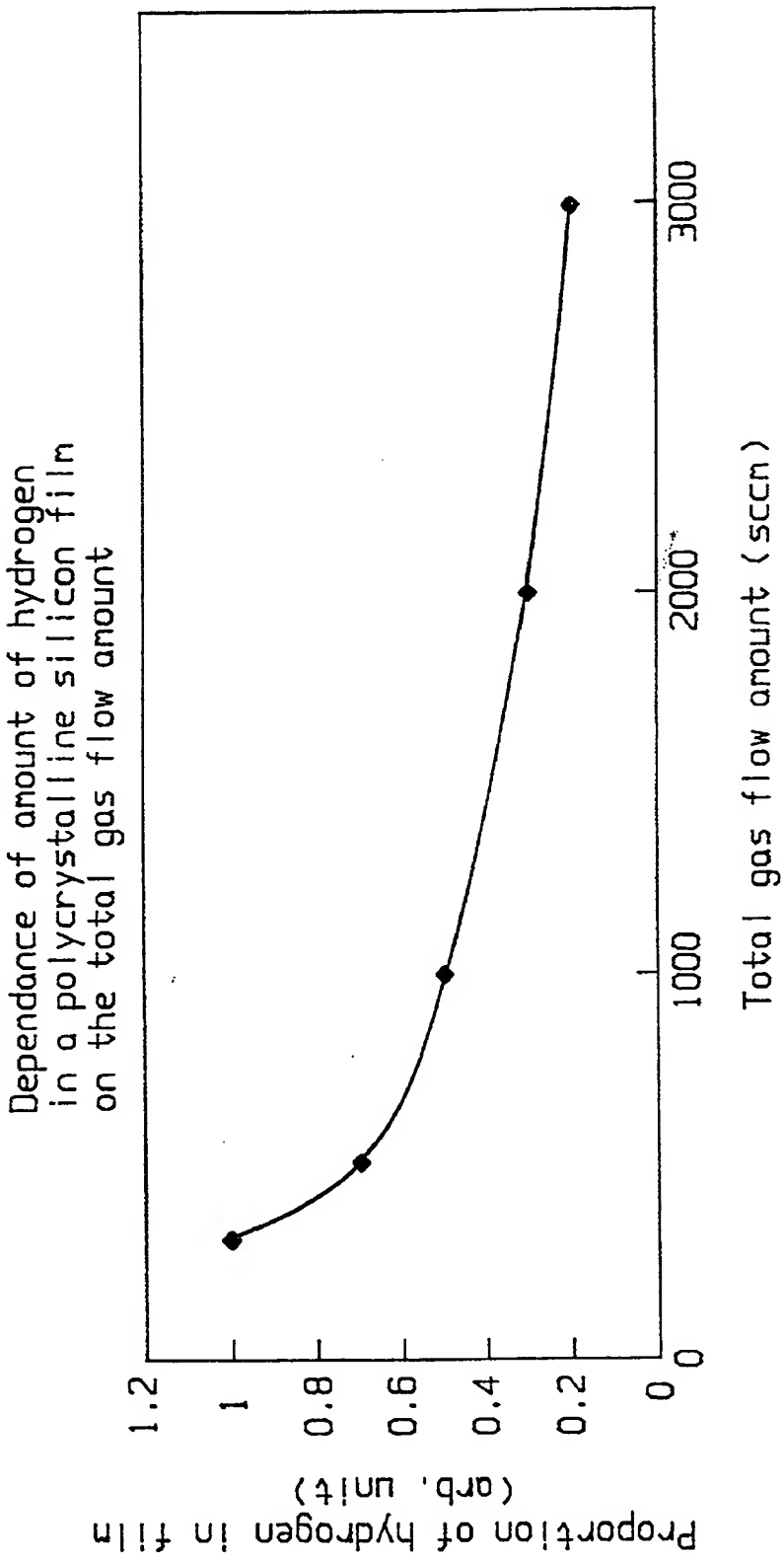
Dependance of amount of hydrogen
in a polycrystalline silicon film
on the total gas flow amount
Proportion of hydrogen in film
(arb. unit)
1.2
1
0.8
0.6
0.4
0.2
0
0
1000
2000
3000
Total gas flow amount (sccm)

Fig. 75

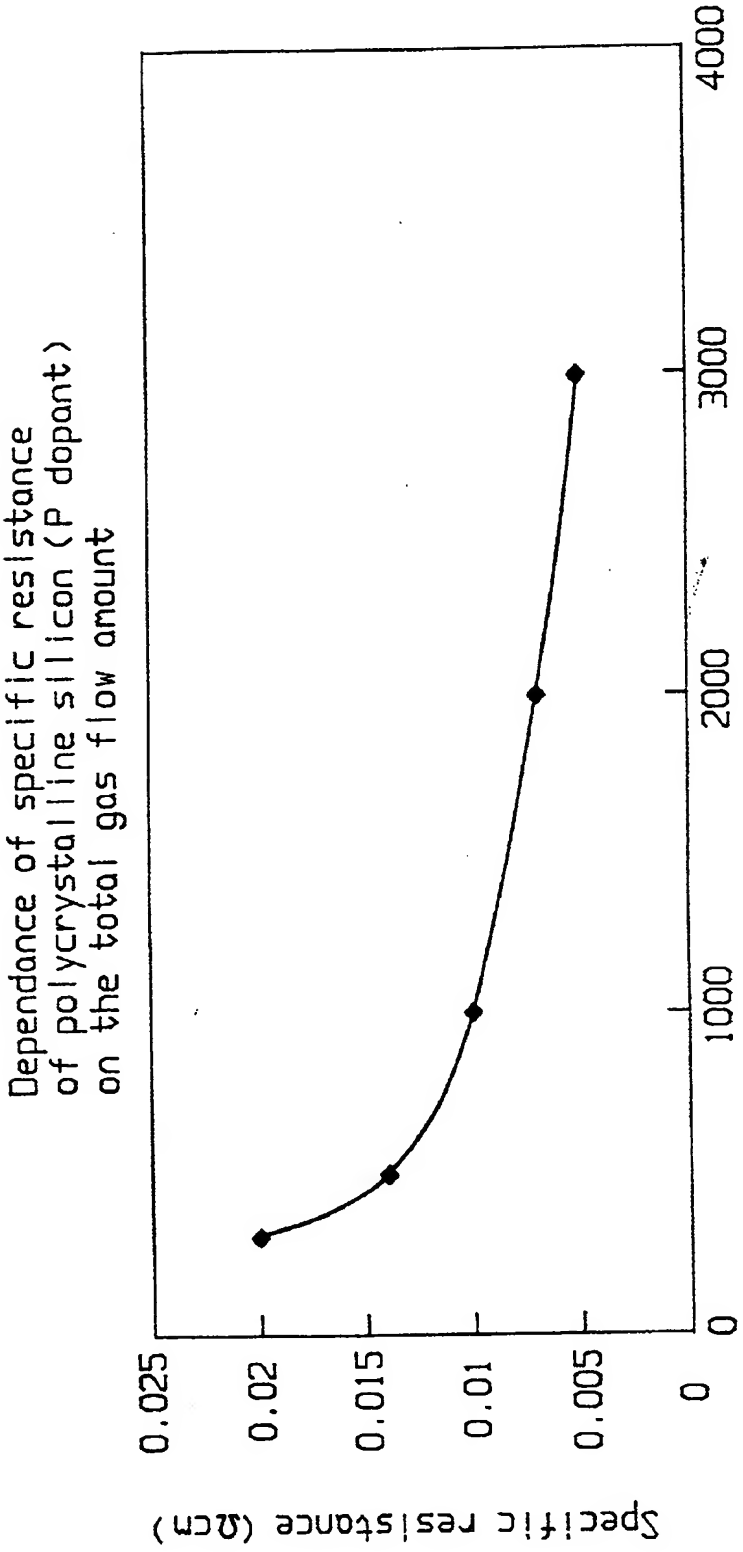
Dependance of specific resistance
of polycrystalline silicon (P dopant)
on the total gas flow amount
Specific resistance (Ωcm)
0.025
0.02
0.015
0.01
0.005
0
0
1000
2000
3000
4000
Total gas flow amount (sccm)

Fig. 76

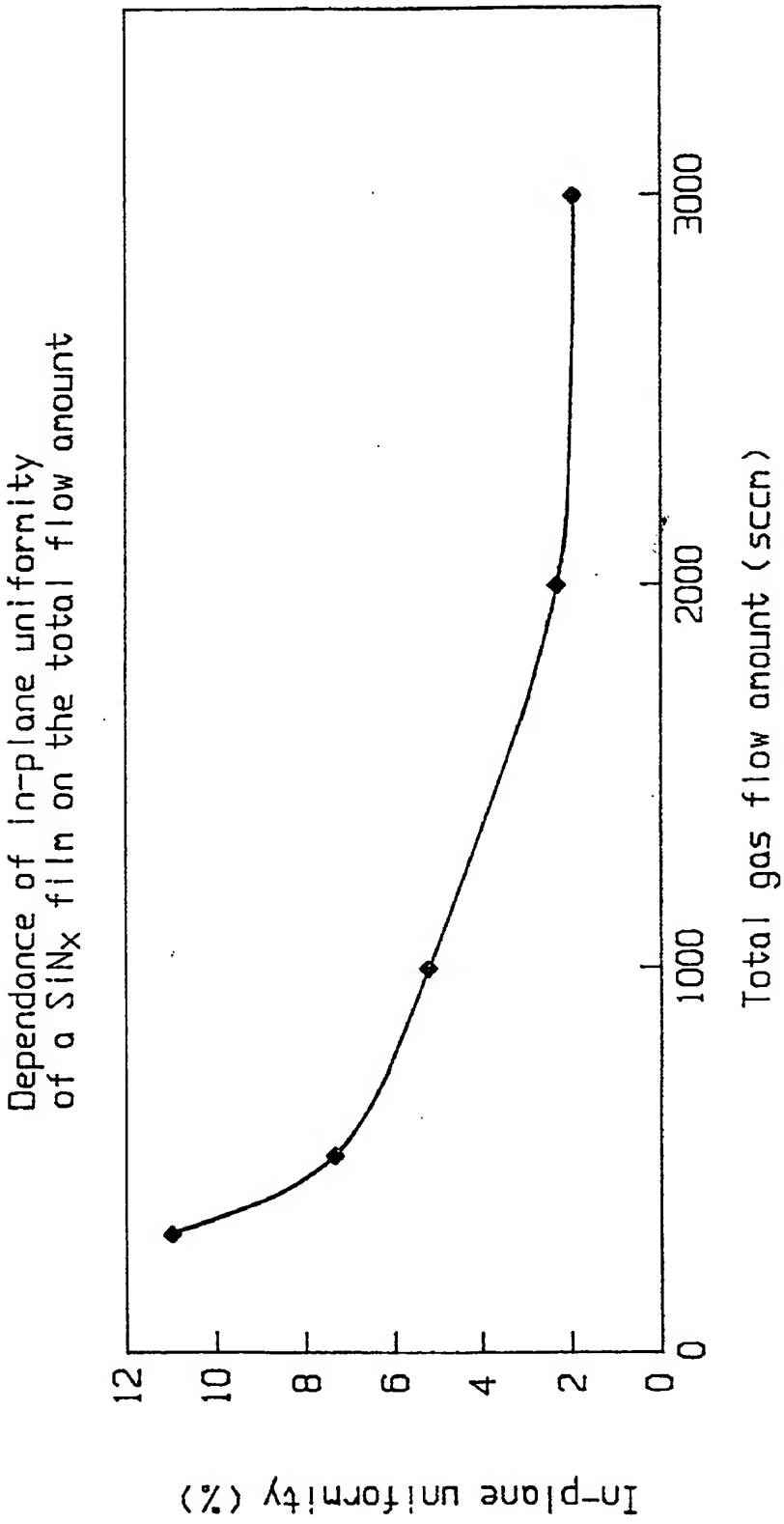
Dependance of In-plane uniformity
of a SiNx film on the total flow amount
In-plane uniformity (%)
0
2
4
6
8
10
12
0
1000
2000
3000
Total gas flow amount (sccm)

Fig. 77

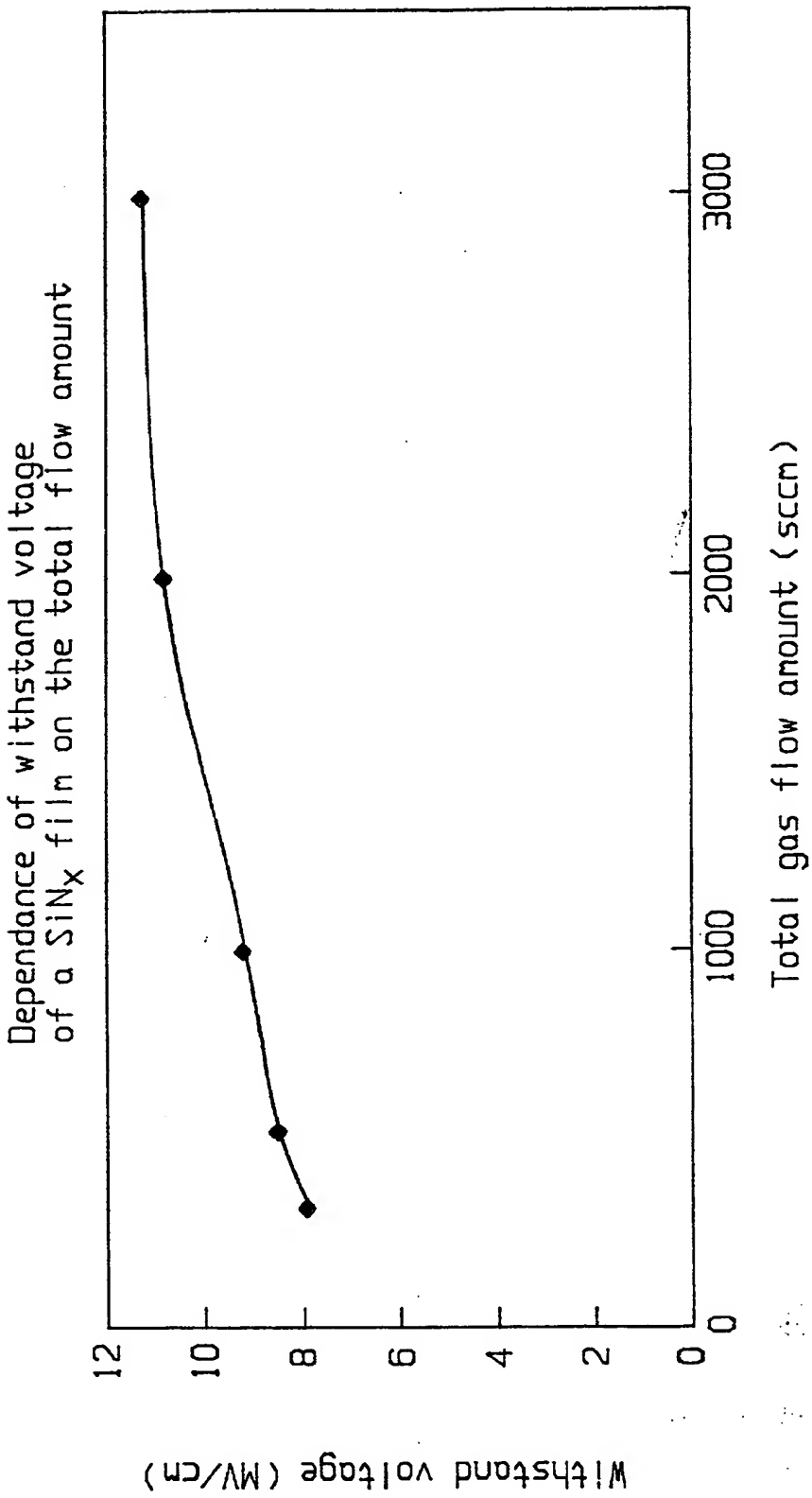
Dependance of withstand voltage
of a SiN_X film on the total flow amount
Withstand voltage (MV/cm)
0
2
4
6
8
10
12
0
1000
2000
3000
Total gas flow amount (sccm)

Fig. 78

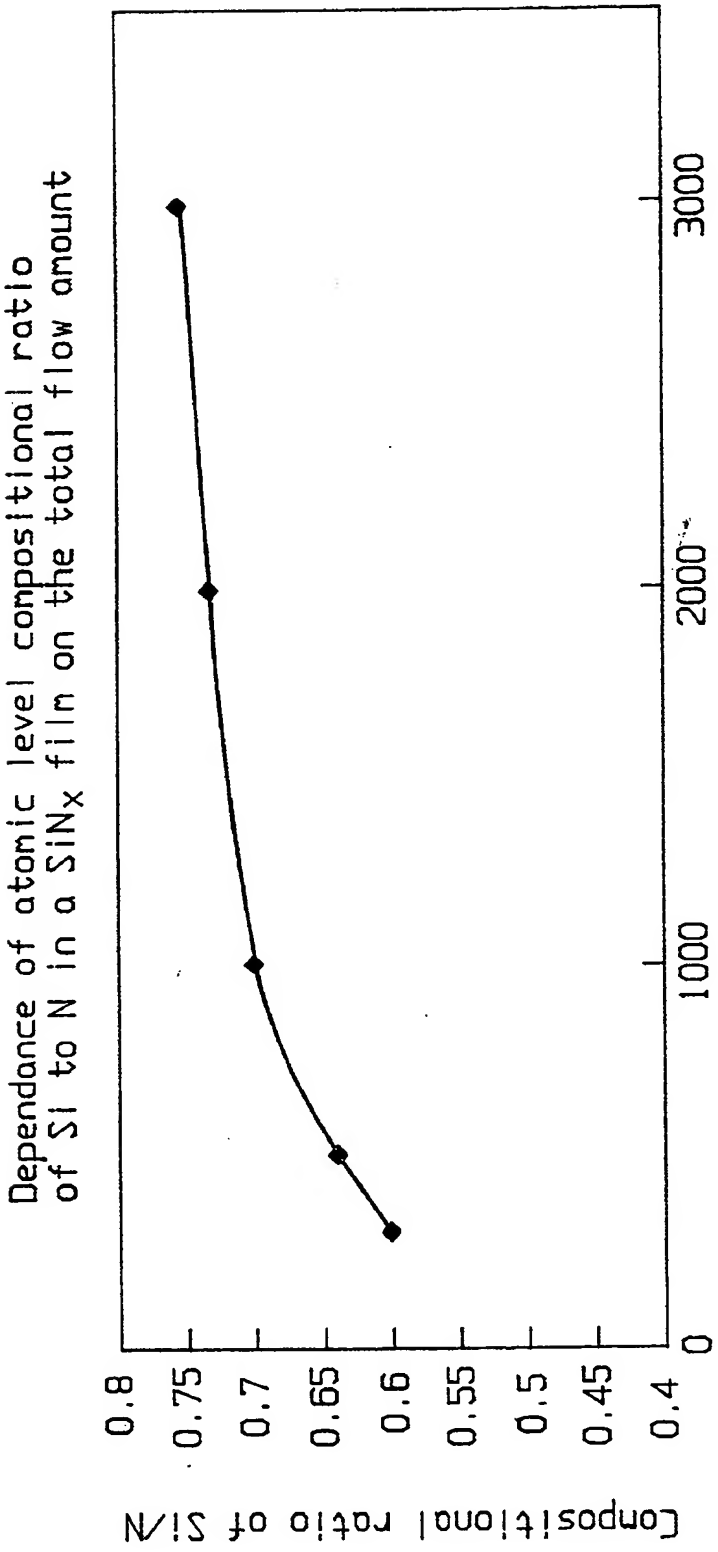
Dependance of atomic level compositional ratio
of Si to N in a SiN_x film on the total flow amount
Compositional ratio of Si/N
0.8
0.75
0.7
0.65
0.6
0.55
0.5
0.45
0.4
0
1000
2000
3000
Total gas flow amount (sccm)

Fig. 79

Dependence of the deposition rate of a fluorocarbon film on total gas flow amount

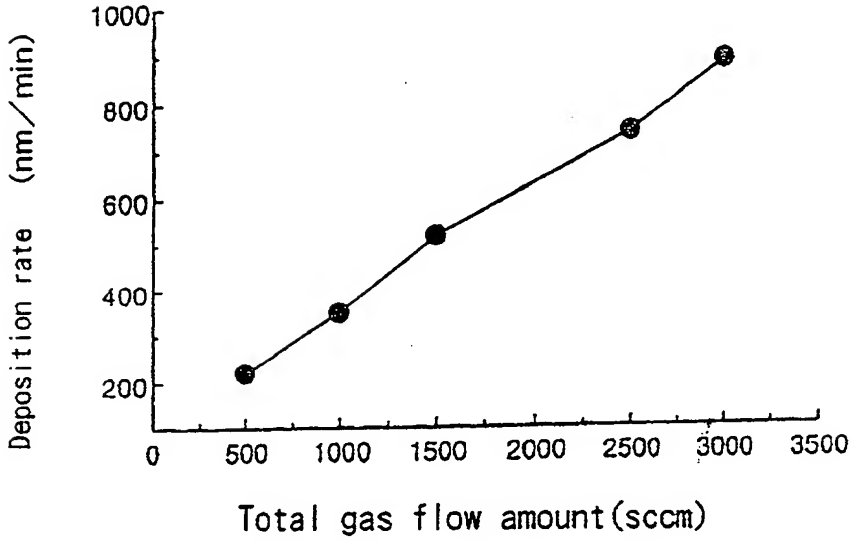

Fig. 80

Dependance of in-plane uniformity of the deposition rate of a fluorocarbon film on total gas flow amount on wafer

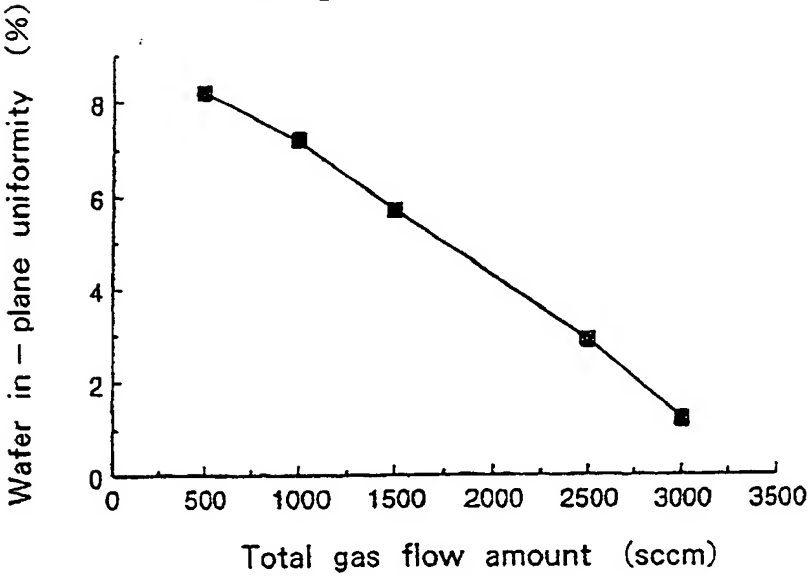

Fig. 81

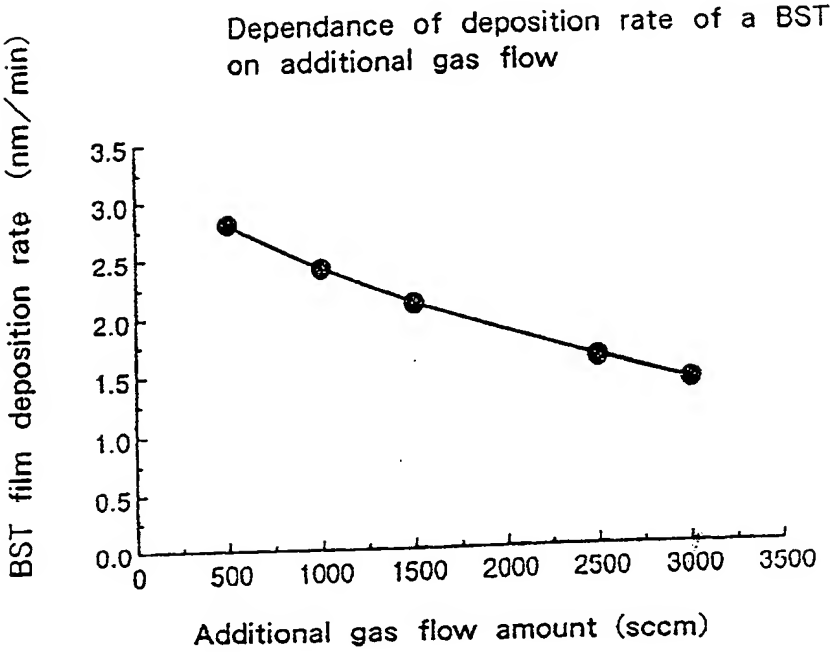
Dependance of deposition rate of a BST film on additional gas flow
BST film deposition rate (nm/min)
3.5
3.0
2.5
2.0
1.5
1.0
0.5
0.0
0
500
1000
1500
2000
2500
3000
3500
Additional gas flow amount (sccm)

Fig. 82

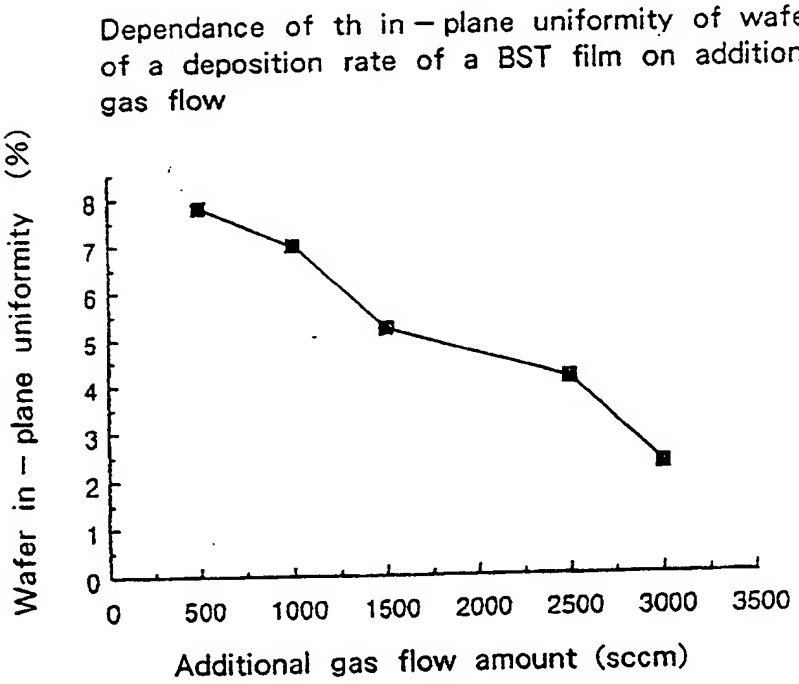
Dependance of th in – plane uniformity of wafer of a deposition rate of a BST film on additional gas flow
Wafer in – plane uniformity (%)
8
7
6
5
4
3
2
1
0
0
500
1000
1500
2000
2500
3000
3500
Additional gas flow amount (sccm)

Fig. 83

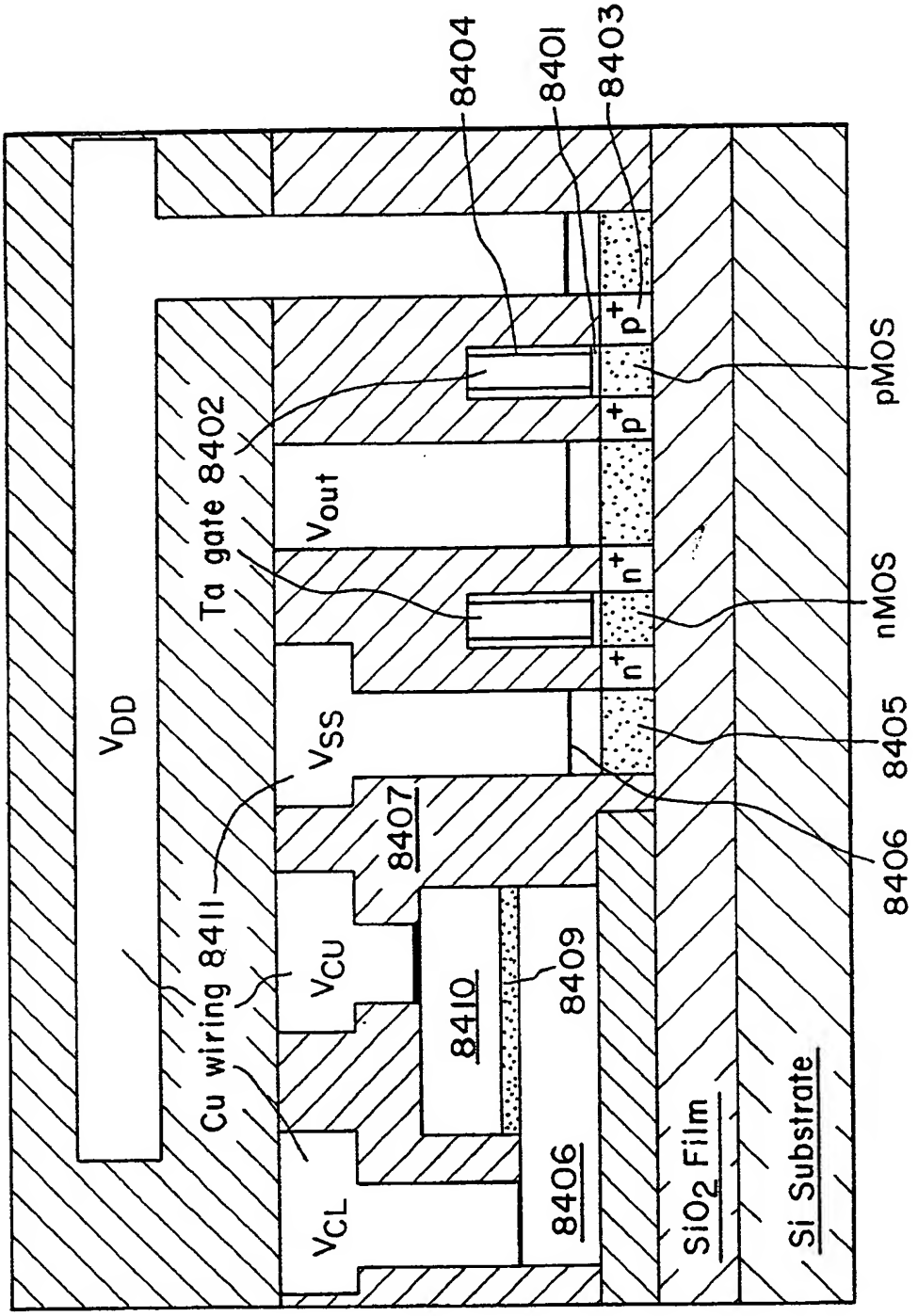
8404
8401
8403
p+
p+
pMOS
Ta gate 8402
Vout
n+
n+
nMOS
VDD
VSS
8405
8407
8406
Cu wiring 8411
VCU
8410
8409
VCL
8406
SiO2 Film
Si Substrate

Fig. 84

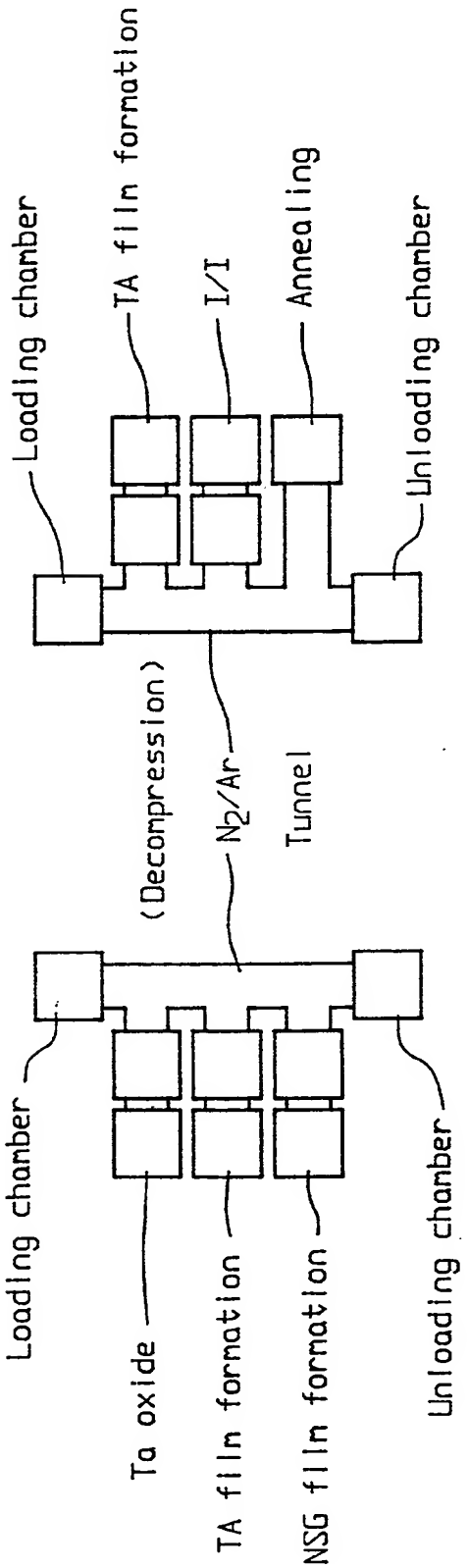

Insulating film formation 6101

Fig. 85A

Tantalum silicide formation

Fig. 85B

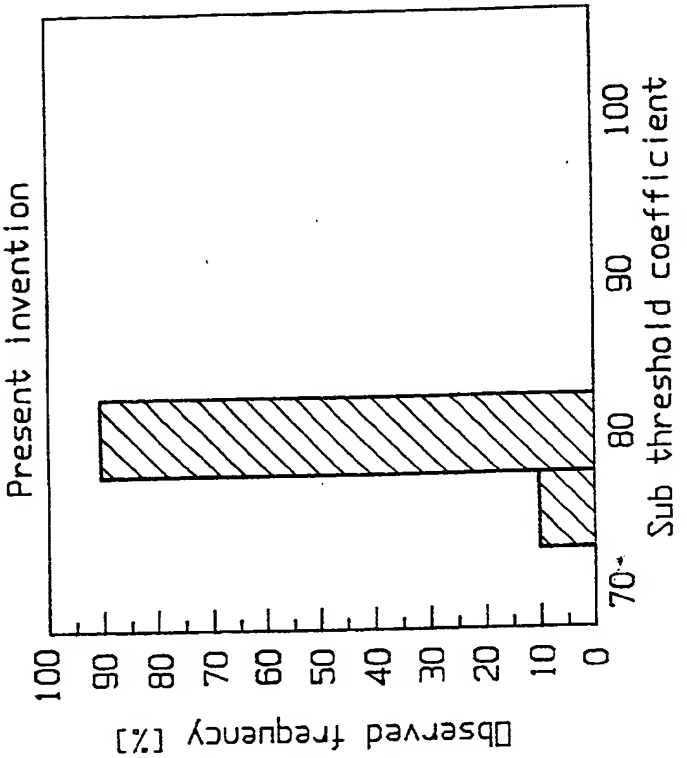

Fig. 86B

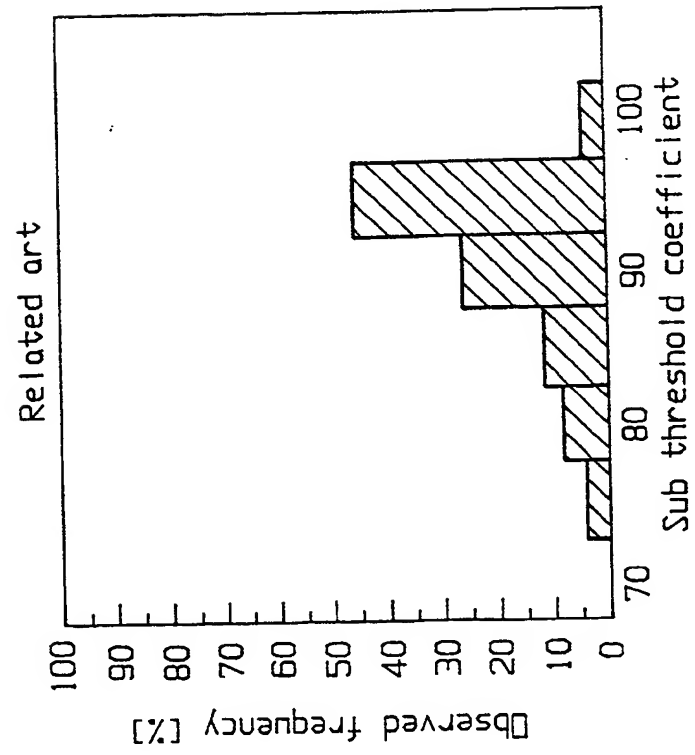

Fig. 86A

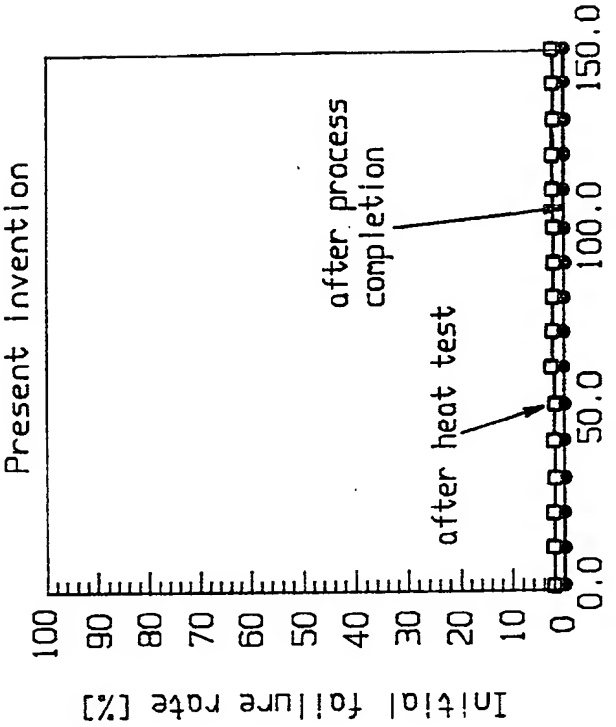

Fig. 87B

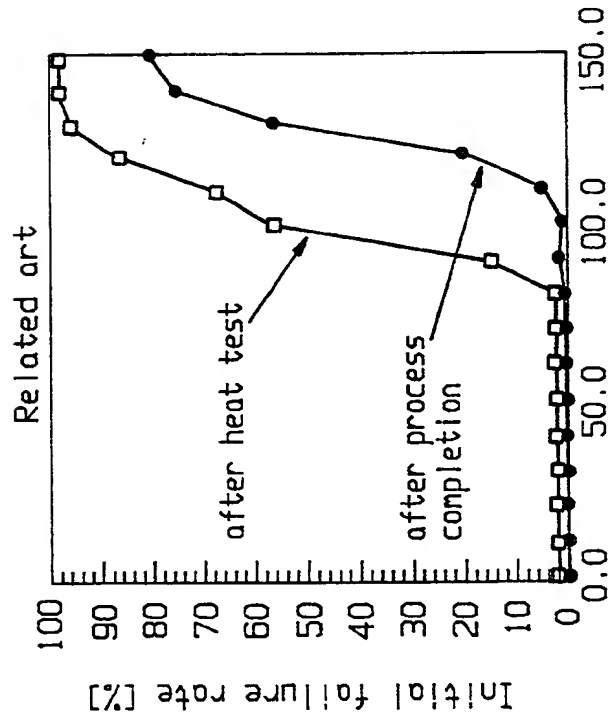

Fig. 87A

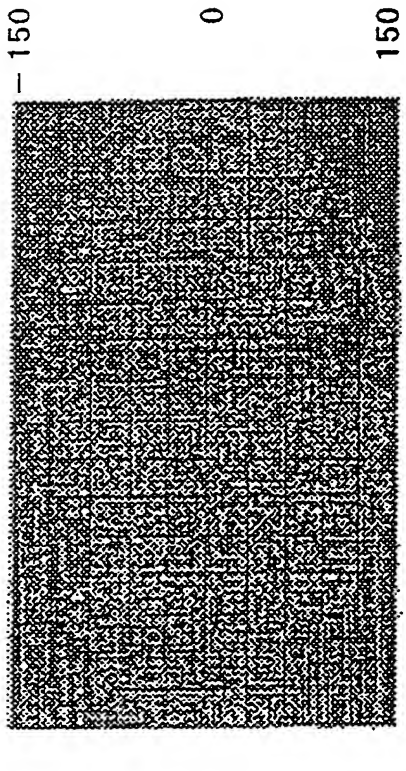

Fig. 88B Present invention

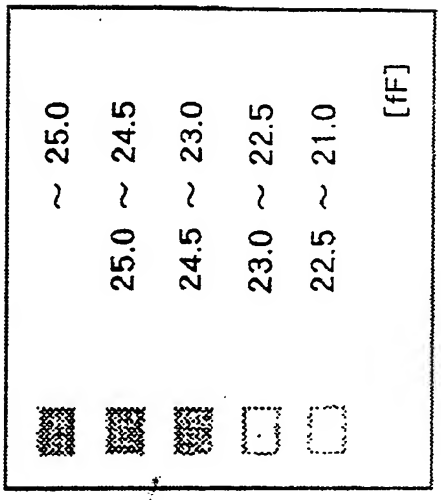

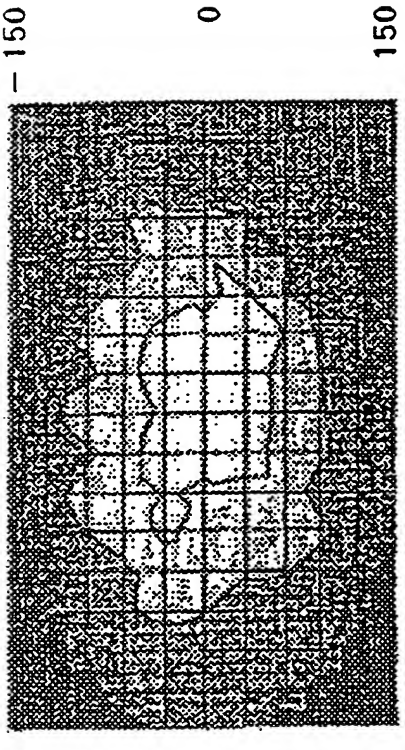

Fig. 88A Related art

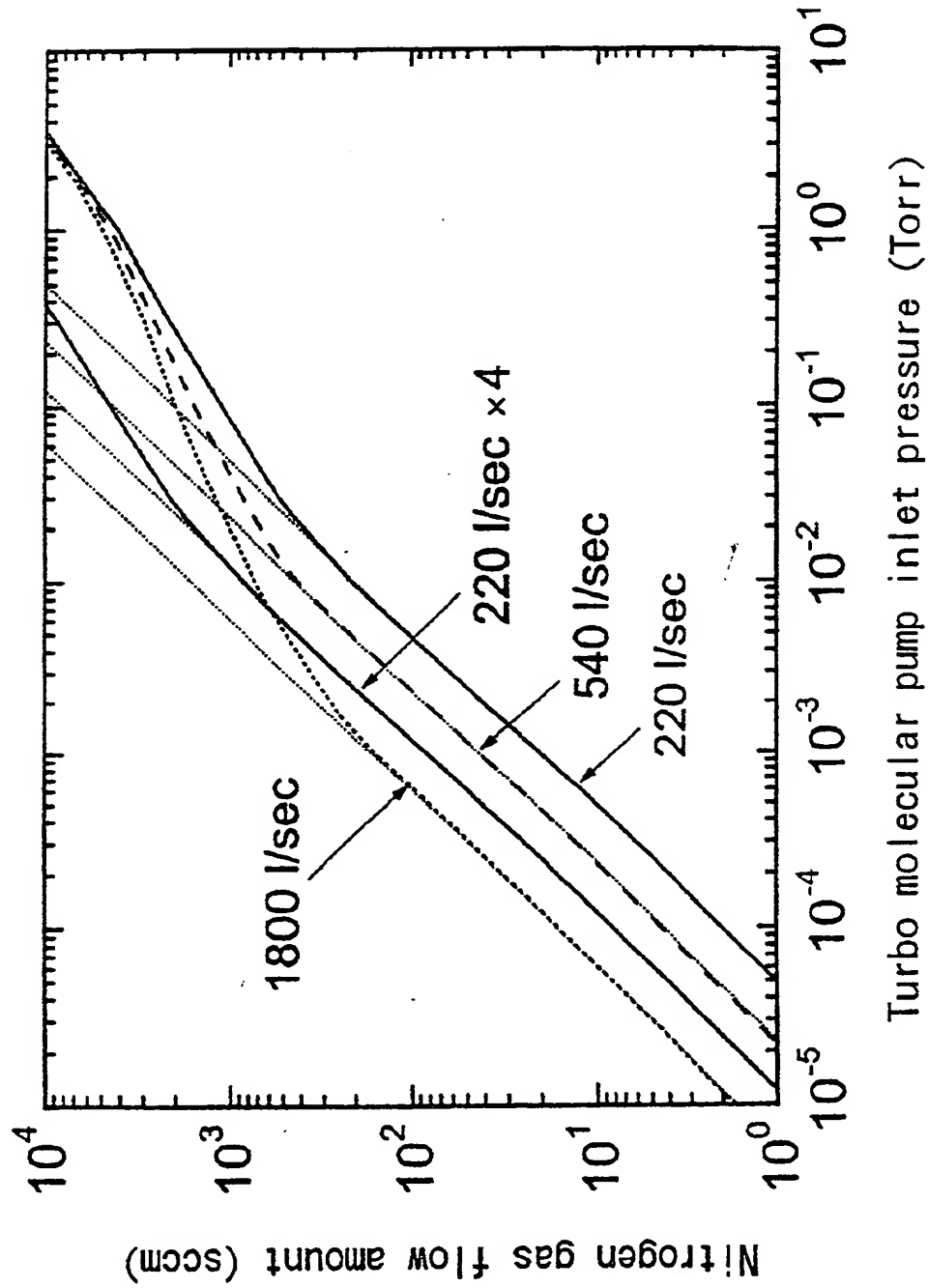
Nitrogen gas flow amount (sccm)
10^4
10^3
10^2
10^1
10^0
1800 l/sec
220 l/sec ×4
540 l/sec
220 l/sec
10^{-5}
10^{-4}
10^{-3}
10^{-2}
10^{-1}
10^0
10^1
Turbo molecular pump inlet pressure (Torr)

Fig. 8g

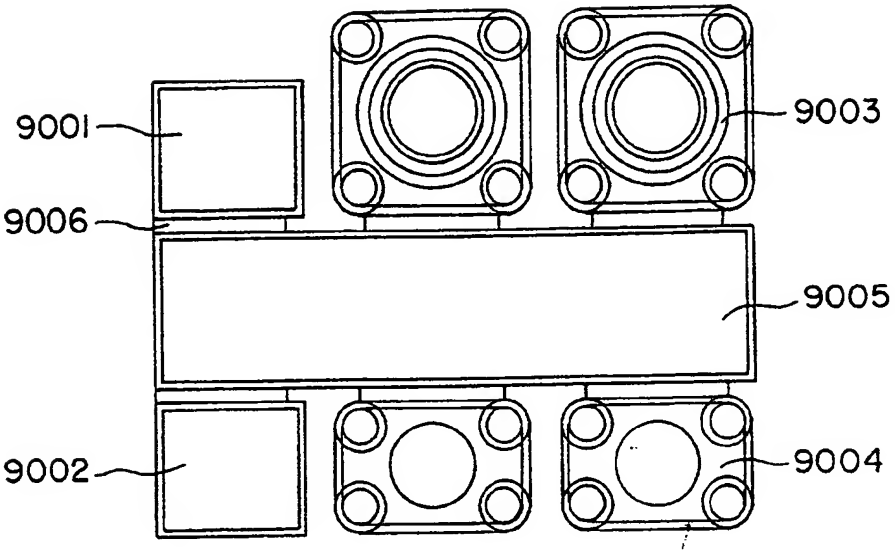

Cluster tool comprising assembly of rectangular process chamber (1)

Fig. 90

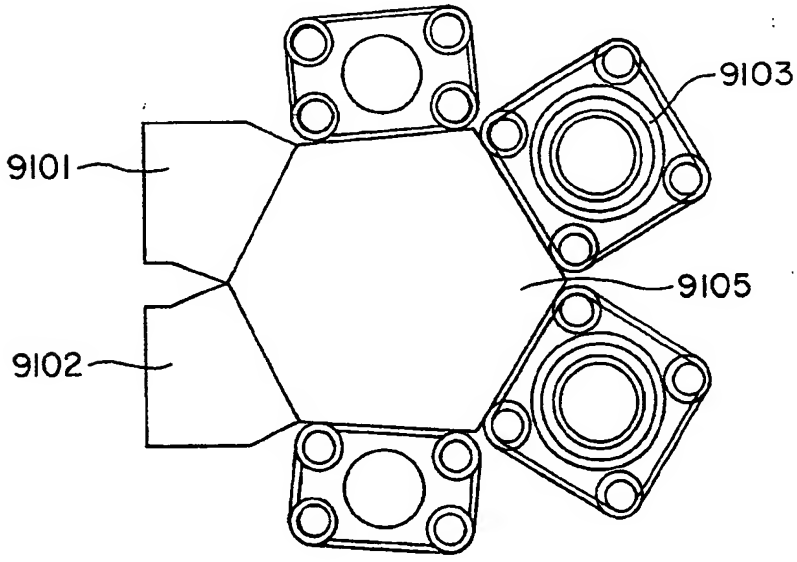

Cluster tool comprising assembly of rectangular process chamber (2)

Fig. 91

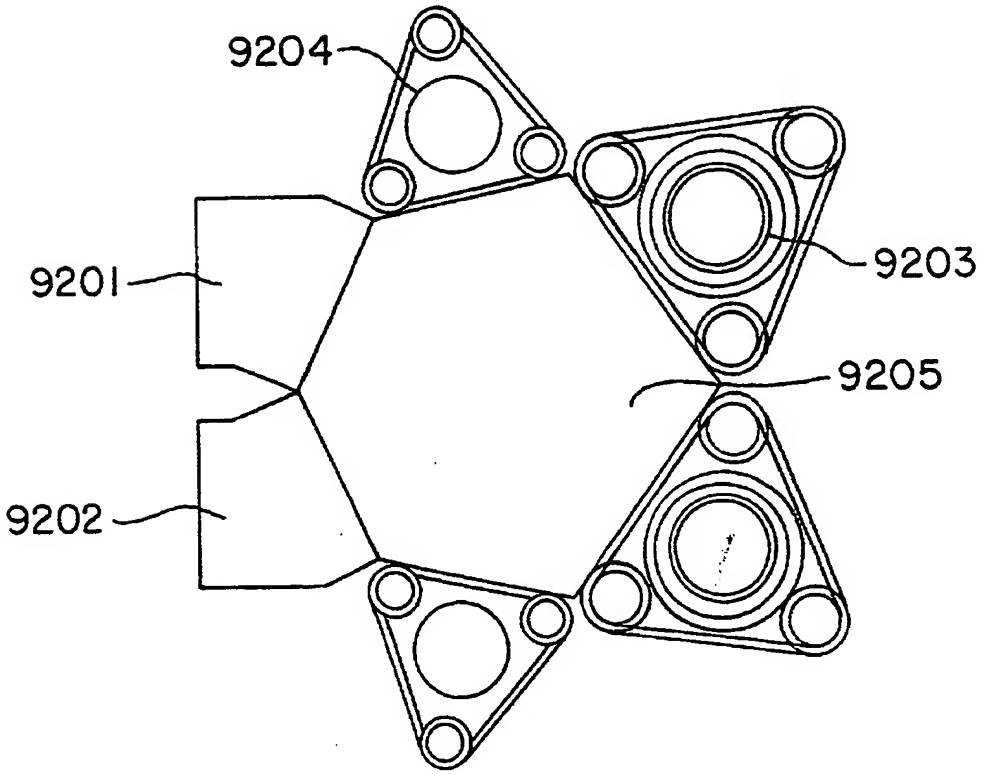

Cluster tool comprising assembly of triangular process chamber

Fig. 92

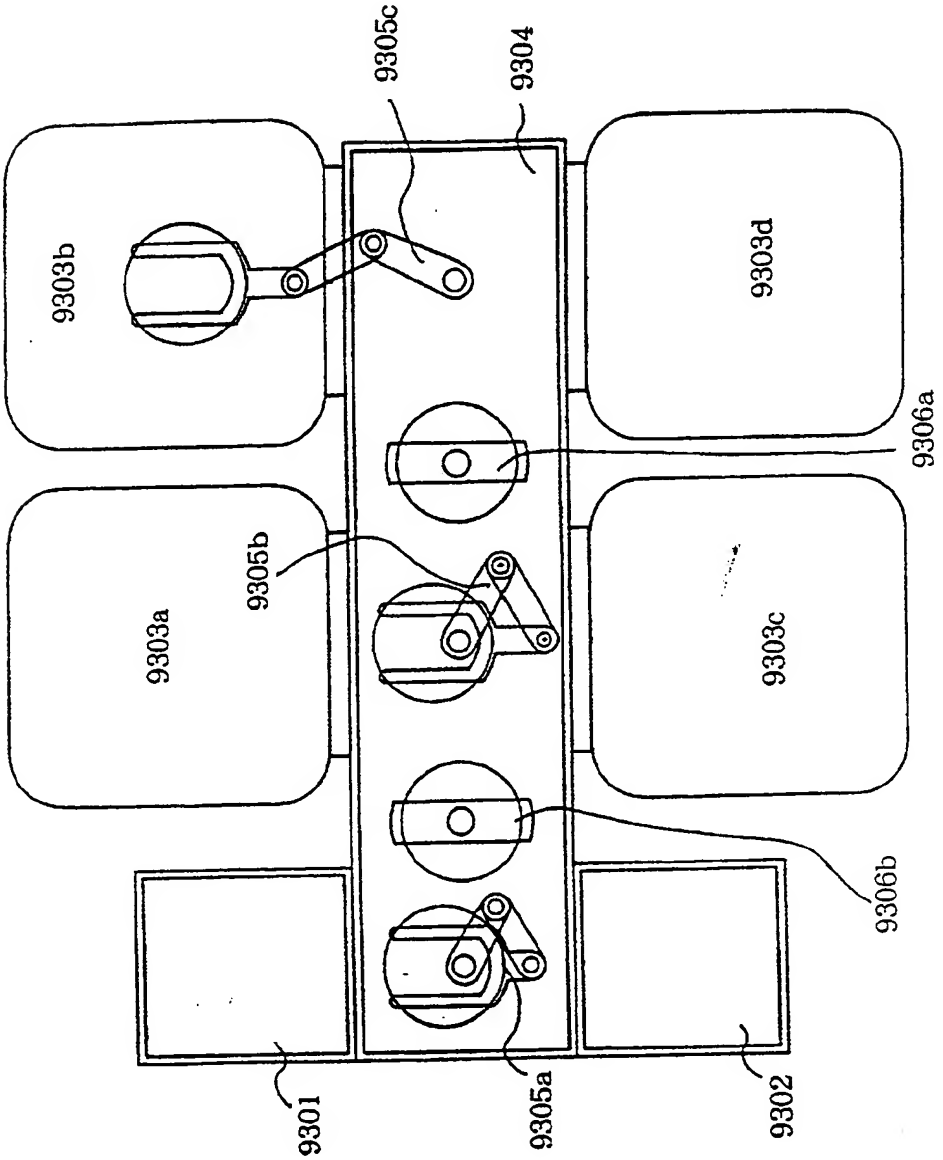
9305c
9304
9303b
9303d
9306a
9305b
9303a
9303c
9306b
9301
9305a
9302

Fig. 93

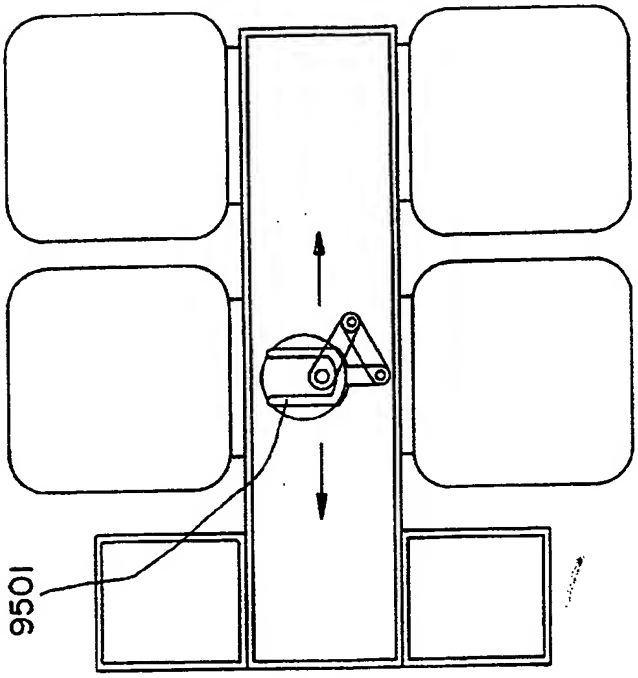

Fig. 95

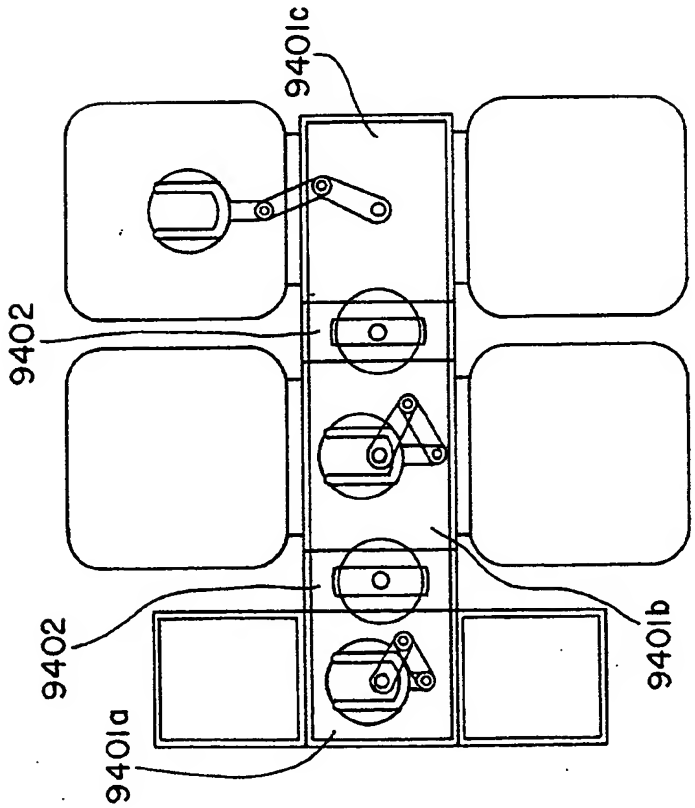

Fig. 94